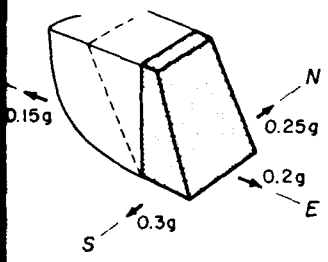

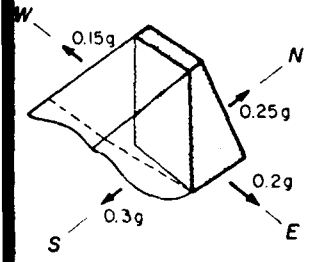

US Army Corps of Engineers

GEOTECHNICAL LABORATORY

MISCELLANEOUS PAPER GL-85-1

SEISMIC DESIGN OF GRAVITY RETAINING WALLS

by

Robert V. Whitman, Samson Liao

Department of Civil Engineering
Massachusetts Institute of Technology
77 Massachusetts Avenue
Cambridge, Massachusetts 02139

January 1985
Final Report

Approved for Public Release; Distribution Unlimited

Prepared for DEPARTMENT OF THE ARMY
US Army Corps of Engineers
Washington, DC 20314-1000
Under CWIS Work Units 31173 and 31589
Monitored by Geotechnical Laboratory
US Army Engineer Waterways Experiment Station
PO Box 631, Vicksburg, Mississippi 39180-0631

Destroy this report when no longer needed. Do not return it to the originator.

The findings in this report are not to be construed as an official Department of the Army position unless so designated by other authorized documents.

The contents of this report are not to be used for advertising, publication, or promotional purposes. Citation of trade names does not constitute an official endorsement or approval of the use of such commercial products.

Unclassified

SECURITY CLASSIFICATION OF THIS PAGE *(When Data Entered)*

REPORT DOCUMENTATION PAGE		READ INSTRUCTIONS BEFORE COMPLETING FORM
1. REPORT NUMBER Miscellaneous Paper GL-85-1	2. GOVT ACCESSION NO. AD-A152 325	3. RECIPIENT'S CATALOG NUMBER
4. TITLE *(and Subtitle)* SEISMIC DESIGN OF GRAVITY RETAINING WALLS		5. TYPE OF REPORT & PERIOD COVERED Final report 6. PERFORMING ORG. REPORT NUMBER
7. AUTHOR(s) Robert V. Whitman, Samson Liao		8. CONTRACT OR GRANT NUMBER(s)
9. PERFORMING ORGANIZATION NAME AND ADDRESS Department of Civil Engineering Massachusetts Institute of Technology Cambridge, Massachusetts 02139		10. PROGRAM ELEMENT, PROJECT, TASK AREA & WORK UNIT NUMBERS CWIS Work Units 31173 and 31589
11. CONTROLLING OFFICE NAME AND ADDRESS DEPARTMENT OF THE ARMY US Army Corps of Engineers Washington, DC 20314-1000		12. REPORT DATE January 1985 13. NUMBER OF PAGES 156
14. MONITORING AGENCY NAME & ADDRESS *(if different from Controlling Office)* US Army Engineer Waterways Experiment Station Geotechnical Laboratory PO Box 631, Vicksburg, Mississippi 39180-0631		15. SECURITY CLASS. *(of this report)* Unclassified 15a. DECLASSIFICATION/DOWNGRADING SCHEDULE
16. DISTRIBUTION STATEMENT *(of this Report)* Approved for public release; distribution unlimited.		
17. DISTRIBUTION STATEMENT *(of the abstract entered in Block 20, if different from Report)*		
18. SUPPLEMENTARY NOTES Available from National Technical Information Service, 5285 Port Royal Road, Springfield, Virginia 22161.		
19. KEY WORDS *(Continue on reverse side if necessary and identify by block number)* Retaining walls--design and construction (LC) Richards-Elms retaining wall design method (WES)		

20. ABSTRACT *(Continue on reverse side if necessary and identify by block number)*

The report discusses the seismic design of gravity walls retaining granular backfill without pore water. The general features of behavior are illustrated by field experiences, results from laboratory model tests and from theoretical analyses. Both the conventional method of design and the Richards-Elms method, based upon an analogy to a sliding block, are reviewed. A shortcoming of the sliding block analogy is discussed, and corrections obtained using a two-block model are presented. Several sources of uncertainty are examined in detail:

(continued)

DD FORM 1 JAN 73 1473 EDITION OF 1 NOV 65 IS OBSOLETE

Unclassified

SECURITY CLASSIFICATION OF THIS PAGE *(When Data Entered)*

20. ABSTRACT (Continued)

the random nature of ground motions, uncertainty in resistance parameters, and model errors, including the important influence of deformability in the backfill. All of these results are then combined to develop a probabilistic method for predicting seismically induced displacements of walls and an improved version of the Richards-Elms method of design. The risk that walls designed by the conventional method might experience excessive displacements is analyzed.

PREFACE

This report was prepared by Professor Robert V. Whitman and Mr. Samson Liao of the Department of Civil Engineering, Massachusetts Institute of Technology, Cambridge, Massachusetts, under Purchase Order No. DACW39-83-M-2088 with the US Army Engineer Waterways Experiment Station (WES). The work was conducted during the period April-December 1983 and was jointly sponsored by the Office, Chief of Engineers (OCE), US Army Civil Works Investigation Studies, "Computer-Aided Engineering Software," CWIS Work Unit 31589, and "Special Studies for Civil Work Soils Problems, CWIS Work Unit 31173. The respective OCE Technical Monitors were Messrs. Lucian G. Guthrie and Richard F. Davidson, respectively. Dr. P. F. Hadala, Assistant Chief, Geotechnical Laboratory (GL) was the WES Technical Monitor. The work was under the general direction of Dr. W. F. Marcuson III, Chief, GL.

COL Tilford C. Creel, CE, and COL Robert C. Lee, CE, were the Commanders and Directors of WES during the period of this study. Mr. F. R. Brown was Technical Director.

TABLE OF CONTENTS

1 INTRODUCTION

The design of gravity retaining walls in an earthquake-prone environment is usually based upon static analysis using an equivalent seismic coefficient. This can be a suitable approach, provided that the seismic coefficient is determined from a rational analysis of actual dynamic behavior. However, the use of seismic coefficients in current practice is largely empirical and sometimes inconsistent, leading to designs that may be either excessively conservative or unsafe.

In 1969, Richards and Elms presented a rational method for the selection of a suitable seismic coefficient, based upon the concept of an allowable permanent displacement. This approach is generally compatible both with the design philosophy used to design gravity retaining walls against static loads and with that used to design many other structures against earthquake loads. Richards and Elms utilized an analogy between the behavior of a gravity retaining wall and that of a block sliding on a plane, which is an oversimplification of the actual behavior of a wall-backfill system. Consequently, they suggested the use of a liberal safety factor, which to some extent takes into account the effects of these oversimplifications and other uncertainties in the analysis.

The work described in this report improves upon and extends the Richards-Elms approach to design by considering corrections to the simple sliding block analogy, and by introducing a rational basis for the selection of a suitable safety factor for use in the

approach. The essence of the proposed method is the following expression for prediction of the residual displacement experienced by a gravity retaining wall during an earthquake:

$$d_{Rw} = \bar{d}_{Rv} \cdot R_{2/1} \cdot Q \cdot R_{\phi} \cdot M \qquad (1.1)$$

where d_{Rw} is the predicted residual displacement

$\bar{d}_{Rv}$ is the mean (expected) residual displacement for a sliding block exposed to ground motion characterized by a small number of parameters (such as peak acceleration A and peak velocity V).

$R_{2/1}$ is a deterministic term accounting for a specific kinematic deficiency in the single sliding block model.

Q is a term accounting for the unpredictable details in the random nature of future earthquake shaking.

R_{ϕ} is a term accounting for the uncertainty in the parameters characterizing the backfill, wall and foundation soil.

M is a term accounting for other, and as yet, poorly understood deficiencies of the simple sliding block model.

The scope of this report is restricted to gravity retaining walls with granular backfills subjected to earthquakes, where soil liquefaction is not of importance. It also primarily deals with the translational mode of retaining wall movements, treating rotational movements as a secondary concern. Chapter 2 presents an overview of the complex nature of the dynamic retaining wall problem, and Chapter 3 discusses the conventional approach to design. Subsequent chapters treat and discuss each of the individual terms in Equation 1.1 in detail.

It should be noted that further research and development remains to be done to render the basic Richards-Elms procedure completely satisfactory. Nevertheless, based on the present knowledge summarized in this report, an improved design procedure is presented in Chapter 9.

2 - GENERAL FEATURES OF DYNAMIC BEHAVIOR

2.1 COMPLEX BEHAVIOR AND SIMPLIFIED MODELS

Analysis of the behavior of gravity retaining walls during earthquake loading is a complex soil-structure interaction problem potentially involving plastic deformations and large strains. Even with the use of numerical procedures, such as the finite element method, it is not presently feasible nor possible to simulate all the phenomenon that would occur. As in all branches of engineering, simplified models with various approximations and assumptions are necessary to make complex problems more tractable, particularly for purposes of design.

Various simplified models, useful for engineering design of retaining walls, will be presented in subsequent chapters of this report. In this chapter, the intent is to illustrate and examine the complexities of retaining wall behavior, and to highlight some of the major aspects of the problem that have been considered in the simplified models. However, more importantly, the phenomena that have <u>not</u> been considered in the simplified models are also identified, to provide a basis for judging the limitations of the models.

A general overview of retaining wall behavior is presented here, based on a review of field observations, laboratory model experiments, and the results of a relatively sophisticated finite element model. Further aspects of some particular details of these observations and data will be discussed, as necessary, in subsequent chapters.

the earth pressure thrust is the force in the spring (labeled 'A') connecting the two masses representing the wall and the backfill wedge.

If the ground is suddenly accelerated to the right and slip occurs as in Fig. 2.7(c), a force would develop in the spring 'A' because of differences in the inertia forces between the two masses and differences in the stiffness of the shear springs. However, there would be no force in the spring 'B', and so the force in the spring 'A' would be fairly small, and perhaps even slightly tensile. On the other hand, when a sudden acceleration is applied to the left as in Fig. 2.7(d), the force in spring 'B' is activated to resist the inertia forces of the two masses. As a result, slip movements do not occur, but a relatively large force would be present in spring 'A', the analog of the earth pressure.

The above arguments have tried to explain in only a purely intuitive fashion the complex nature of forces and displacements in a elastic-plastic retaining wall model. However, the major point of emphasis as it applies to gravity wall design is that there is not a clear direct correlation between the maximum earth pressure force and the amount of relative displacement that occurs. Focusing too much upon the forces exerted by the backfill may lead to meaningless results, and it is more essential think in terms of displacements in design.

The location of the resultant dynamic earth pressure force was observed to vary with time in a complex manner in the finite element model. Parametric studies using a finer mesh model (than that shown in Fig. 2.5), indicated that the time variation of the

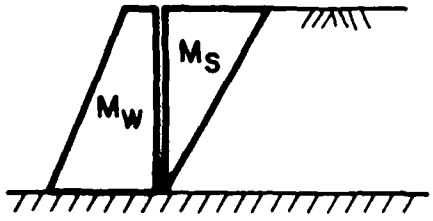

(a) Elastic-Plastic Retaining Wall

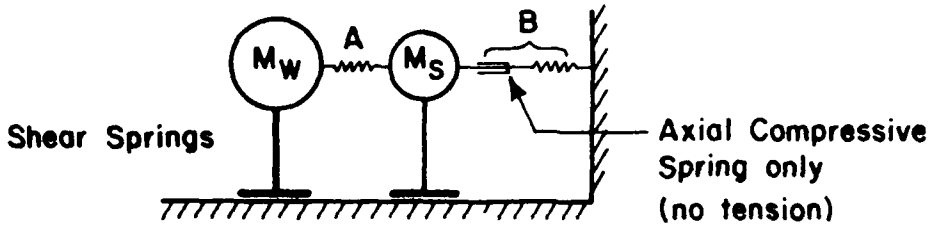

(b) Idealized Lumped Mass System

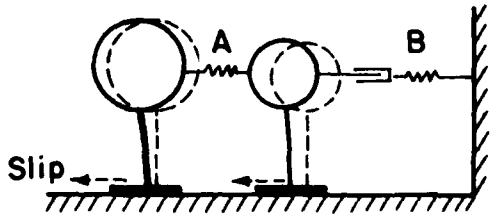

(c) Occurrence of Slip

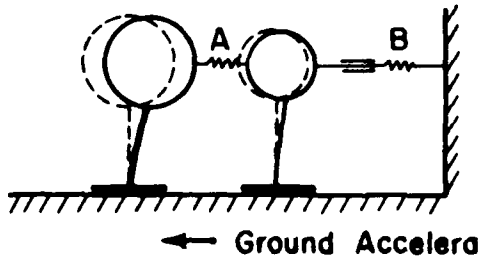

(d) No Slip, Elastic Deformations Only

FIG. 2.7 AN INTUITIVE MODEL OF ELASTIC-PLASTIC RETAINING WALL BEHAVIOR.

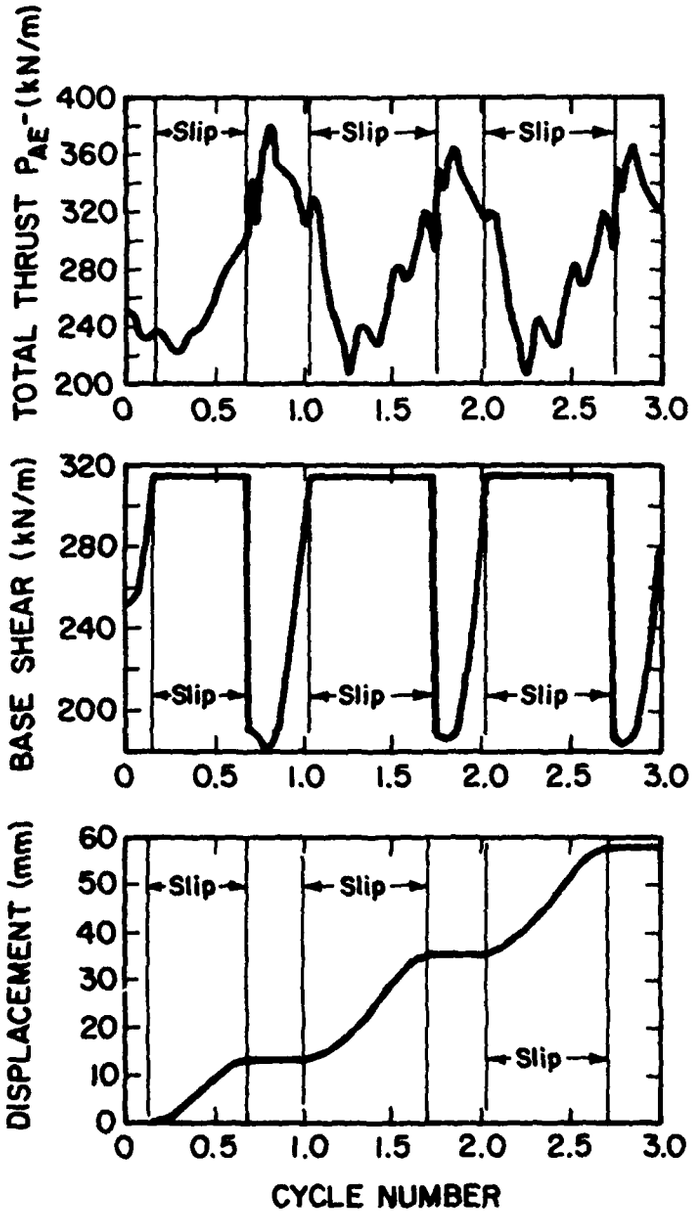

FIG. 2.6 TYPICAL RESULTS FROM FINITE ELEMENT MODEL FOR RETAINING WALL SUBJECTED TO 3 CYCLES OF SINUSOIDAL GROUND MOTION.

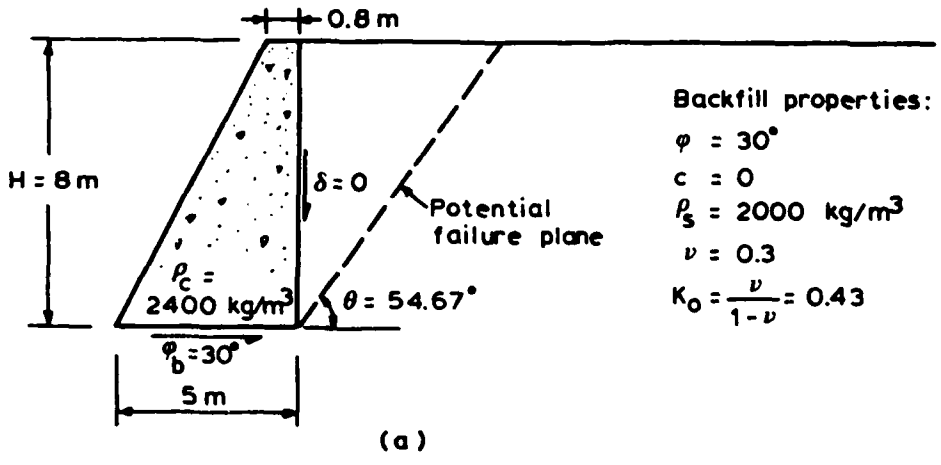

(a)

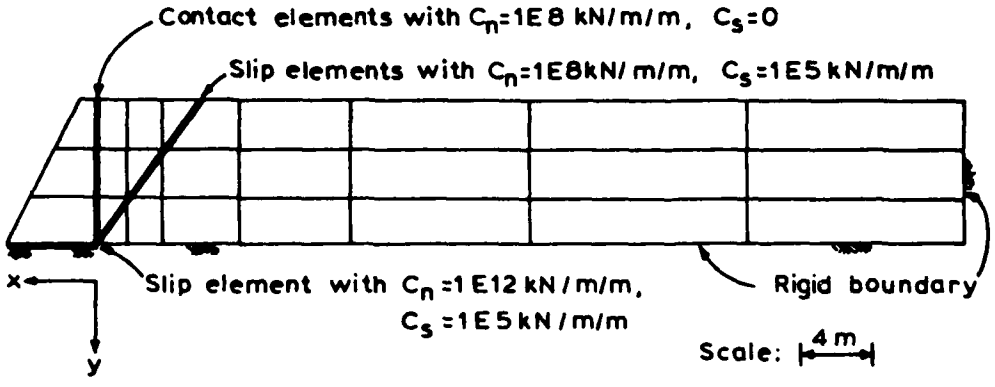

C_n = Normal stiffness of slip elements

C_s = Shear stiffness of slip elements

(b)

FIG. 2.5 FINITE ELEMENT MODEL OF A RETAINING WALL (AFTER NADIM, 1982).

2.4 FINITE ELEMENT RESULTS

Though even sophisticated finite element analyses are simplified models of actual behavior, they can nevertheless offer insight into physical processes that are difficult to observe or measure experimentally. The finite element idealization of a retaining wall used in a study by Nadim (1982) is shown in Fig. 2.5. The material properties of this model are linearly elastic, except for the essentially rigid-plastic elements at the base of the wall, at the wall-soil interface, and along a preselected failure plane through the backfill. This model is able to account for elastic deformation of the backfill as well as for the development of a Coulomb-type failure wedge.

A typical set of results, obtained using 3 cycles of sinusoidal motion at the base of the grid, is shown in Fig. 2.6. There are three intervals (marked "slip" on the figure) during which the wall slides upon the base. In these intervals, the shear force at the base of the wall is constant and the thrust between backfill and wall is relatively low. On the other hand, the maximum thrusts from the backfill occur at times when no slip is occurring, and when the base shear resistance is fairly low.

An explanation for the lack of direct correlation between the earth pressure force and the amount of wall slippage (at any given time) is illustrated in Fig. 2.7. Here, the finite element model is further idealized as a lumped mass system consisting of two masses and axial and lateral-shear springs. A unique feature imagined for one of the axial springs (labeled 'B') is its ability to transmit compressive forces, but not tension. The analog of

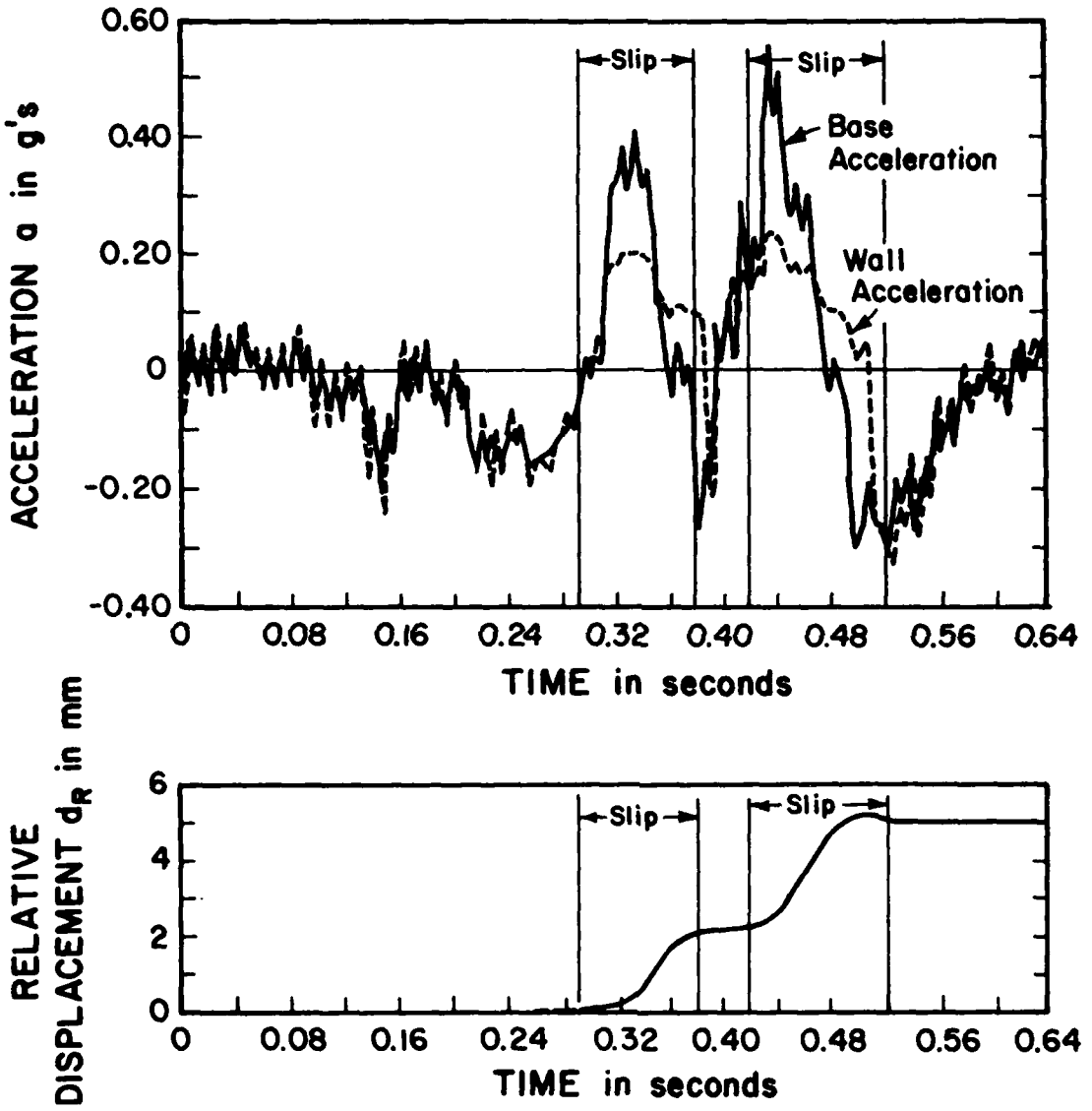

FIG. 2.4 TYPICAL MEASUREMENTS OF ACCELERATION AND RELATIVE DISPLACEMENT - IN EXPERIMENT PERFORMED BY LAI (1979).

(Figure based on reduced data from Jacobsen, 1980).

Typical measurements of acceleration and relative displacement of the model wall obtained by Lai (1979) are shown in Fig. 2.4. The first feature to note is that the total slip of the model retaining wall does not occur in a single movement (i.e., catastrophically), but rather occurs in a stepwise fashion as a series of smaller incremental displacements. During the time intervals when slip is not occurring, the acceleration of the model wall follows closely the input base acceleration. The occurrence of slip is associated with wall accelerations that are less than the peak base motions, and there appears to be a critical acceleration at which slip starts to occur. Also, slip occurs in only the direction away from the backfill, implying that passive pressures are more than sufficient to resist wall movements into the backfill.

A problem common to all model tests is the lack of similitude in stresses and loads from using small scale models. In part, this scaling problem can be alleviated by conducting tests in a centrifuge, as has been reported by Ortiz, et al. (1981) and by Bolton and Steedman (1982) in their experiments on model retaining walls. Currently, there is an extensive research program on retaining walls being carried out at the Cambridge University Centrifuge facility, but the results of those model tests are not available to the writers at the time of publication of this report. It is almost certain that these series of tests will provide further insight into retaining wall behavior, and may change some of the conclusions stated here.

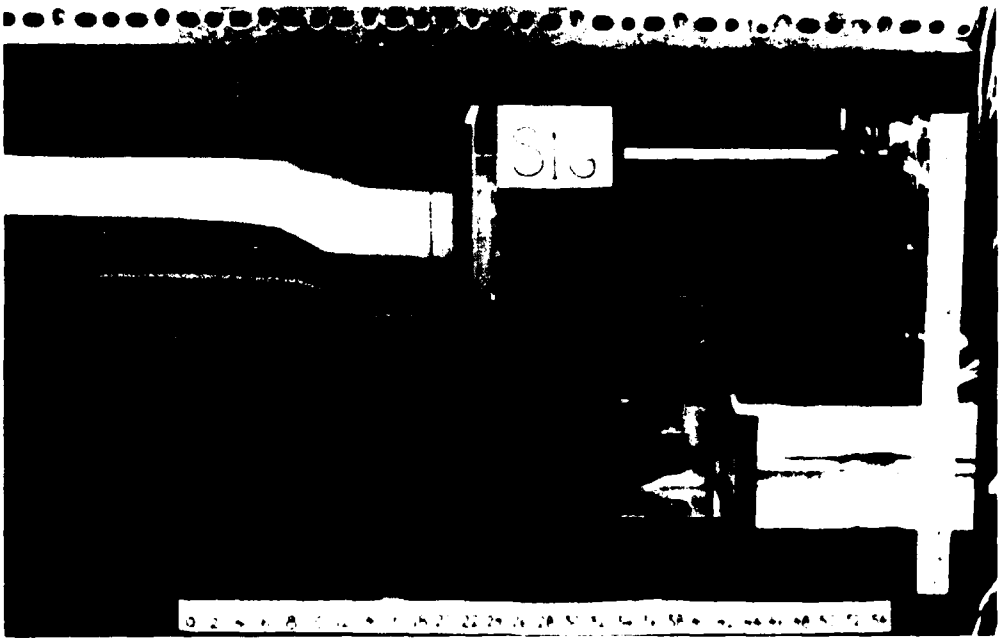

FIG. 2.3 MODEL TEST SHOWING TRANSLATIONAL MODE OF FAILURE (FROM LAI, 1979).

Note: Scale is marked in cm.

- The formation of a single predominant failure plane in the backfill, along which slip occurs.
- A significant amount of backfill settlement.
- The occurrence of distortional shear strains in the backfill failure wedge.
- The plastic deformation of the soil in the area near the toe of the wall as a result of wall rotation.

Lai (1979) performed a series of experiments using L-shaped model retaining walls approx. 12.6 inches (320 mm) high with a base width of 8.7 inches (220 mm). The model walls were made of aluminum, and additional steel plates could be secured to the base of the wall to vary the total weight of the wall. The dynamic excitation was provided by a shaking table which could simulate both periodic and earthquake excitations.

A photograph of one of Lai's model tests after failure is shown in Fig. 2.3. In contrast to the rotational failures, translational movements produce very little distortional strain in the failing backfill soil wedge, and can be approximated as a rigid body motion. However, plastic deformations of the soil at the toe of the soil wedge must occur in the process of movement. Similar to the result shown for rotational failure, Lai noted the formation of a single predominant failure plane, though other planes developed in the failing wedge with larger movements. Also, there is clear evidence that increasing the weight of the wall leads to flatter inclinations of the failure plane.

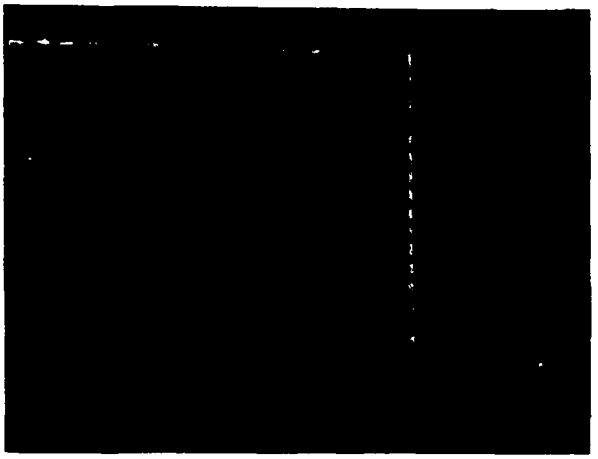

(a) Before starting test of gravity wall.

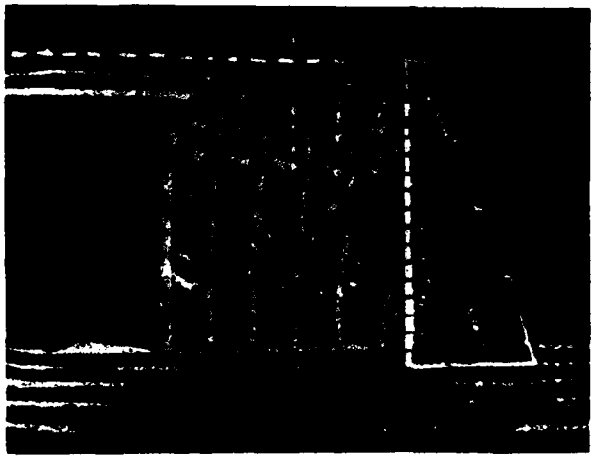

(b) Condition of gravity wall after 1 minute of vibration.

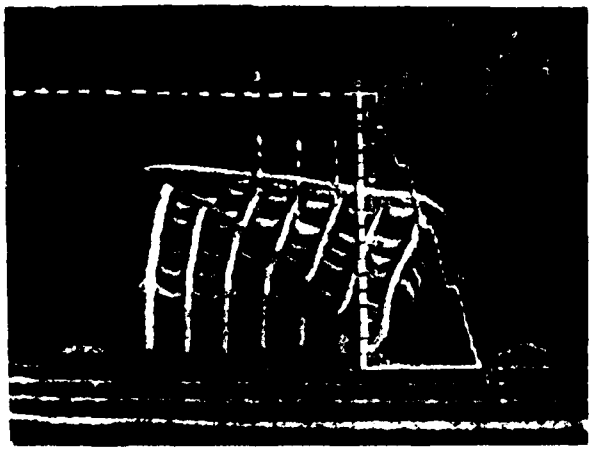

(c) Condition of gravity wall after $2\frac{1}{2}$ minutes of vibration.

FIG. 2.2 MODEL TEST SHOWING ROTATIONAL MODE OF FAILURE (FROM MURPHY, 1960).

Note: Scale is marked in inches.

(1970), and more recently by Nadim (1982). Generally, the experiments that have been performed can be classified into two groups:

- Experiments primarily concerned with the measurement of dynamic earth pressures and/or structural response.
- Experiments to measure the movements of retaining wall and observe general failure patterns during shaking.

The first group, involving experiments to measure dynamic earth pressure, has had limited success in the comparison of results with theoretical solutions, in particular the Mononobe-Okabe equation. Specific details of these comparisons with theory will be discussed in Chapter 3. It has generally been observed that the distribution of earth pressure does not increase linearly with depth as in the case for static pressures. Also, the location of the resultant of the total force is usually located above the lower third point along the height of the wall. Several of these experiments involved model walls that were fixed or restrained, and subsequently did not correspond to true field conditions.

The second group of experiments are generally closer in their simulation of actual field conditions. Murphy (1960) conducted tests on a model gravity retaining wall made of solid rubber shaken with sinusoidal base motion with a period of 1.48 seconds. Figure 2.2 shows the sequence of failure of the retaining wall. Although the wall weight is improperly scaled and there are undoubtedly frictional effects (i.e. model against glass container), several significant behavioral features can be noted:

by Nadim (1980), but the results are of a preliminary nature.

Settlements of the backfill behind a wall generally accompany outward movements of the wall. Evans (1971) reports fill settlements of the order of 10% to 12% of the fill height. Such orders of magnitude of downwards movements of the backfill associated with outwards movement of the wall are consistent with the concept of the development of a wedge of soil failing along a plane behind the wall.

It has been observed that movements are not always associated with damage or failure. Evans (1971) noted that of the 39 bridges examined in the vicinity of the 1968 Inangahua earthquake in New Zealand, 23 showed measureable movement (without damage), and only 15 were damaged. This is an important concept which is used by Richards and Elms (1979) in the proposed design method.

Designing to limit the amount of outward movement is a rational method to avoid failure not only for the translational mode, but perhaps also for rotational modes of failure. In the case of bridge abutments, if the amount of translation is restricted so that contact and restraint by the bridge superstructure is avoided, then the likelihood of rotational movements about the top of the retaining wall is greatly reduced.

2.3 MODEL EXPERIMENTS

Tests have been performed by a number of investigators using small scale models of earth retaining structures subjected to dynamic base motion. Reviews and summaries of the various results from these experiments have been reported by Seed and Whitman

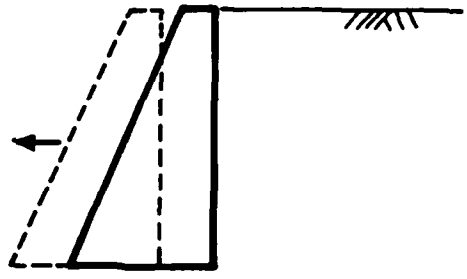

(a) Outward Translation

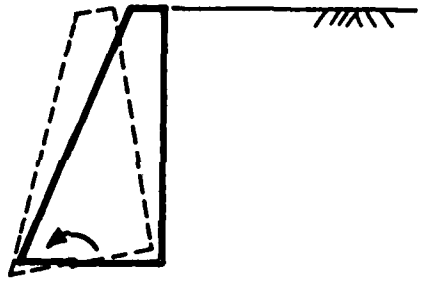

(b) Rotation about the Base

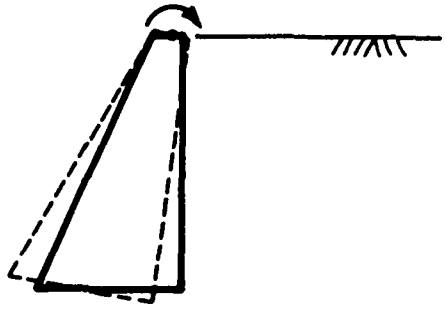

(c) Rotation about the Top

FIG. 2.1 POSSIBLE MOVEMENTS OF GRAVITY RETAINING WALLS.

2.2 FIELD OBSERVATIONS

Many reports of retaining wall movements during earthquakes are available in the literature. Useful summaries of these data have been presented by Seed and Whitman (1970), the Japan Society of Civil Engineers - JSCE (1977), and by Mayes and Sharpe (1981).

Aside from the cases where liquefaction was a cause of failure, three types of retaining wall movements have been observed, as schematically illustrated in Fig. 2.1. These are:

- Outward translations of the wall
- Rotations about the base of the wall
- Rotations about the top of the wall

Most cases of movement involve a combination of translation and rotation. Rotations about the top of the wall appear to be restricted to retaining walls forming part of bridge abutment structures. Mayes and Sharpe (1981) suggest that rotation about the top occurs only after outward motion of the wall brings the top into contact with and restraint by the superstructure. However, the pattern of overall bridge movement in some cases indicate that inertia forces from the superstructure may actually havepushed the top of the wall into the backfill (Evans, 1971).

In the simplified methods presented in subsequent chapters, only the translational mode of movement is considered in analysis. This is because translational movements are more analytically tractable than rotational movements, but it is also an obvious disadvantage of the methods, since it is rare that purely translational movements of walls have been observed. Some analytical work on rotational modes of movement has been reported

location of the earth pressure depended on factors such as the elastic modulus of the backfill and the frequency and amplitude of the input ground motion.

Another feature observed in the finite element model is the amplification of ground motions due to the elastic properties of the wall and backfill. Since the system is elastic, a natural frequency of vibration can be associated with the retaining wall and the soil. If the input ground motion due to an earthquake has a central frequency near the natural frequency, effects similar to resonance will tend to amplify the maximum ground acceleration, and cause larger displacements of the retaining wall.

3 - CONVENTIONAL DESIGN

3.1 GENERAL CONCEPTS

Gravity retaining walls are typically designed using a static equivalent earthquake coefficient. This coefficient is used to evaluate the static plus dynamic force exerted on the wall by the backfill, and should also be used to calculate the inertia force due to the wall. A schematic of these forces is shown in Fig. 3.1, along with definitions and notation for the seismic coefficients. Having found these forces, conventional static design procedures are followed, which means ensuring that the weight of the wall, shear resistance on the base of the wall and passive resistance at the toe are sufficient (with appropriate safety factors) to resist sliding, overturning and bearing capacity failure.

In concept, the use of a seismic coefficient (also called the pseudo-static method of analysis), is equivalent to a static tilting of the problem at an angle ψ computed as:

$$\psi = \tan^{-1} \left(\frac{N_H}{1-N_V}\right) \qquad (3\text{-}1)$$

where N_H = the horizontal seismic coefficient

N_V = the vertical seismic coefficient

with positive (+) inertia force directions as noted in Fig. 3.1. Figure 3.2 illustrates this concept for a simple case where $N_V = 0$.

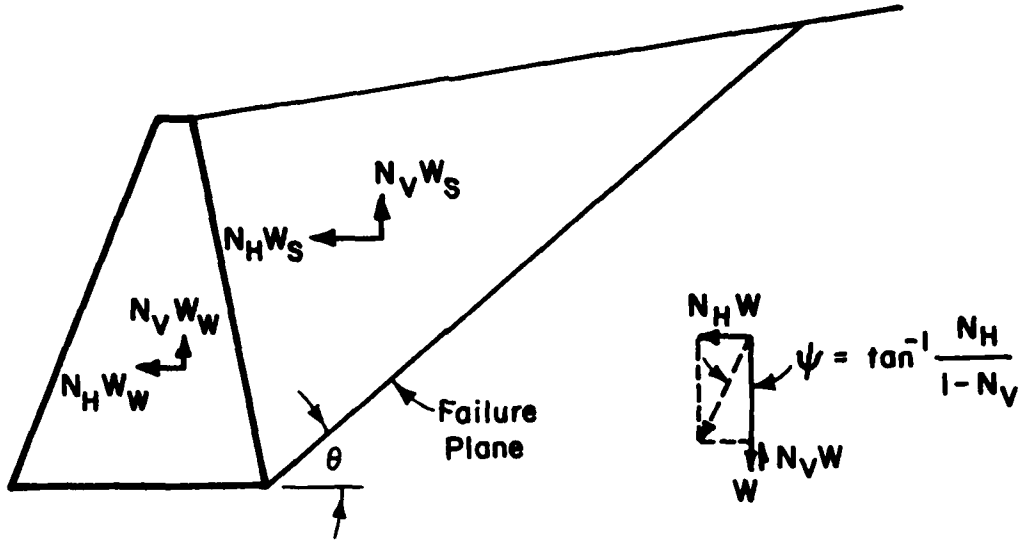

W_W = Weight of Retaining Wall

W_S = Weight of Soil Backfill Wedge

N_H = Horizontal Seismic Coefficient

N_V = Vertical Seismic Coefficient

FIG. 3.1 SCHEMATIC OF STATIC EQUIVALENT SEISMIC COEFFICIENTS AND EARTHQUAKE INERTIA FORCES FOR CONVENTIONAL DESIGN.

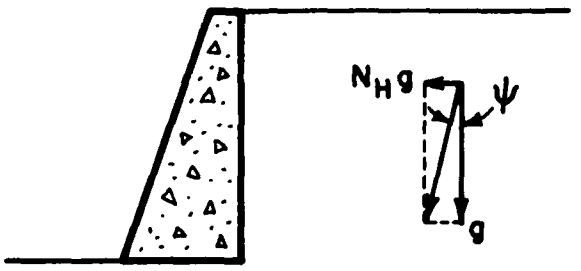

(a) Retaining Wall with Gravitational and Horizontal Seimic Force Vectors

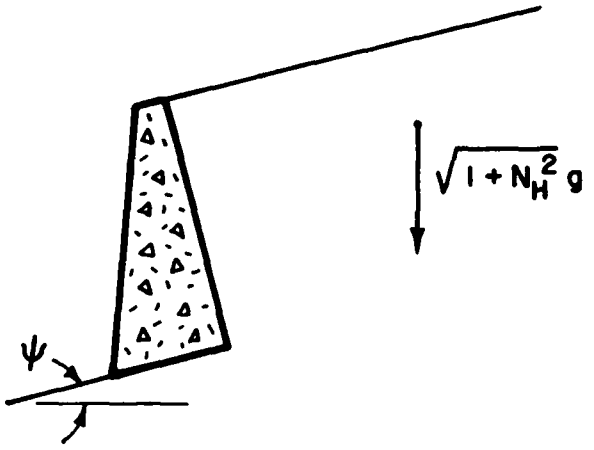

(b) Equivalent Static Problem with Gravitational Force Only

FIG. 3.2 INTERPRETATION OF THE ψ-ANGLE IN CONVENTIONAL SEISMIC COEFFICIENT ANALYSIS ($N_V = 0$).

As can be readily seen, a logical conclusion from this interpretation of the angle, Ψ is that Ψ can not exceed the angle of repose (ϕ) for cohesionless flat backfill (Richard and Elms, 1979). Since the steepest slope that can be formed is at the angle of repose, $\Psi > \phi$ would correspond to an impossible non-equilibrium condition. Similarly, for a backfill inclined at angle i, Ψ would be restricted to have values less than ϕ-i. Physically, as Ψ increases, the critical angle of the failure plane becomes flatter, until at $\Psi = \phi$-i, the failure plane becomes parallel to the backfill slope.

3.2 EVALUATING DYNAMIC EARTH PRESSURE

3.2.1 Mononobe-Okabe Equation

Although retaining wall seismic stability analyses can be performed by assuming several trial slip planes of failure in the backfill (as in slope stability analysis), usually earth pressures are calculated using some version of the Mononobe-Okabe equation (Mononobe, 1929 and Okabe, 1926). In its complete form, the equation is written as:

$$P_{AE} = 1/2\,\gamma\,H^2\,(1-N_V)\,K_{AE} \qquad (3.2.a)$$

where

$$K_{AE} = \frac{\cos^2(\phi-\Psi-\beta)}{\cos\Psi\,\cos^2\beta\,\cos(\Psi+\beta+\delta)\left[1+\sqrt{\frac{\sin(\phi+\delta)\,\sin(\phi-\Psi-i)}{\cos(i-\beta)\,\cos(\Psi+\beta+\delta)}}\right]^2} \qquad (3.2.b)$$

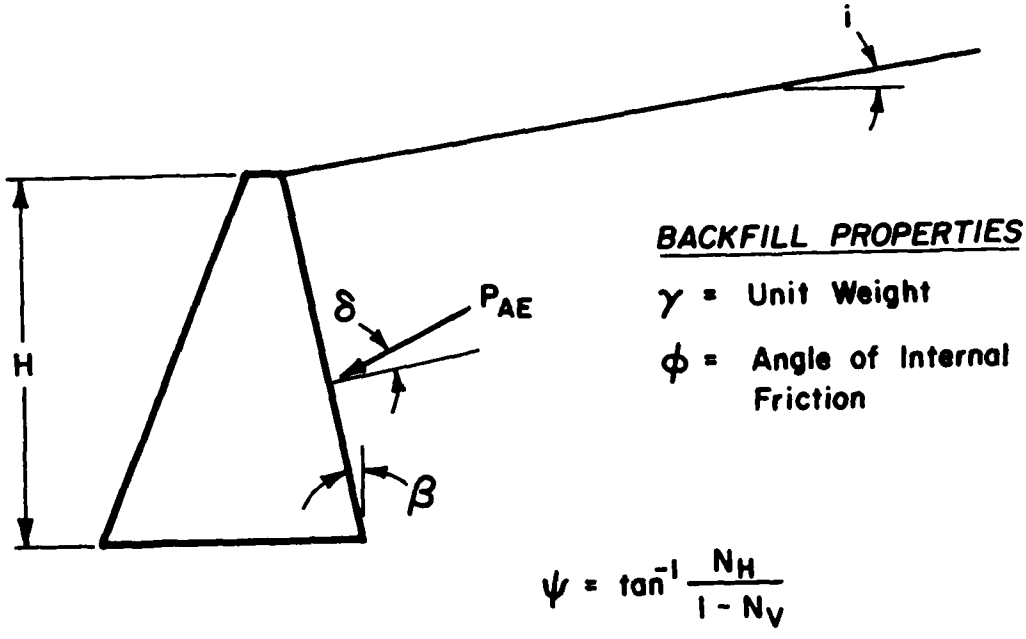

FIG. 3.3 DEFINITION OF PARAMETERS FOR MONONOBE-OKABE EQUATION.

P_{AE} is the combined active static and dynamic thrust, and the other quantities in the equation are:

γ = unit weight of the backfill

H = height of the backfill

ϕ = angle of internal friction of the backfill

δ = angle of friction between the backfill and the wall

β = angle of inclination of the back of the wall (with respect to vertical)

i = angle of inclination of the backfill

The above variables are illustrated in Fig. 3.3. N_V and Ψ are as previously defined (Eqn. 3.1).

Figure 3.4 provides various charts of the quantity K_{AE} or K_{AE} cos δ plotted against the horizontal seismic coefficient N_H. K_{AE} cos δ represents the horizontal component of the dynamic earth pressure. Fig. 3.4 illustrates the sensitivity of the Mononobe-Okabe equation to changes in the various input parameters. Based on the observation that the inclination of the lines in Fig. 3.4 are all approximately at the same slope (of about 3/4) for a relatively wide range of N_H, ϕ, and δ, Seed and Whitman (1970) proposed a useful approximate equation for K_{AE}:

$$K_{AE} \simeq K_A + (3/4)N_H \qquad (3.3)$$

where K_A is the static earth pressure coefficient, determined using appropriate values of ϕ, β, i, and δ.

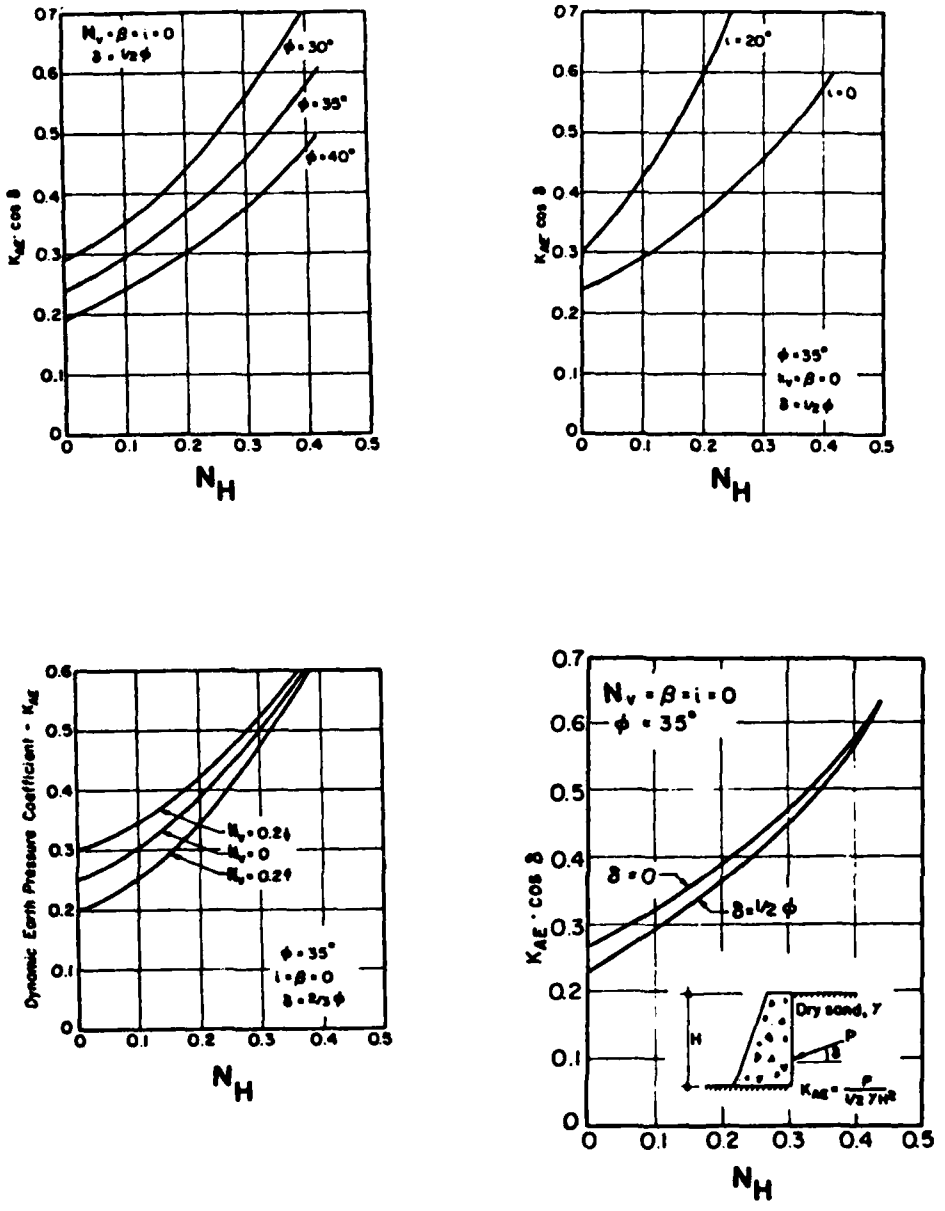

FIG. 3.4 EFFECTS OF CHANGES IN VARIOUS PARAMETERS ON THE DYNAMIC EARTH PRESSURE COEFFICIENT K_{AE} (AFTER SEED AND WHITMAN, 1970).

The location of the total thrust P_{AE} is indeterminate from the Mononobe-Okabe analysis. Usually, it is recommended that the resultant force be located above the lower third point of the wall. Seed and Whitman (1970) suggest that the dynamic component of P_{AE} be placed at the upper third point, with the net result being that the combined dynamic and static thrust P_{AE} would be located at or near mid-height of the wall.

3.2.2 Validity of Mononobe Okobe Equation

The Mononobe-Okobe equation is nothing more than Coulomb's equation for active earth pressure, modified to incorporate a horizontal inertia body force as well as a vertical gravitational body force. Indeed, as discussed previously, Equation 3.2 may be derived simply by starting from Coulomb's equation and tilting the wall and backfill until the resultant of all body forces is vertical (e.g. see Antia, 1982).

Equation 2.1 is subject to all of the same limitations as the static Coulomb equation. Failure lines through the backfill are assumed to be straight, which is an approximation but a good one. Most important is the requirement that there be sufficient strain along the assumed failure line to mobilize the full shearing resistance of the soil in the active sense. That is to say, there must indeed be active conditions. If the full shearing resistance of the backfill is realized throughout the failure wedge, and if the horizontal inertia body force is constant within this wedge, then the static plus dynamic stress between backfill and wall must be distributed linearly with depth. In many cases, these may be

questionable assumptions, the deviation from which would lead to quite different stress patterns.

Other dynamic earth pressure equations have been suggested, usually derived on the assumption that the backfill is linearly elastic with no limitation upon the shear stresses that can occur. A summary of these various solutions is presented by Nadim (1982). Not surprisingly, such equations often predict much larger dynamic thrusts, and a different distribution of lateral stress with depth, than an analysis based upon Coulomb's assumptions.

As described in Chapter 2, various experiments have been performed using shaking tables with the purpose of checking upon the validity of the Mononabe-Okabe equation. In general, the conclusion has been that the observed total dynamic thrusts agree reasonably well with those predicted by the theory. However, many of these tests have not satisfied conditions that permit sliding to occur along a failure plane through the backfill. In addition, the dynamic thrust varies during a cycle of loading, and it is not clear which observed value should be compared to the Mononobe-Okabe value.

Hence it is not surprising that there are experiments showing disagreement with theory, because of experimental conditions that do not simulate the behavior of gravity retaining walls. On the other hand, at least some of the reported experimental confirmation of the Mononobe-Okabe Equation may be only fortuitious.

3.3 DISCUSSION OF THE SEISMIC COEFFICIENT METHOD

3.3.1 Format of Typical Seismic Coefficients

The use of a static equivalent earthquake coefficient is a reasonable approach for the design of gravity retaining walls, provided that neither the backfill nor the foundation soils beneath the wall experiences a dramatic loss of strength (i.e., liquefaction) during earthquake shaking. A key element in this approach is the proper selection of the seismic coefficient to use in the Mononobe-Okabe Equation.

The seismic coefficient method is used for the design of most civil engineering projects. Building codes and other design manuals provide recommended values for this coefficient, which is primarily dependent on the geographical location of the project with respect to regions as defined by seismic zoning maps. In most codes, the coefficient is modified by factors that are dependent on:

- The type of foundation soil profile at the project site
- The type of the structure (e.g. buildings vs. bridges)
- The natural period of the structure
- The importance of the structure (e.g. hospitals vs. warehouses)

The last of these above factors, often referred to as the "importance factor", is an attempt at incorporating a subjective risk/benefit element into the seismic coefficient.

The various maps and recommendations that have been developed are strictly for the horizontal seismic coefficients. Although the general Mononobe-Okabe equation can accommodate both vertical

and horizontal accelerations, the present lack of recommendations for the vertical components of acceleration prevents considering this factor in conventional design. Also, the vertical component of earthquake motion is generally not considered to be of as much significance as the horizontal component.

3.3.2 Comparison of Two Seismic Coefficient Maps

Two examples of seismic coefficient maps of the United States are shown in Figures 3.5 and 3.6. Figure 3.5 is the seismic coefficient zoning map currently used by the U.S. Army Corps of Engineers - USACE (1983), and Fig. 3.6 is from the tentative building code proposed by the Applied Technology Council (ATC-3-06, 1978). Similar maps for the United States are published in the Uniform Building Code (UBC) and in the ANSI regulations.

Comparison of the two maps in Figures 3.5 and 3.6 indicate apparent differences in the delimiting of seismic zones and the magnitudes of seismic coefficients. The ATC maps show coefficients that are double the values shown on the USACE map. However, the USACE coefficients are intended to be applied directly, while the ATC coefficients should be modified using various factors as previously described. For free-standing gravity retaining walls, the current ATC recommendation (Mayes and Sharpe, 1981) is to use $N_H = 1/2\ N_O$, where N_O is the value of the seismic coefficient shown on Fig. 3.6. Thus in the final comparison, the two maps do not conflict as significantly as at first glance. Nevertheless, differences do exist and it should be

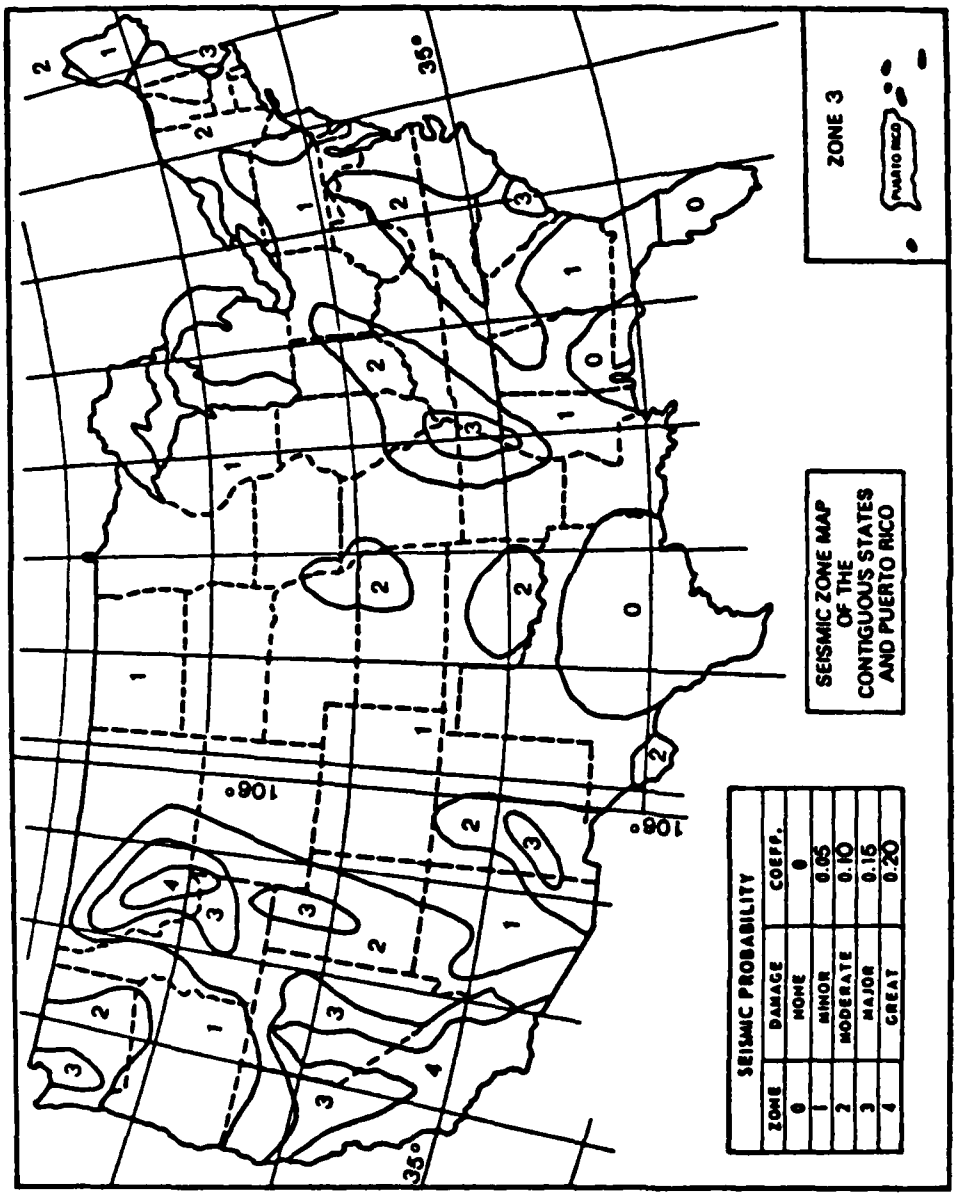

FIG. 3.5 SEISMIC ACCELERATION COEFFICIENT MAP (AFTER USACE, 1983).

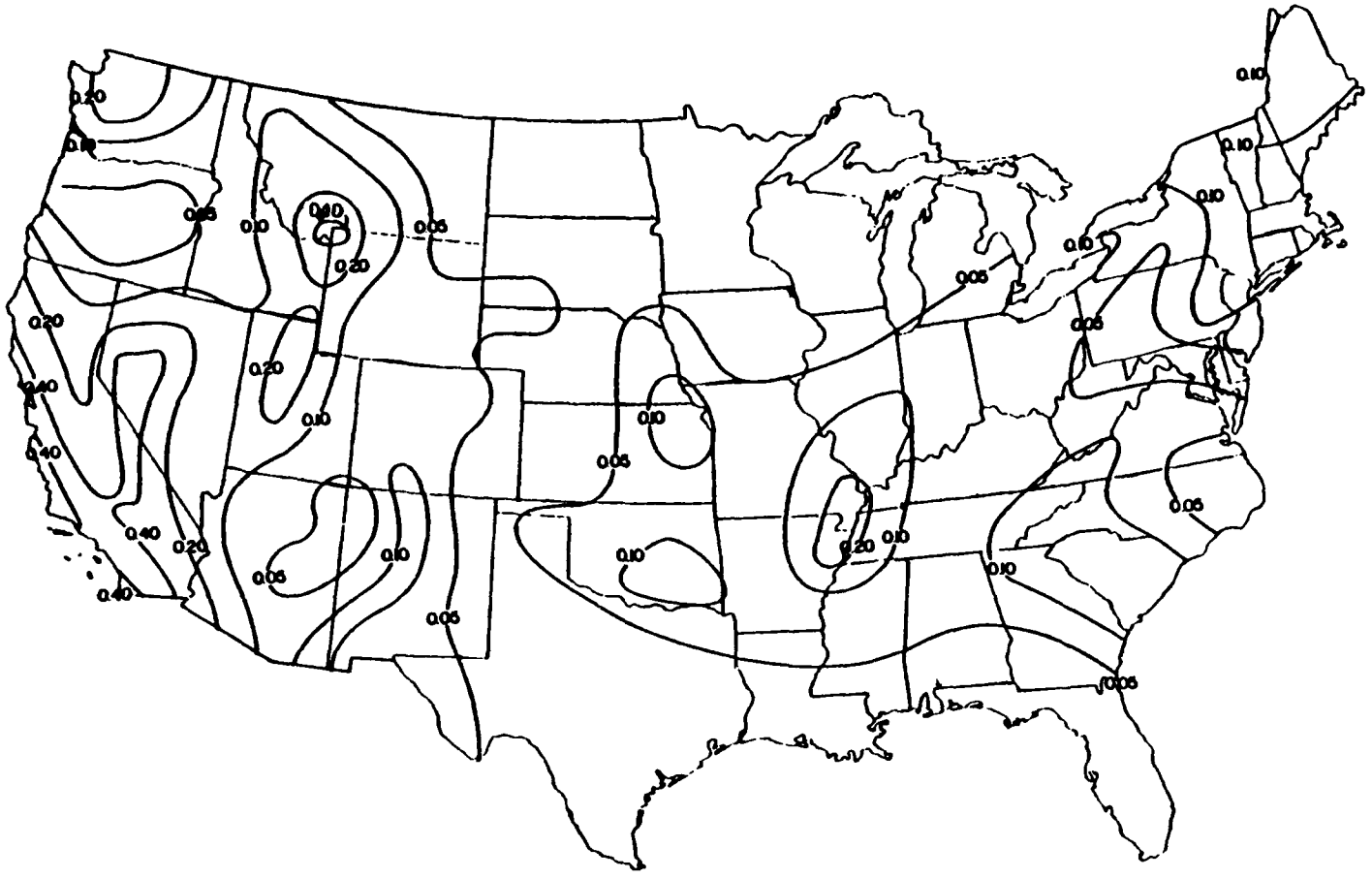

FIG. 3.6 SEISMIC ACCELERATION COEFFICIENT (N_o) - CONTINENTAL UNITED STATES (AFTER ATC-3-06, 1978).

$$N = \frac{\tan\phi_b - \frac{\gamma H^2}{2W_w} K_a}{1 + \frac{3\gamma H^2}{8W_w}} \qquad (4.5)$$

Once $a_T = Ng$ is obtained by solving Eqn. 4.4 or by using the approximate solution of Eqn. 4.5, it is a simple matter to use Eqn. 4.1 to estimate the retaining wall displacement. This computation is illustrated in Example 4.2.

4.4 RICHARDS-ELMS DESIGN PROCEDURE

The design of a gravity retaining wall essentially requires calculating the weight of the wall W_w, given an imposed limit for allowable displacements. This is the inverse problem of solving for displacements discussed in the previous section. The procedure proposed by Richards and Elms is as follows:

1. Decide upon an acceptable maximum displacement d_R.
2. Calculate N using Eqn. 4.1 in the form:

$$N = \left[0.087 \frac{V^2}{Ag} \frac{1}{d_R}\right]^{1/4} A \qquad (4.6)$$

3. Use the Mononobe-Okabe equation (Eqn. 3.2b) to calculate P_{AE}. In doing so, the appropriate values of β, ϕ, δ, and i should be used.

4. Calculate the required weight of the wall using Eqn. 4.4 in the form:

$$T = F_I + (P_{AE})_H \tag{4.2a}$$

Making the appropriate substitutions, we obtain

$$B_N \tan\phi_b = \frac{W_w}{g} \quad a_T + (P_{AE})_H$$

$$[W_w + P_{AE})_V] \tan\phi_b = \frac{W_w}{g} \quad a_T + (P_{AE})_H \tag{4.2c}$$

Solving for a_T:

$$a_T = [\{W_w + (P_{AE})_V\} \tan\phi_b - (P_{AE})_H] \frac{g}{W_w} \tag{4.3}$$

or

$$\text{or} \quad N = \tan\phi_b - \frac{(P_{AE})_H - (P_{AE})_V \tan\phi_b}{W_w} \tag{4.4}$$

Richards and Elms recommend using the Mononobe-Okabe equation (Eqn. 3.2) for evaluating P_{AE}, and hence the above equation cannot, in general, be solved explicitly since P_{AE} is a non-linear function of a_T (or N). Iterative methods or an approximate graphical procedure as illustrated in Example 4.1 can be used to solve the equation. If the Seed-Whitman approximation for P_{AE} (Eqn. 3.3) is used and if $\delta + \beta = 0$, then a simple explicit expression for N <u>can</u> be obtained:

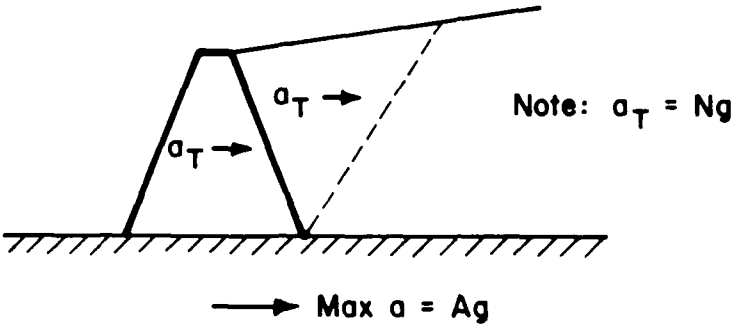

(a) Wall and Backfill Accelerations

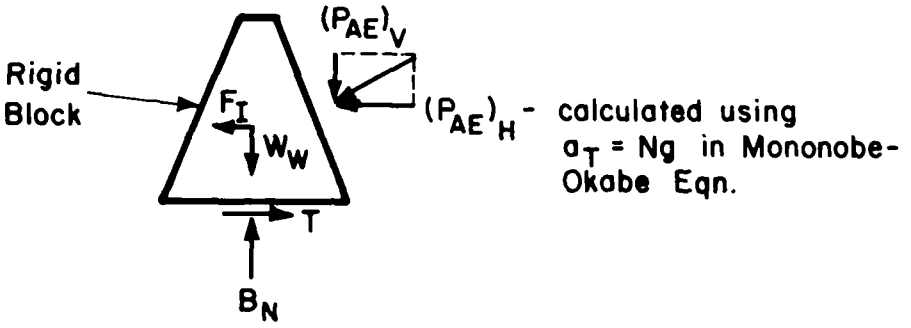

(b) Free Body Diagram of Wall

FIG. 4.5 IDEALIZATION OF THE RETAINING WALL PROBLEM BY RICHARDS AND ELMS (1979).

corresponding displacements would be 0.35 in. and 1.4 in.

Based on these results, Richards and Elms proposed an alternate and very convenient equation for calculating the block displacements d_R in the medium to low range of N/A (the range of interest in design) as:

$$d_R = 0.087 \frac{V^2}{Ag} \left(\frac{N}{A}\right)^{-4} \tag{4.1}$$

where N and A are previously defined and V is the maximum ground velocity. This equation is also plotted in Fig. 4.4 for comparison with the data and with Newmark's curves.

4.3 EVALUATING RETAINING WALL DISPLACEMENTS

Although Eqn. 4.1 is based on the results of a sliding block model originally intended for use in predicting movements of dams and embankments, it can be easily applied to predict retaining wall movements. The only difference in application arises from a slightly more complicated evaluation of the limiting acceleration $a_T = Ng$. For a block on a horizontal plane, N is simply equal to $\tan\phi_b$. However, additional vertical and horizontal earth pressure forces, respectively denoted as $(P_{AE})_V = P_{AE} \sin(\delta + \beta)$ and $(P_{AE})_H = \cos(\delta + \beta)$ and shown in Fig. 4.5, must be considered in the equilibrium equations for the retaining wall.

Summing forces in the horizontal direction, using the free body diagram in Fig. 4.5(b) and imposing the requirements of equilibrium:

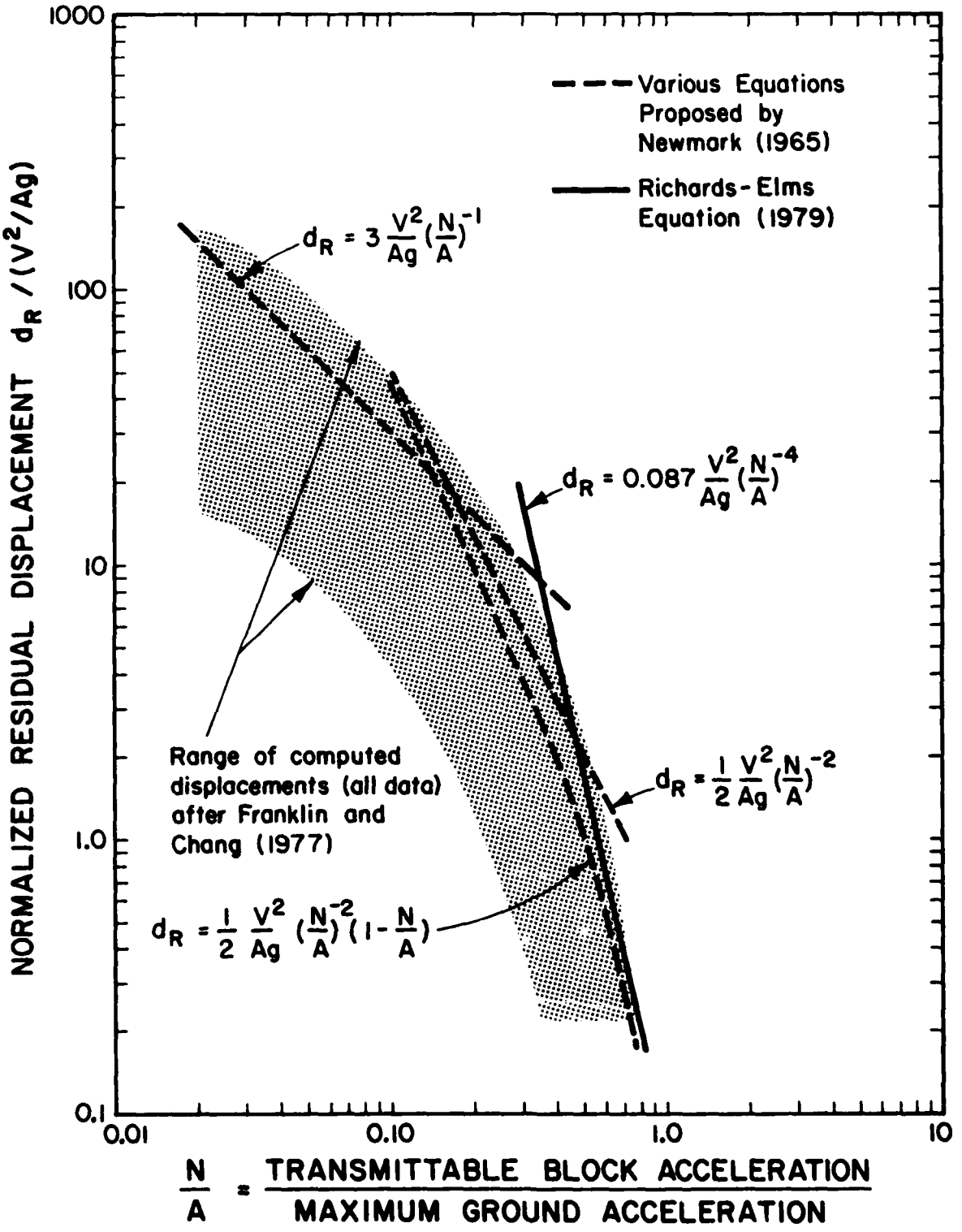

FIG. 4.4 RANGE OF NORMALIZED DISPLACEMENTS USING NEWMARK SLIDING BLOCK MODEL, AND VARIOUS EQUATIONS APPROXIMATING THE UPPER ENVELOPE.

shown were obtained using several strong motion records from the San Fernando earthquake. Note that there is considerable scatter in the calculated displacement for each factor of N/A, as a result of differing characteristics of the various earthquake records.

The data in Fig. 4.3 were plotted using a "standardized" displacement scale, obtained by scaling the earthquake inputs to a maximum acceleration Ag = 0.5g and a maximum velocity V = 30 in/sec. These same data can be replotted using a normalized dimensionless displacement scale by dividing the calculated displacements by V^2/Ag. Figure 4.4 shows such a plot with the ranges of normalized displacements from all earthquakes used by Franklin and Chang in their analyses. Also shown are several expressions suggested by Newmark giving conservative estimates for the residual displacements, each most applicable for a different range of N/A. Note that while these expressions are not true upper bounds, they do form nearly an upper envelope for most of the computed points.

To illustrate the implications of these results, the quantity V^2/Ag typically ranges from 1 in. (for moderate earthquake with a peak acceleration of 0.2g) to 4 in. (for a major earthquake with a peak acceleration of 0.6g). In many problems of interest the value N/A ranges from 0.3 to 0.7. At N/A = 0.3, the normalized residual displacement falls in the range from 0.4 to 10.0 so that displacements during a moderate earthquake would be from 0.4 to 10 inches, while those in a major shaking would range from 1.6 in. to 40 in. At N/A = 0.7, the upper envelope value of normalized displacement is 0.35, so that for minor and major earthquakes, the

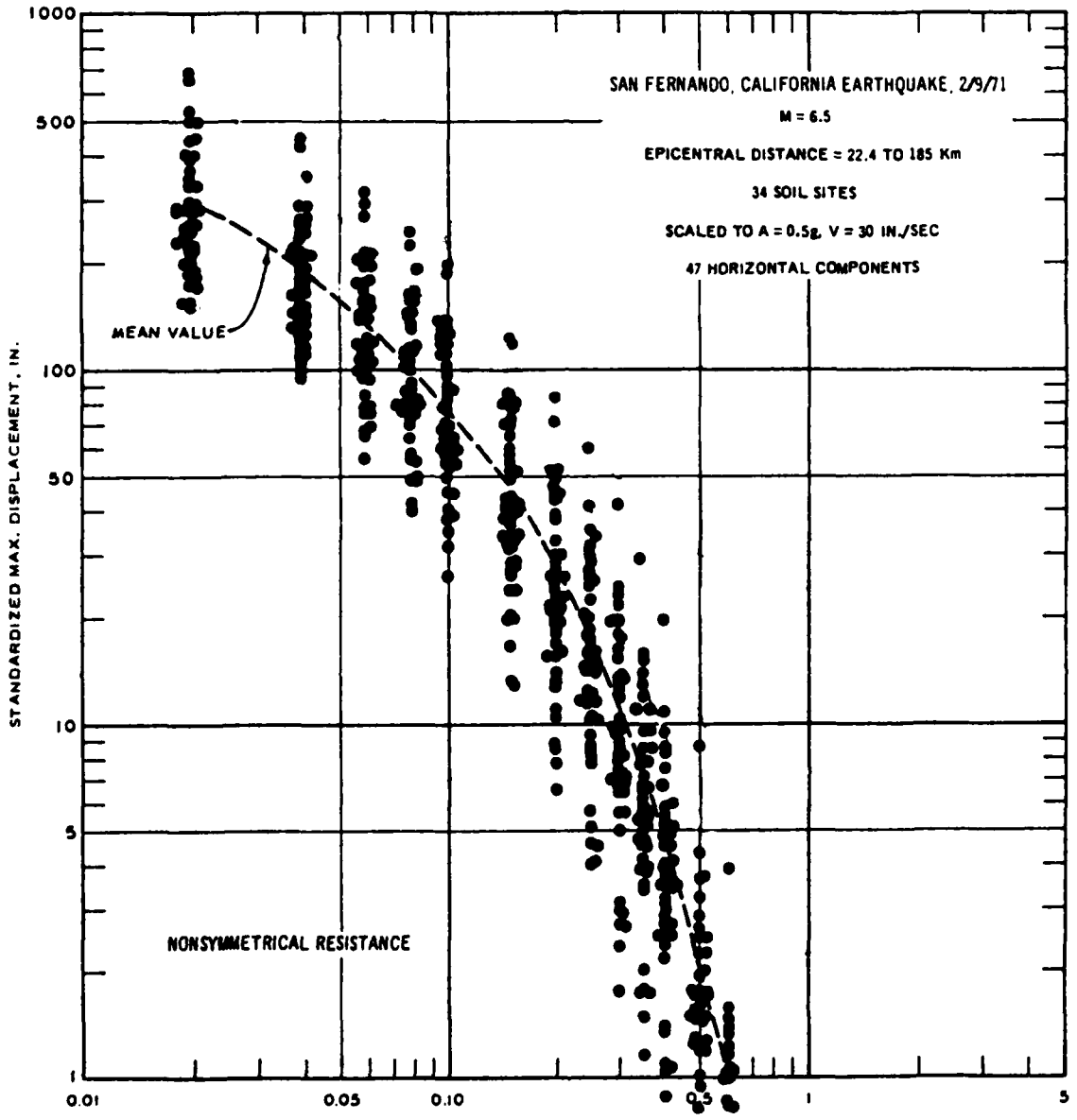

$$\frac{N}{A} = \frac{\text{Transmittable Block Acceleration}}{\text{Maximum Ground Acceleration}}$$

FIG. 4.3 EXAMPLE OF RESULTS USING NEWMARK SLIDING BLOCK MODEL (AFTER FRANKLIN AND CHANG, 1977).

transmitted to the block through friction forces is $a_T = Ng$ where the subscript 'T' denotes the transmittable horizontal or limiting acceleration. Then the consequent acceleration experienced by the block is shown by the dashed lines in Fig. 4.2(a).

The resulting velocity profile as a function of time can be deduced as shown in Fig. 4.2(b). The plane's velocity increases linearly at a slope Ag and levels off at time t_o, the end of the rectangular input pulse. However, the block continues to accelerate until its velocity catches up to the velocity of the plane (at time t_m) and this limits the time interval of the acceleration impulse experienced by the block. The resulting relative displacement between the block and the plane is simply the shaded area shown in Fig. 4.2(b), i.e. the difference in the integrals of plane and block velocities over time.

The basic concepts described above can be applied to more complex earthquake acceleration time histories, using a relatively simple computer program. An additional feature that must be included is the non-symmetric resistance of friction forces, i.e., slip occurs only in one direction. This is consistent with the physical behavior of retaining walls in that passive pressures are generally more than sufficient to resist wall movements into the backfill during earthquake shaking.

An example of the type of results obtained by Newmark (1965) and later expanded by Franklin and Chang (1977) is shown in Fig. 4.3. This figure is a plot of standardized residual block displacements d_R versus the ratio of transmittable block acceleration to maximum ground acceleration $a_T/a = N/A$. The data

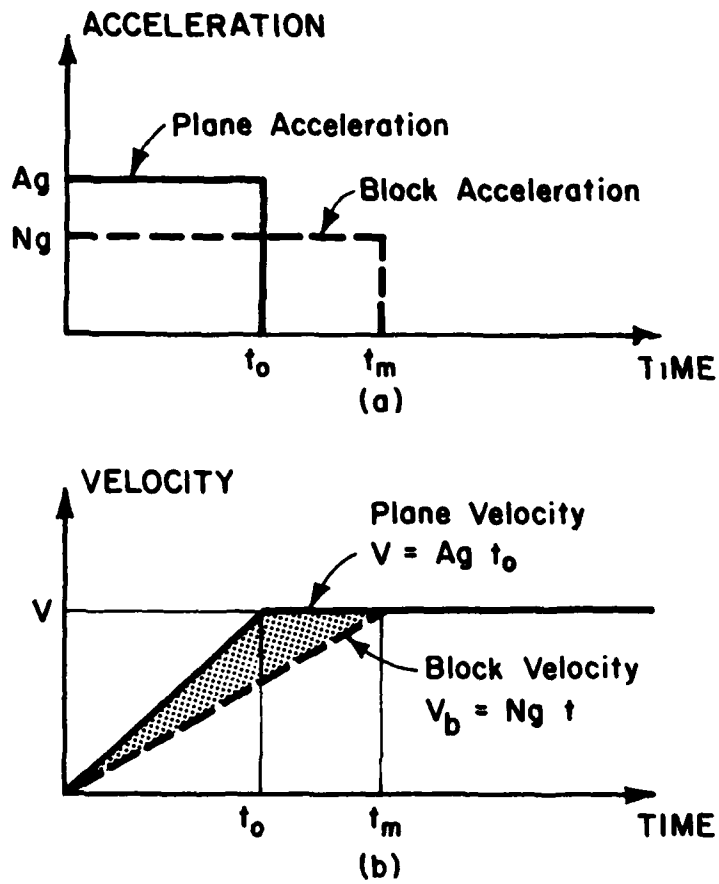

FIG. 4.2 ACCELERATION AND VELOCITY PROFILES OF BLOCK AND PLANE SUBJECTED TO A RECTANGULAR PULSE EXCITATION.

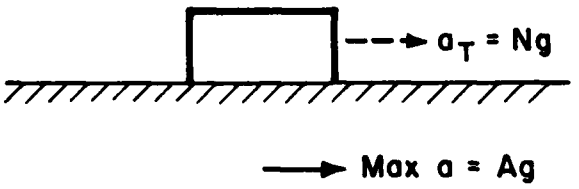

(a) Notation for Block and Plane Accelerations

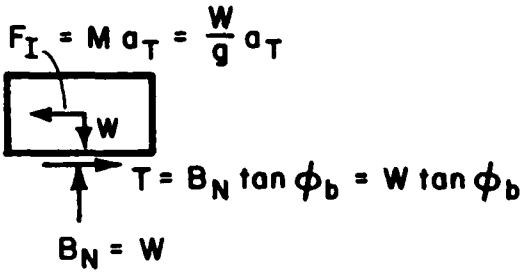

F_I = Inertia Force

W = Weight

B_N = Base Normal Force

T = Shear Force

(b) Free Body Diagram of Block

FIG. 4.1 NOTATION AND FORCES FOR SLIDING BLOCK ON A PLANE.

4 - RICHARDS-ELMS METHOD

4.1 GENERAL

Recognizing the shortcomings of the conventional approach for seismic design of gravity retaining walls, Richards and Elms (1979) developed a design philosophy based on the concept of an allowable permanent displacement. In the end, the design of a wall is still accomplished using an equivalent static seismic coefficient, but with a more rational basis for the selection of this coefficient.

The key to the Richards-Elms approach is the method of calculating the amount of residual wall movement. The approach is similar to the method suggested by Newmark (1965) to evaluate the amount of slip occurring in dams and embankments during earthquakes. The Newmak sliding block model is discussed in the next section, which is also intended to introduce notation and to set the stage for discussions of more complex models for evaluating retaining wall displacements.

4.2 NEWMARK'S SLIDING BLOCK MODEL

Consider the rigid block shown in Fig. 4.1 with weight W and mass M = W/g, where g is the gravitational constant. It is assumed that the coefficient of friction between the block and the plane is $\mu = \tan\phi_b$. Suppose that a rectangular earthquake impulse (solid lines) shown in Fig. 4.2(a) is applied to the plane. The magnitude of the plane's acceleration a is equal to Ag. Suppose also, that the maximum acceleration which can be

3.3.5 CONCLUSION ON SEISMIC COEFFICIENTS

The conclusion that is arrived at from the above discussion is that there <u>are</u> rational ways to select and use the conventional seismic coefficient in design. However, the emphasis of design should not concentrate on the evaluation of equilibrium of forces, but rather on the evaluation of the retaining wall slip that should be allowed to occur during a major earthquake. In a recent document issued by the USACE, it is stated that:

> "... the seismic coefficient method, often referred to as the pseudo-static method, is no longer regarded as being appropriate for analysis of embankment or foundation response in seismic loading. Therefore its use for this purpose should be discontinued."
>
> (USACE, 1983)

The above statement should equally apply to gravity retaining walls.

much higher than the seismic coefficient. Thus, it is recognized that buildings designed using these recommended coefficients can be expected to yield, should a major earthquake occur. However, these designs are such that the yielding should not cause unacceptable damage or danger of injuries and fatalities.

The implication for gravity retaining walls designed using a seismic coefficient method is that slip of the of the wall will likely occur during major earthquakes. This is especially true in light of the fact that relatively low factors of safety are usually recommended in conjunction with seismic design. The design manual used by the Naval Facilities Engineering Command (NAVFAC, 1982) DM-7.2 currently allows a factor of safety between 1.1 and 1.2 for seismic analysis, and for quay walls in Japan the recommended factor of safety against sliding is 1.0 (JSCE, 1977). Although the USACE does not have specific factor of safety guidelines for retaining walls (USACE, 1965), it is inferred from the guidelines for dams (USACE, 1970) that a factor of safety of 1.0 would be acceptable in earthquake design.

An alternative to designing retaining walls using the seismic coefficient would be to instead use the peak ground acceleration expected for a future earthquake. However, this practice is considered to be generally uneconomical if the inertia force of the wall is considered in the design. It has also been suggested that the horizontal earth pressure P_{AE} be evaluated using the peak ground acceleration and that the inertia of the wall be ignored. However, this is an illogical procedure and cannot consistently lead to sound designs.

noted that for walls which are restrained from horizontal movement, $N_H = 1.5\ N_O$ is recommended by the ATC code.

3.3.3 Judgement in Formulation and Use

The recommended seismic coefficients in the various codes and manuals are derived partly from theory and partly from experience data during actual earthquakes. Considerable judgement is necessary to formulate the zoning maps and to determine suitable values of seismic coefficients. Thus it is not surprising that the differences in various codes and manuals should occur, and also that updating of the values of the seismic coefficients occur from time to time.

It is also important to note that the intended use of the various recommendations may significantly affect seismic coefficient values. For example, the USACE maps were originally formulated primarily for use in designing earth dams, which make up a significant part of the USACE's constructed projects. Thus, applying the USACE coefficients to other structures should be done cautiously. In Japan, a similar situation exists with seismic coefficients and maps differing for port and harbour structures, roadways, buildings, etc. (JSCE, 1977).

3.3.4 Seismic Coefficients and Safety Factors

Seismic coefficients typically have lower values than the peak ground accelerations that have occurred during earthquakes. In designing buildings, it is expected that the peak accelerations (due to amplification of ground motion in the structure) could be

$$W_w = \frac{(P_{AE})_H - (P_{AE})_V \tan\phi_b}{\tan\phi_b - N} \qquad (4.7)$$

5. Apply a factor of safety of 1.5 to the wall weight W_w.

A design problem, using the above procedure, is illustrated in Example 4.3.

4.5 COMMENTS ON THE RICHARDS-ELMS METHOD

The Richards-Elms procedure is rational and simple to apply. It is, in effect, a counterpart of a procedure used for buildings (Newmark and Hall, 1982) where the ratio of design seismic coefficient is chosen on the basis of the ductility ratio (of expected strain to yield strain) that a structure possesses before there is extreme structural damage or danger of collapse. Its major disadvantages are that it does not consider certain kinematic restrictions upon retaining wall behavior, the deformability of the backfill or possible tilting, and the statistical variability of earthquake ground motions. In a fashion, these factors have been taken into account in the factor of safety of 1.5 on the wall weight, which is somewhat conservative compared to usual values of recommended safety factors ranging from 1.0 to 1.2, as discussed in Section 3.3. However, it is not clear that there is a rational basis for the suggested safety factor of 1.5 on wall weight.

The remainder of this report will consider some of the deficiencies in the Richards-Elms procedure, and will suggest improvements and corrections, while retaining the essential simplicity and soundness of the basic approach.

EXAMPLE 4.1

Given: Retaining wall and backfill with properties shown in Figure E4.1.

Find: The maximum transmittable acceleration N, using the Richards-Elms method.

Solution: The weight of wall W_w is calculated to be 32.81 K/ft. From Eq. 3.2a, $P_{AE} = (1/2)(0.120)(25)^2 K_{AE} = 37.5 K_{AE}$ K/ft. Assuming values of N, values for ψ and K_{AE} are calculated from Eqs. 3.1 and 3.2b. A new value of N is then computed from Eq. 4.4. Results of these computations appear in Table E4.1 and are graphed in Fig. E4.2. The answer is given by the intersection of a curve through the computed points and a line through the origin at 45°.

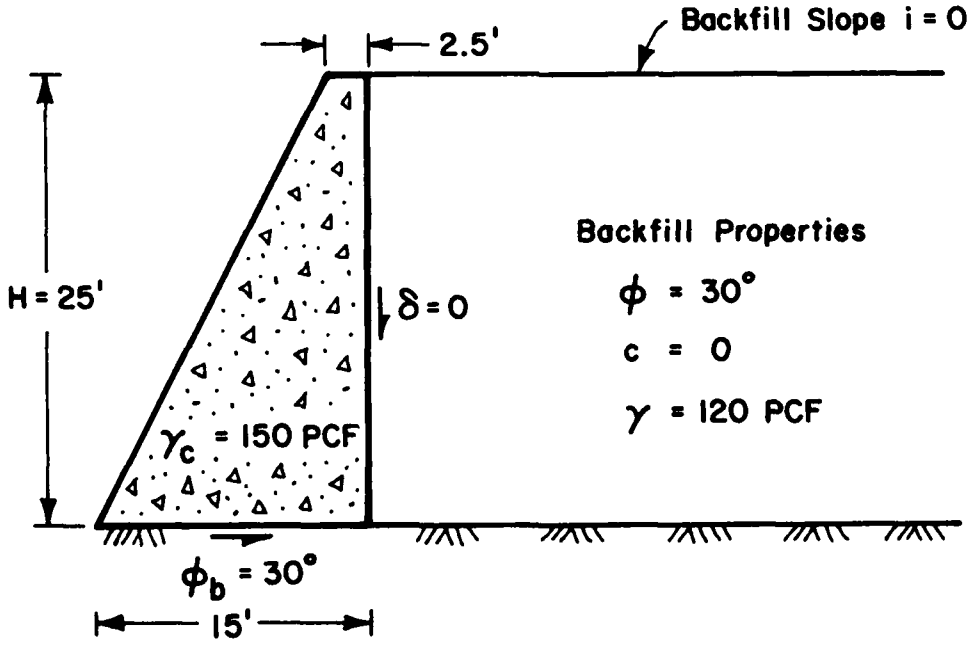

FIG. E4.1

EXAMPLE 4.1 (continued)

Table E4.1

ASSUMED N	ψ	$(K_{AE})_H$	COMPUTED N
0.05	2.86°	0.364	0.161
0.10	5.71°	0.397	0.123
0.15	8.57°	0.433	0.082
0.20	11.31°	0.473	0.036

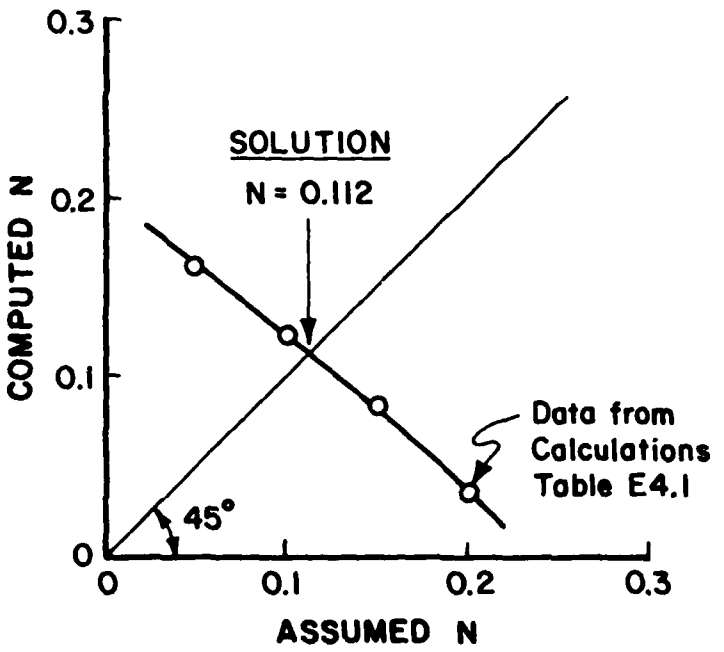

FIGURE E4.2

For comparison, N is also computed using Eq. 4.5, yielding

N = 0.106

EXAMPLE 4.2

Given: The wall in Example 4.1.

Find: The permanent displacement caused by an earthquake characterized by A = 0.3 g's and V = 15 in/s, using the Richards-Elms approach.

Solution: From Eq. 4.1:

$$d_R = 0.087 \frac{15^2}{0.3(386)} \left(\frac{0.112}{0.3}\right)^{-4}$$

$$= 0.087\ (1.94)(51.48)$$

$$= 8.7 \text{ in.}$$

EXAMPLE 4.3

Given: The backfill and frictional resistance properties in Example 4.1.

Find: For a wall 25 feet high, the required weight of wall if an earthquake with A = 0.3 g's and V = 15 in/s is to cause a permanent displacement of 1 inch, according to the Richards-Elms approach.

Solution:

Step 1 - d_R = 1 inch

Step 2 - From Eq. 4.6, N = 0.192

Step 3 - Eq. 3.1 gives $\psi = 10.89°$

- Eq. 3.2b yields $K_{AE} = 0.467$

- Eq. 3.2a gives $P_{AE} = 17.51$ K/ft.

Step 4 - From Eq. 4.7, $W_w = 45.44$ K/ft.

Step 5 - Applying a safety factor of 1.5 to computed W_w:

Required weight of wall = 68.2 K/ft.

5 - KINEMATIC CONSTRAINTS UPON MOTION OF BACKFILL

5.1 THE TWO BLOCK MODEL

In the Richards-Elms model, the retaining wall is modelled as a single sliding block on a plane, when in fact the actual behavior is much more complex. A more realistic model is the two-block model developed by Zarrabi (1979), which is shown schematically in Fig. 5.1. In this model the wall is represented as a block on a horizontal plane, and the wedge of soil (behind the wall) that "fails" during sliding is represented by another rigid block on an inclined plane.

The kinematic constraints on the two-block model are that during sliding, contact force and acceleration continuity must be maintained between the two blocks themselves, and between each of the blocks and their respective sliding planes. This gives rise to three equations of acceleration continuity that must be satisfied simultaneously with the equations of equilibrium.

The most significant constraint in terms of the mechanics of the problem is that of maintaining contact between the sliding soil wedge and the inclined plane. For outward movement of the wall to occur, there must be a simultaneous outward and downward movement of the soil wedge. Thus, even when there is no vertical ground acceleration, the backfill wedge would still experience vertical accelerations.

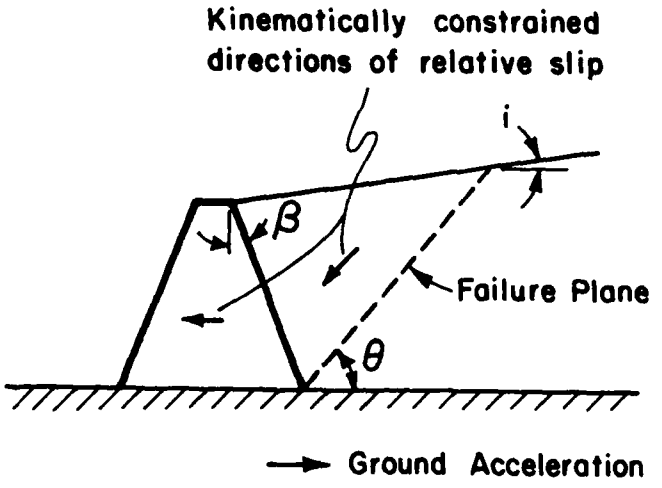

(a) Actual Physical Situation

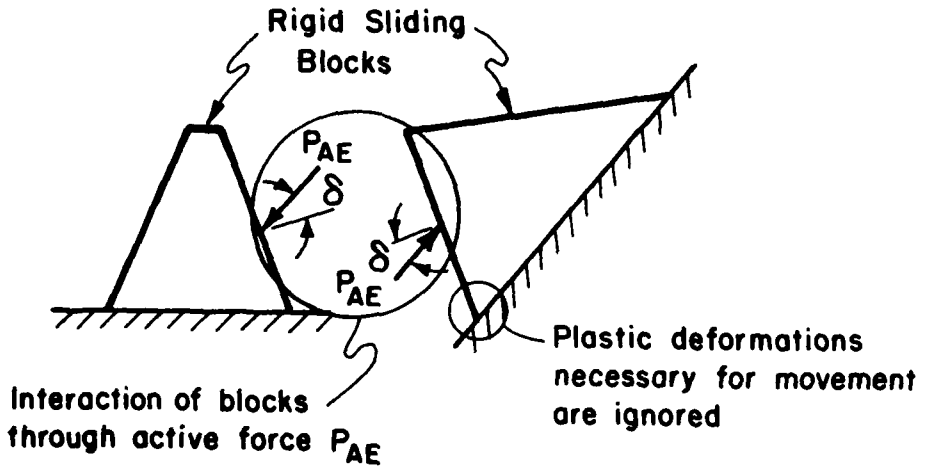

(b) Two Block Model Idealization by Zarrabi

FIG. 5.1 SCHEMATIC OF IDEALIZATION OF RETAINING WALL PROBLEM BY ZARRABI (1979).

5.2 COMPARISON WITH SINGLE-BLOCK MODEL

Vertical accelerations in the backfill wedge affect the active earth pressure P_{AE} between the wall and the soil. This is reflected by the Ψ term and the factor $(1-N_V)$ in the Mononobe Equation (Eqn. 3.2). It can be shown that for continuity of acceleration normal to the failure plane at any instant in time, the following equation must hold:

$$N_V(t) = A_V(t) + [A_H(t) - N_H(t)] \tan [\theta(t)] \qquad (5.1\text{-a})$$

or

$$N_H(t) = A_H(t) + [A_V(t) - N_V(t)] \cot [\theta(t)] \qquad (5.2\text{-b})$$

where $A_H(t)$ is the horizontal ground acceleration coefficient.

$A_V(t)$ is the vertical ground acceleration coefficient.

$N_H(t)$ is the transmittable horizontal acceleration coefficient of the wall and soil wedge.

$N_V(t)$ is the transmittable vertical acceleration coefficient of the soil wedge.

$\theta(t)$ is the angle of inclination of the failure plane with respect to horizontal (see Figure 5.1).

The notation (t) indicates the above quantities to be variable with time. Thus, the transmittable acceleration at any instant in time is dependent upon the ground acceleration at the same time. This is in sharp contrast to the single-block model proposed by Richards and Elms where the transmittable acceleration is constant with time.

A schematic comparison of the sliding processes of the Zarrabi (two-block) and Richards-Elms (single-block) models is shown in Fig. 5.2. In the two-block model there is a threshold,

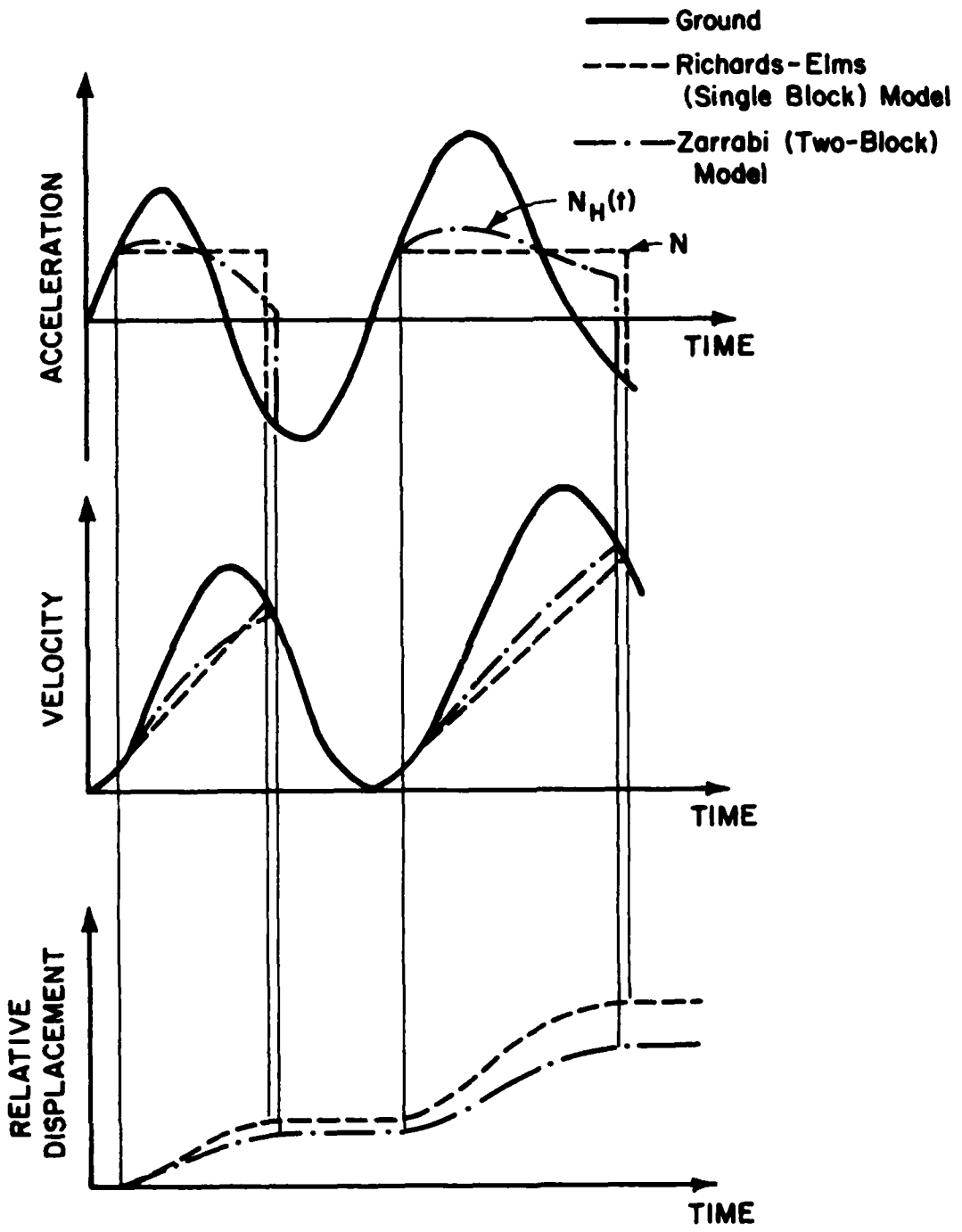

FIG. 5.2 SCHEMATIC COMPARISON OF SLIDING PROCESSES OF THE RICHARD-ELMS (R-E) AND ZARRABI MODELS.

acceleration N_T required to initiate slip. Provided that comparable assumptions are made concerning the properties of the backfill, the value of N_T is exactly the same as the value of N used for the Richards-Elms procedure. However, after initiation of slip, the limiting acceleration N_H at any time during a cycle of slip can be greater or less than $N_T g$.

As a result, the active thrust P_{AE} is also changing during sliding. An illustration of how this physically occurs is shown in Fig. 5.3 for the case where there is no vertical ground acceleration ($A_V = 0$). When the ground acceleration $A_H g$ exceeds the transmittable acceleration $N_H g$ [Fig. 5.3(a)], the vertical backfill wedge acceleration $N_V g$ is in the downward direction. Hence, the inertia force is in the opposite upward direction, effectively causing a decrease in the weight of the soil and a subsequent decrease in P_{AE}. The reverse occurs during the later stages of slip when $A_H g < N_H g$ as shown in Fig. 5.3(b)

The equations applicable to the evaluation of residual slip in the two-block model was developed by Zarrabi (1979). The solution procedure for these equations is fairly complicated in that during slip, the value of N_H must be evaluated at every time-step. Also, since θ is a function of N_H and N_V, the solution for N_H must be obtained iteratively. Wong (1982) subsequently developed a more efficient scheme, in which part of the solution to the governing equations is precomputed and stored in computer memory, thus requiring fewer iterations. Alternatively, it might be assumed that θ remains fixed in which case the Mononabe-Okabe equation no longer applies and the basic equations for dynamic

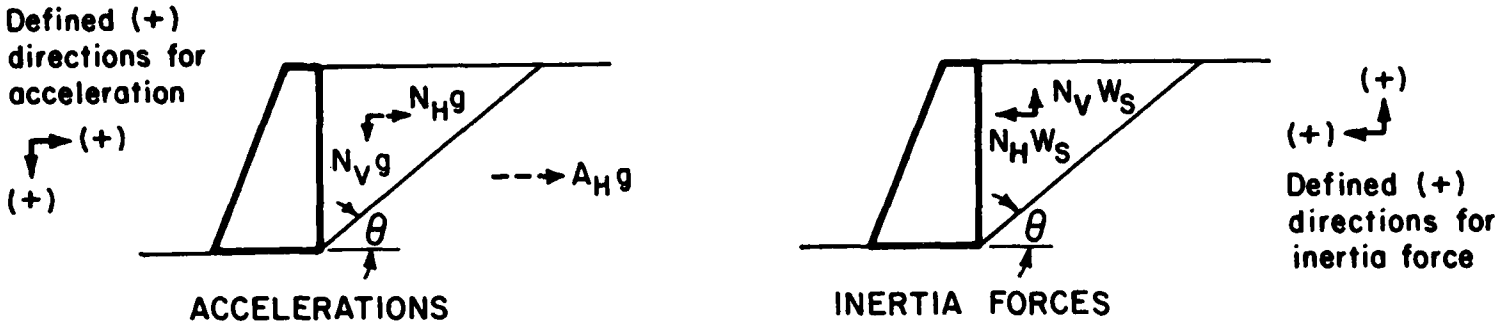

(a) $A_H > N_H \Longrightarrow$ Smaller P_{AE}

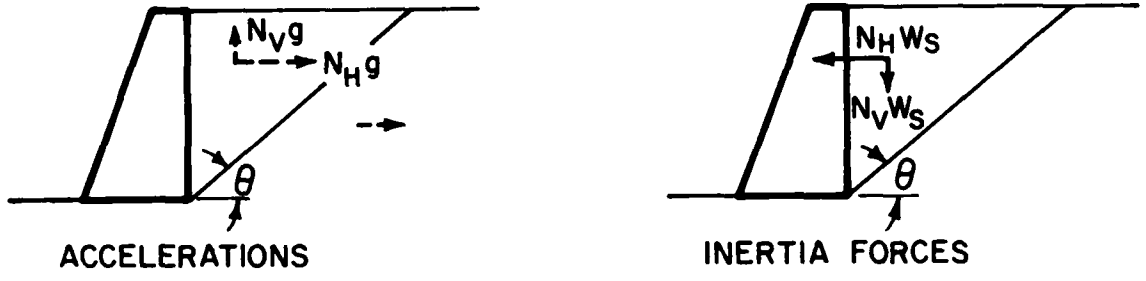

(b) $A_H < N_H \Longrightarrow$ Larger P_{AE}

FIG. 5.3 ILLUSTRATION OF DIRECTIONS OF BACKFILL ACCELERATIONS AND INERTIA FORCES DURING SLIP.

equilibrium and continuity are solved simultaneously at each time step.

There is one other feature of Zarrabi's two-block model that deserves mention at this point. This is the implicit non-symmetrical resistance of two-block model, so that unlike the Richards-Elms/Newmark model, no explicit assumptions regarding the non-symmetrical nature of the sliding block resistance are necessary.

5.3 NUMERICAL RESULTS

The net result of the kinematic constraints in the two-block model is that the calculated residual displacements are smaller than those using the single-block model. This is illustrated in Fig. 5.4, which shows the ratio $R_{2/1}$ plotted against N/A (for the single-block model) or N_T/A (for the two-block model), where $R_{2/1}$ is defined as:

$$R_{2/1} = \frac{\hat{d}_R}{d_R} = \frac{\text{Residual displacement of two-block model}}{\text{Residual displacement of single-block model}}$$

Note also that the values of A, N and N_T, as used here, are not functions of time, but are constants depending on the earthquake record or the wall/backfill properties.

The results shown in Fig. 5.4 are based on limited results using the average values of residual displacement calculated using four earthquakes (Antia, 1982). The unit weight of the soil, the wall height and the height of the wall are properties that can be collectively described by the value of N_T. However, the soil and

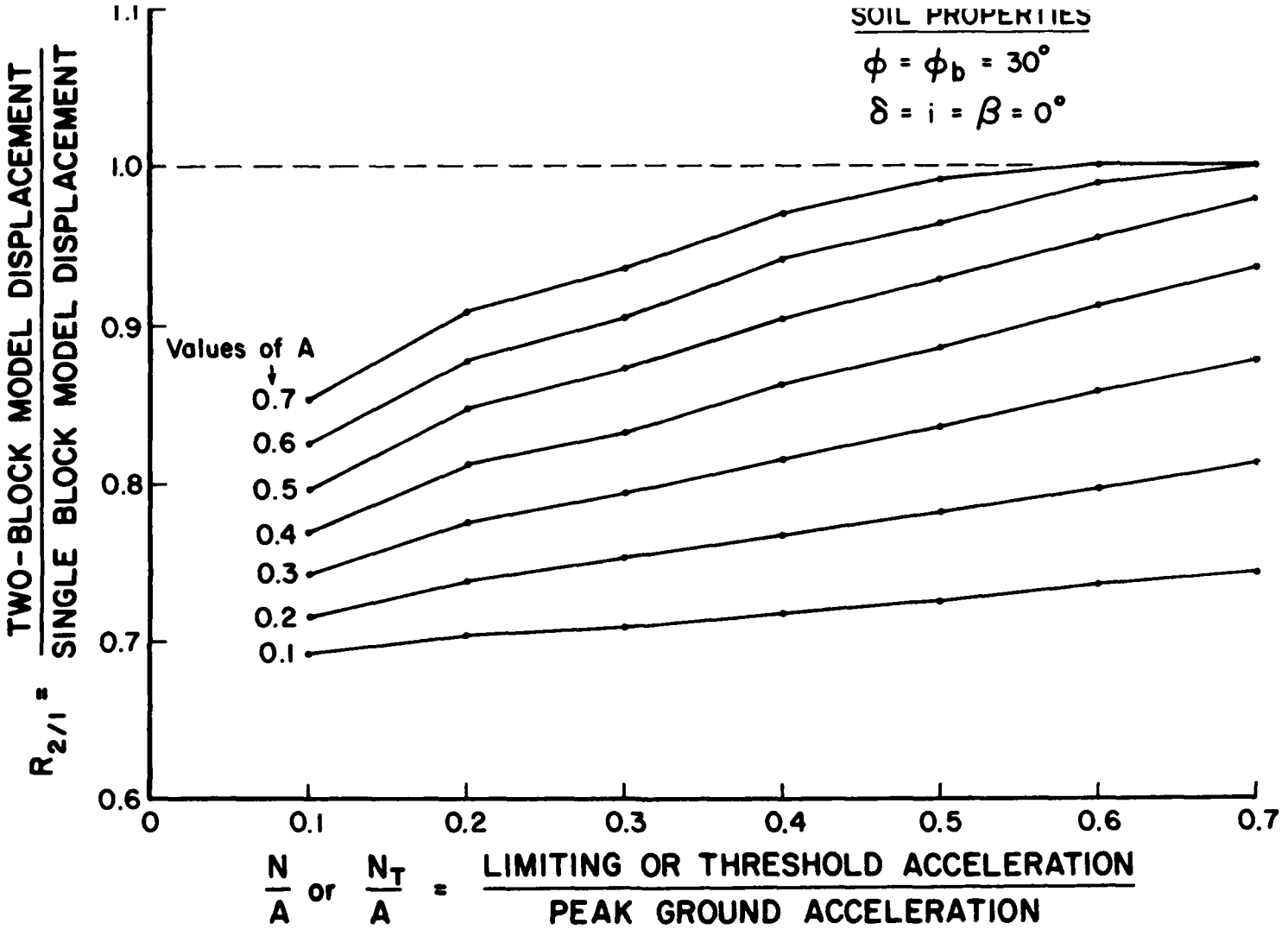

FIG. 5.4 COMPARISON OF TWO-BLOCK AND SINGLE BLOCK MODEL RESULTS AS A FUNCTION OF N/A OR N_T/A (AFTER ANTIA, 1982).

backfill properties cannot be as easily incorporated in a single parameter,and the results shown in Fig. 5.4 are only for a typical case which might be encountered in practice ($\phi = \phi_b = 30^\circ$; $\delta = i = \beta = 0$).

It is seen from Fig. 5.4 that the differences between the two models (smallest $R_{2/1}$) are greatest for small values of N/A and/or for small values of A. An explanation for this trend is that as either N or A increases, the angle of the failure plane $\theta(t)$ becomes generally smaller (flatter). Hence, $N_v(t)$ which is directly related to tan $[\theta(t)]$ becomes smaller (Eqn. 5.1-a), so that the vertical acceleration and its effects are reduced. In the limit, as A or N becomes large (roughly corresponding to Ψ becoming large), the angle $\theta(t)$ would be nearly zero (horizontal), and hence no vertical backfill motions would result from purely horizontal ground motions.

The reason for the ratio $R_{2/1}$ being consistently less than one is not completely clear at the present. It would be not unreasonable to envision that although $N_H(t)$ and hence P_{AE} vary with time during slip, that on the average, the results of the two-block model should be same as the single-block model. Intuitively, however, the mere fact of adding "constraints" to a model implies a restriction of otherwise freer motions. Another intuitive notion, from a work-energy viewpoint, is that the two-block model has more energy-dissipating mechanisms than the single-block model. Whereas in the single-block model, the earthquake energy causing motion can only be dissipated through friction forces at the base of the wall, the two-block model has

The goodness of fit is shown in Fig. 6.3; for N/A between 0.1 and 0.7, the value predicted by this equation is within 10% of the computed $\bar{d}_{Re}$ (within 5% for N/A $\geq$ 0.4). This expression does not, as it ideally should, go to zero as N/A approaches unity although it predicts insignificant values in that range.

The scatter of the record means $\bar{d}_{Ro}$ is indicated by the coefficients of variation in the second line of Table 6.1, which are statistics for the random variable $F_s = \bar{d}_{Ro}/\bar{d}_{Re}$. For intermediate values of N/A, the uncertainty from record to record is about the same as for differently oriented walls during any one shaking. At larger N/A, the orientation effect has much greater uncertainty.

Again, all these results were developed using only the horizontal components of recorded ground motions.

6.5 EFFECT OF VERTICAL ACCELERATIONS

Downward acceleration of the plane supporting a block will decrease the normal force at the interface, thus decreasing the transmittable acceleration and increasing the tendency to slip. Conversely, upward acceleration increases resistance to slip. In a ground motion with many peaks of acceleration causing slip, the effects of the vertical component of ground motion may be expected to cancel. Hence the vertical component of ground motion has generally been ignored when computing sliding block displacements.

The actual effect of vertical ground accelerations has been studied using the suite of 14 earthquake records described above. For each computation, the vertical component of acceleration was

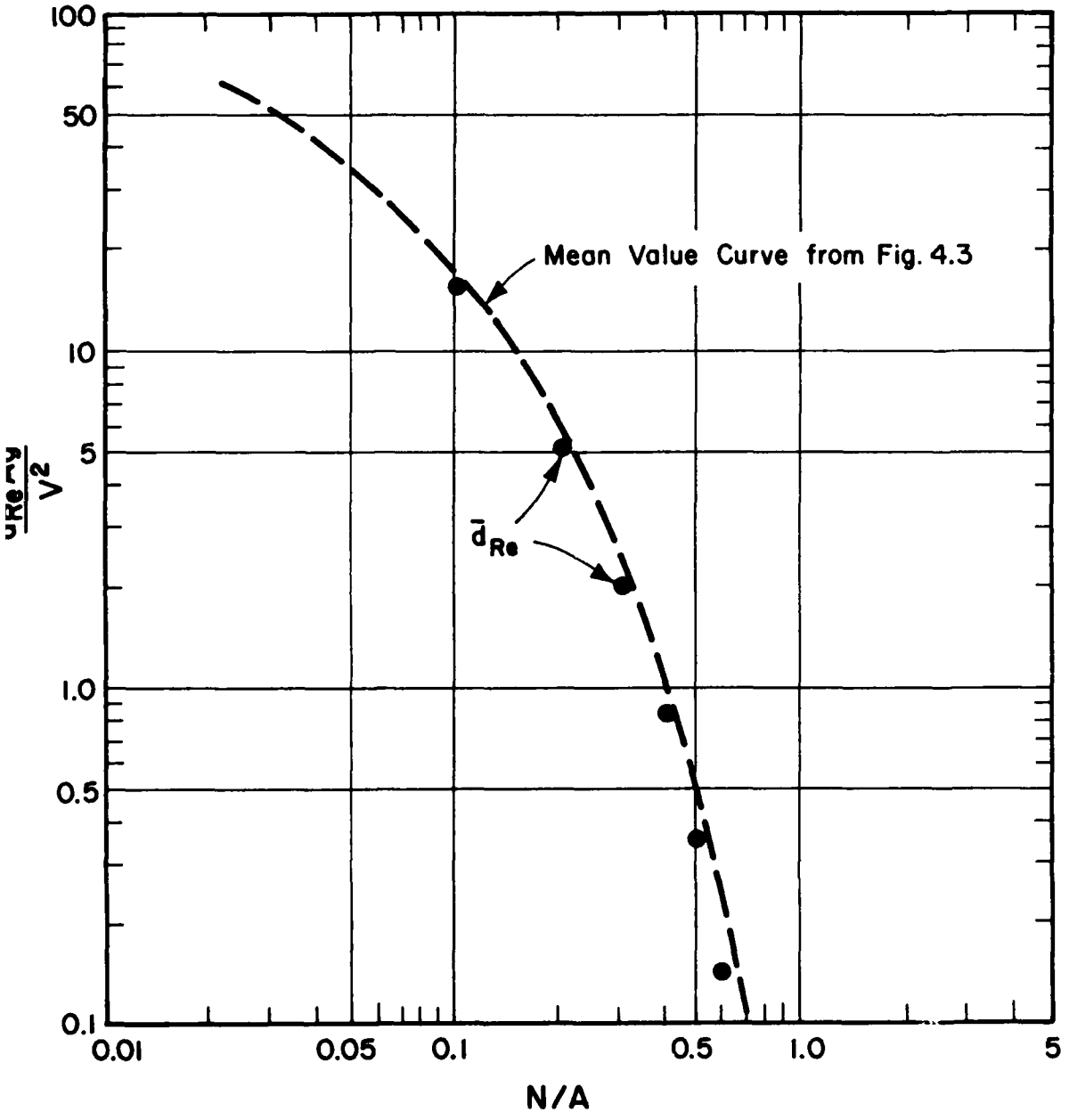

FIG. 6.2 MEAN DISPLACEMENTS FROM THIS STUDY COMPARED WITH THOSE FROM FRANKLIN AND CHANG (1977).

exponential with a spike at the origin. For N/A of 0.4 and 0.5, it is somewhat similar to a log-normal distribution.

All of these results were computed using only the horizontal components of the recorded ground motions.

6.4 SCATTER AMONG DIFFERENT SITES AND EVENTS

The next step was to examine the record means $\bar{d}_{Ro}$. For each selected N/A, each of these fourteen values was first normalized to a common peak acceleration and peak velocity using V^2/Ag scaling. (As previously discussed, A is the largest absolute acceleration from both components of a record, and V is the peak absolute velocity from the component containing that acceleration.) Then the 14 normalized values of $\bar{d}_{Ro}$ were averaged to obtain the overall mean displacement $\bar{d}_{Re}$; that is:

$$\bar{d}_{Re} = \text{Ave } [\bar{d}_{Ro}] \tag{6.1}$$

The scatter of the record means about the overall means was also analyzed.

The overall mean displacements, in normalized form, are plotted as a function of N/A in Fig. 6.2. As a result of the scaling scheme used in Wong's analysis, these results fall below the average curve from Fig. 4.3. A simple expression which provides an approximate fit to the mean slips is:

$$\bar{d}_{Re} = \frac{37V^2}{Ag} e^{-9.4N/A} \tag{6.2}$$

Table 6.1

COEFFICIENTS OF VARIATION ARISING FROM UNCERTAIN ASPECTS OF GROUND MOTION

COMPONENT OF UNCERTAINTY		N/A						
		0.1	0.2	0.3	0.4	0.5	0.6	0.7
ORIENTATION OF WALL AT A SITE		0.32	0.42	0.51	0.64	0.86	1.12	1.30
EARTHQUAKE TO EARTHQUAKE		0.53	0.54	0.58	0.58	0.56	0.50	0.41
VERTICAL ACCELERATION	A							
	0.2	↑	↑	<0.05	0.05	0.07	0.15	0.12
	0.3	↑	↑	<0.05	0.07	0.13	0.22	0.27
	0.4	<0.05	<0.05	0.05	0.10	0.18	0.30	0.37
	0.5	↓	↓	0.06	0.12	0.25	0.37	0.57
	0.6	↓	↓	0.07	0.15	0.33	0.44	0.66
	0.7			0.08	0.19	0.42	0.51	0.73

6.3 ORIENTATION EFFECTS

For a complete analysis of this effect, it would be desirable to compute, from the two observed components of each record, the time histories of motions in many directions. However, only the two recorded components have been used in this study to evaluate four possible permanent displacements.

Four values of permanent slip d_{Re} were computed from each of the 14 records for values of N/A from Ø.2 to Ø.7, with no normalization of the records and ignoring vertical accelerations. For each of the records, an average $\bar{d}_{Ro}$ was determined (used for the analysis in Section 6.4), plus four values of the ratio $E_o = d_{Re}/\bar{d}_{Ro}$. Thus for each N/A, 56 values of E_o were obtained. The mean of E_o is, by definition, unity. The coefficients of variation are listed on the first line of Table 6.1.

It may be seen that the scatter in the ratio E_o increases as N/A increases. This occurs because, at the larger N/A, one or more component-directions may not cause any permanent slip. For example, at N/A = Ø.7 the 1940 El Centro record causes no slip in the east-west direction, and very little for a wall oriented so that it can slip to the south. Overall, of the 56 computed slips, 17 are zero for N/A = Ø.7, eight are zero for N/A = Ø.6, and 2 are zero for N/A = Ø.5. Numerous other values are so small as to be essentially zero.

Because of the tendency for an increasing number of zero values as N/A increases, the distribution of E_o changes as N/A changes. For N/A = Ø.1, the distribution was found to be approximately normal. For N/A = Ø.7, it is more nearly

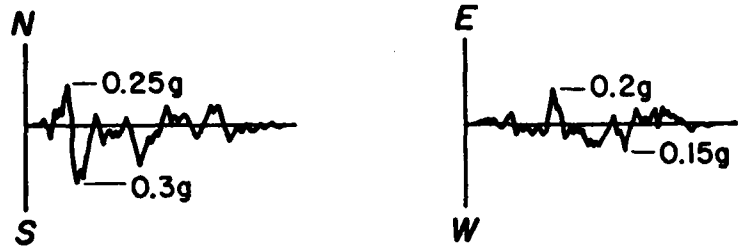

(a) Example N-S and E-W Components of an Earthquake

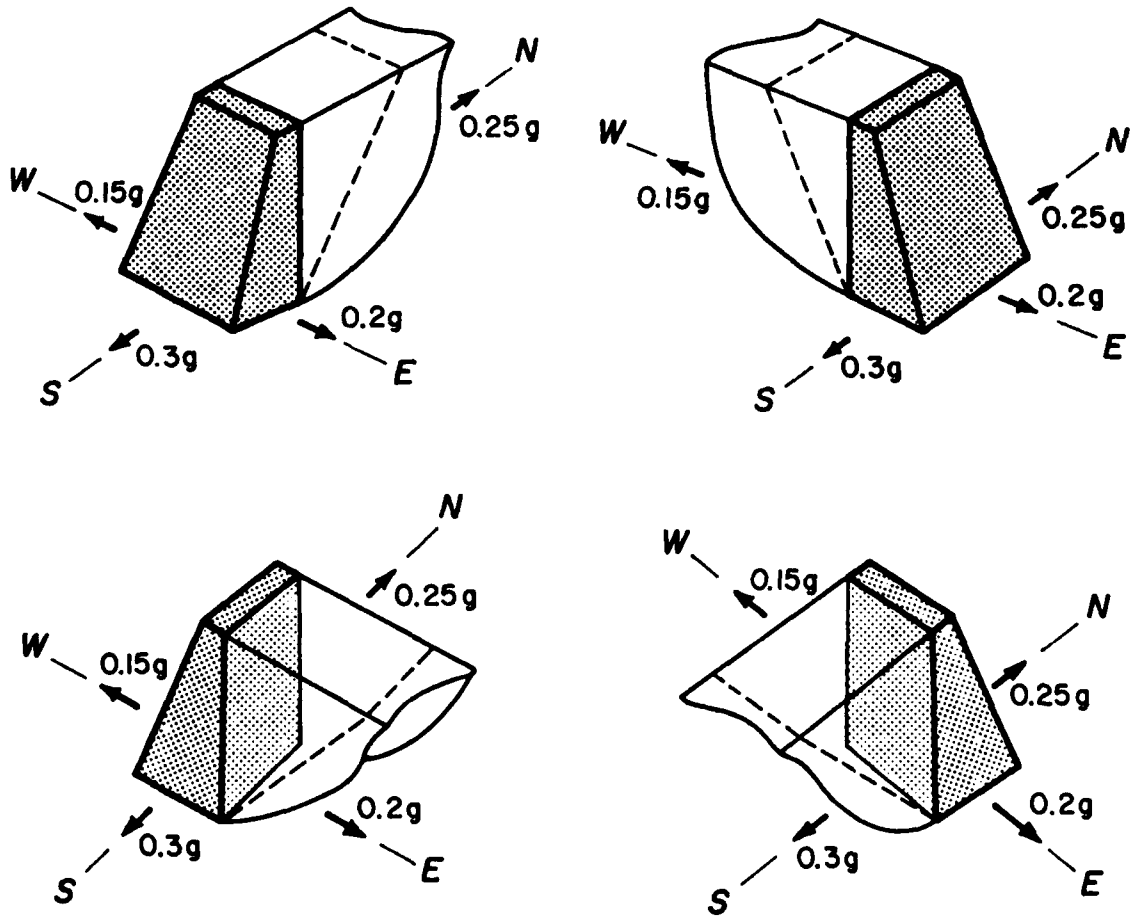

(b) Different Orientations of Retaining Wall with respect to Earthquake Components

FIG. 6.1 EFFECTS OF RETAINING WALL ORIENTATION.

tions are different in the positive and negative sense of each component.

An important implication is that the permanent slip experienced by a retaining wall during an earthquake will depend upon the orientation of the wall. For example, the four retaining walls shown in Fig. 6.1 would be expected to experience differing amounts of permanent displacement during any one earthquake. Indeed, some walls might have permanent displacement while the others would not yield at all. This is an important aspect of uncertainty in the prediction of the motion which may be experienced by any particular wall.

In previous work, it has been usual practice to normalize a component of a record to the maximum acceleration and velocity in that component. However, this procedure tends to obscure the orientation effect just described. In the study by Wong, one acceleration - the largest absolute acceleration from either of the components - was used to normalize both components. This was done because the earthquake motion recorded at a site is always characterized by this largest absolute acceleration, and this number would always be used when judging whether or not a wall (or any other structure) located at the site lived up to expectations.

The choice of a velocity to characterize the ground motions at a site is less obvious. For this study, use has been made of the largest absolute velocity in the component containing the largest peak acceleration. This choice is consistent with past practice and should lead to the least confusion concerning interpretation of results.

characterized by having peak accelerations greater than Ø.15 g resulting from earthquakes with magnitudes between 6.3 and 7.7. (Actually, all but 2 records are for magnitudes between 6.3 and 6.7). The restriction on peak acceleration was imposed so that all records would be typical of those which might cause significant displacement of actual retaining walls, and distortion would not be introduced by scaling of weak motions. The limitation upon magnitude was used to narrow the range of durations of earthquake shaking, which roughly correlates with magnitude. Ideally a similar study should be performed using other sets of records corresponding to smaller and larger magnitudes, but as yet this has not been done.

Analysis of scatter in sliding arising from differences in ground motions has been divided into three parts. First there are the differences in sliding associated with the several components of motion at one location during one earthquake. Second there are the differences from site to site and earthquake to earthquake. Finally there is the effect of the vertical component of ground motion. In the end, the influences of these three effects will be lumped together. However, considering them separately will provide an understanding of the relative importance of the several effects.

6.2 SCALING OF RECORDS

A typical ground motion record has two horizontal components. As a matter of course, the peak accelerations (and velocities) are different for the two components. Moreover, the peak accelera-

6 - RANDOM NATURE OF GROUND MOTIONS

6.1 INTRODUCTION

This is the first of three chapters dealing with uncertainty in the prediction of the residual displacement for a gravity retaining wall. As discussed in the introduction, such uncertainty arises because of differences in the details of ground motions, because of doubts as to the actual resistance of a wall to sliding, and because of errors in the models used to predict residual displacement for a given ground motion and given resistance parameters.

This chapter deals with the consequences of the essentially random nature of ground motions. As discussed in connection with Fig. 4.3, different ground motions each normalized to the same peak acceleration and velocity can produce quite different amounts of sliding for the same N/A. These differences are associated with differing frequency contents, differing distributions of peaks and differing directions of shaking. Because the prediction procedure ultimately recommended in this report uses the simple sliding block model, these various effects are studied using that model. Thus the results potentially apply to all problems for which the sliding block model provides a reasonable prediction of permanent displacement or deformation including certain earth slope movements in earthquakes as well as retaining walls.

The analysis here uses results from a study of the mean and distribution of sliding caused by a suite of normalized ground motion records (Wong, 1982). This study utilized a relatively small set of records - 14 in number and listed in Appendix A -

5.5 SUMMARY

The use of a single-block model analogy by Richards and Elms (1979) tends to overestimate the residual slip of a retaining wall due to earthquake shaking. Zarrabi's model, using the concept of two interacting blocks, provides a better estimate of the actual slip, as confirmed by model tests on a shaking table.

An important issue mentioned briefly in this chapter involves whether it is valid to assume a failure plane inclination θ which varies with the instantaneous ground acceleration. This and other issues regarding how changes in other parameters (ϕ, ϕ_b, i, β and δ) affect the results, are treated in Chapter 8.

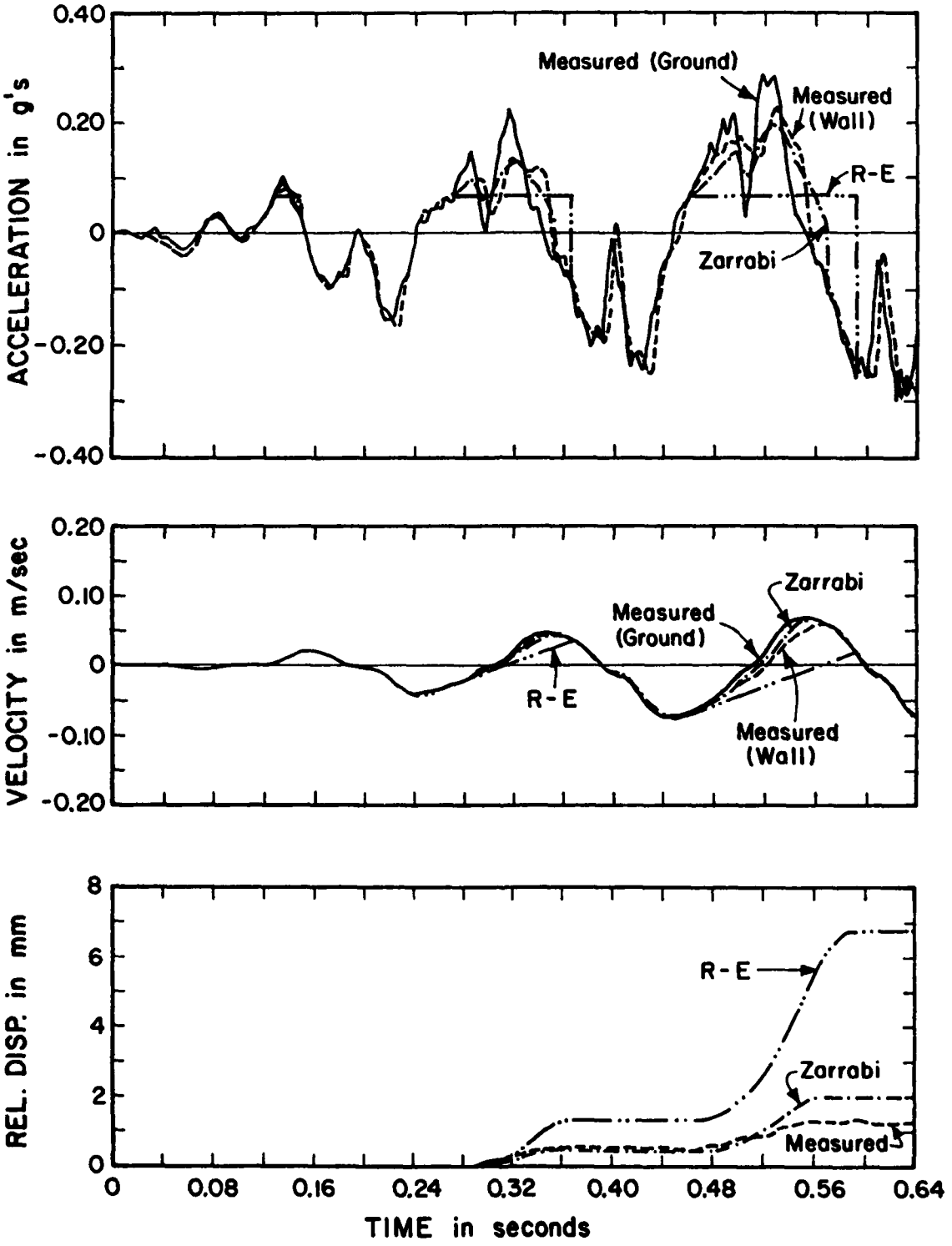

FIG. 5.6 COMPARISON OF RICHARDS-ELMS (R-E) AND ZARRABI SLIDING BLOCK MODELS WITH EXPERIMENTAL RESULTS (FROM JACOBSEN, 1980)(SEE CHAPTER 2 FOR DETAILS OF EXPERIMENTS, WHICH WERE PERFORMED BY LAI, 1979).

experimental results obtained by Lai (1979). These experiments were previously described in Chapter 2.

A typical comparison of theory and experiment is shown in Fig. 5.6. As can be seen, the Zarrabi two-block model is a better simulation of the time histories of acceleration, velocity, and relative displacement. Clearly, the limiting acceleration is not constant as predicted by the single block model. Also noted by Jacobsen was the fact that the two-block model predictions are in better agreement during the beginning of the shaking as compared to the latter part of the shaking. It is conjectured that this is in part due to the physical constraint that the toe of the soil block has to undergo some plastic deformation in order to slide with the wall. The rigid two-block model inherently assumed this effect to be negligible.

An important point with regard to the comparisons made by Jacobsen, is that the calculations he performed should be recognized as "Class C" predictions, i.e. predictions after the fact. In particular, Jacobsen used the angle of inclination θ of the failure plane obtained from the experimental results as input to the computuer simulation models. As opposed to Zarrabi's procedure where θ varied with acceleration, Jacobsen chose instead to use a fixed θ (measured in the model) and found that this gave better agreement with the experimental results.

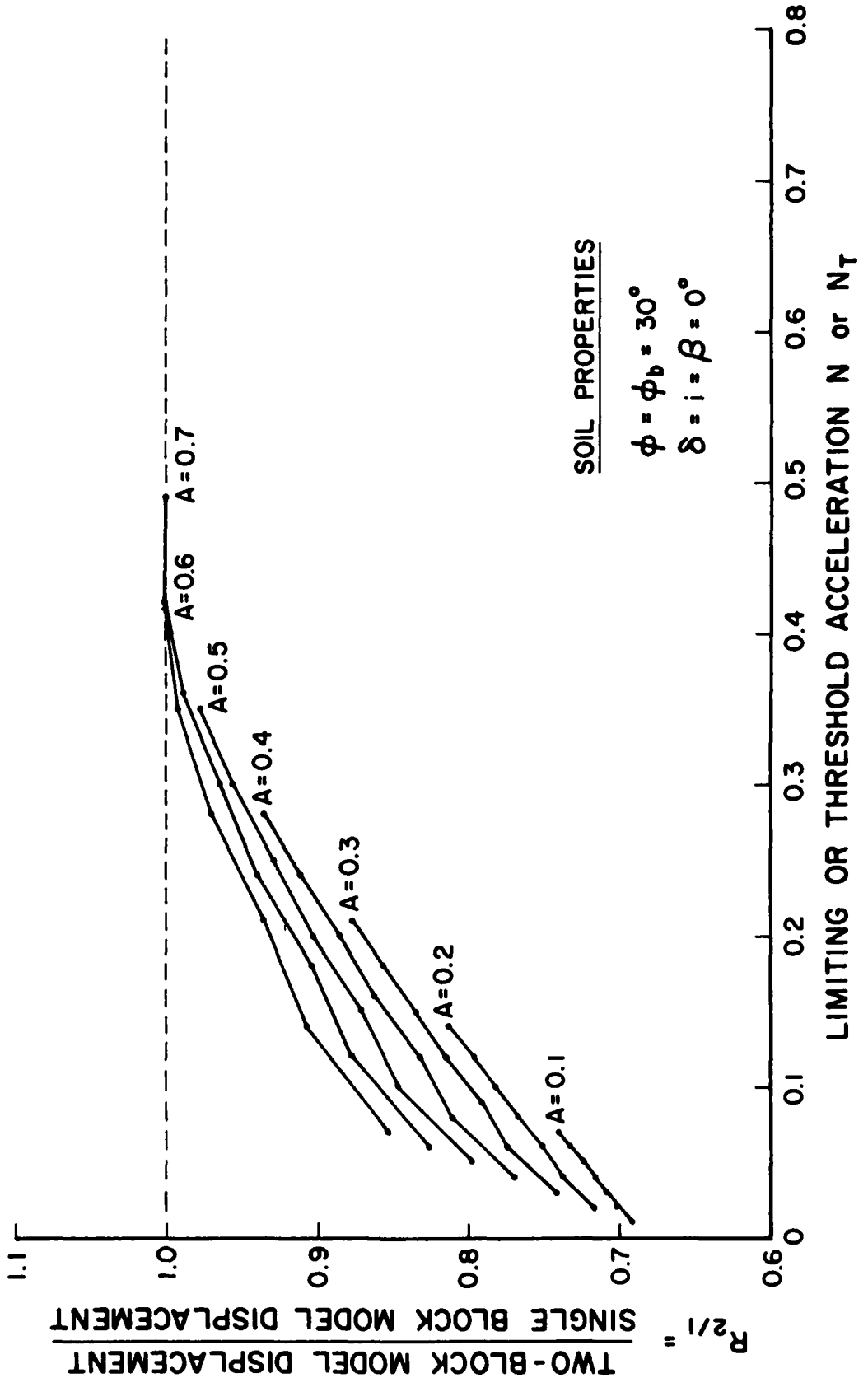

FIG. 5.5 COMPARIONS OF TWO-BLOCK AND SINGLE BLOCK MODEL RESULTS AS A FUNCTION OF N OR N_T (AFTER ANTIA, 1982).

at least an additional frictional energy dissipation surface through the failure plane in the backfill. Though these explanations are intuitively plausible, they would need to be justified rigorously by further research.

Another important observation from the results shown in Fig. 5.4 is that it is not possible to normalize the residual displacements of the two-block model by dividing by V^2/Ag as was the case for the single-block model. If it were possible, then

$$R_{2/1} = \frac{\hat{d}_R}{d_R} \qquad \frac{\hat{d}_{R/(V^2/AG)}}{d_{R/(V^2/Ag)}} \tag{5.3}$$

should only be a function of N/A or N_T/A. Since it is known that $d_R/(V^2/Ag)$ is only a function of N/A (see Section 2.4), but that $R_{2/1}$ depends on A, it can only be concluded that $\hat{d}_R/(V^2/Ag)$ is not solely a function of N/A, and hence cannot be normalized.

However, as a practical matter in design considerations, the results of Fig. 5.4 can be replotted as shown in Fig. 5.5, where the horizontal axis has values of N or N_T instead of N/A or N_T/A. This scheme condenses the values of $R_{2/1}$ to a narrower band of data, minimizing the influence of A. Wong (1982) has suggested that $R_{2/1}$ can be approximated for design purposes as solely a function of N.

5.4 COMPARISON WITH EXPERIMENTAL RESULTS

Jacobsen (1980) performed a detailed comparison of the Richards-Elms single-block and Zarrabi two-block models with

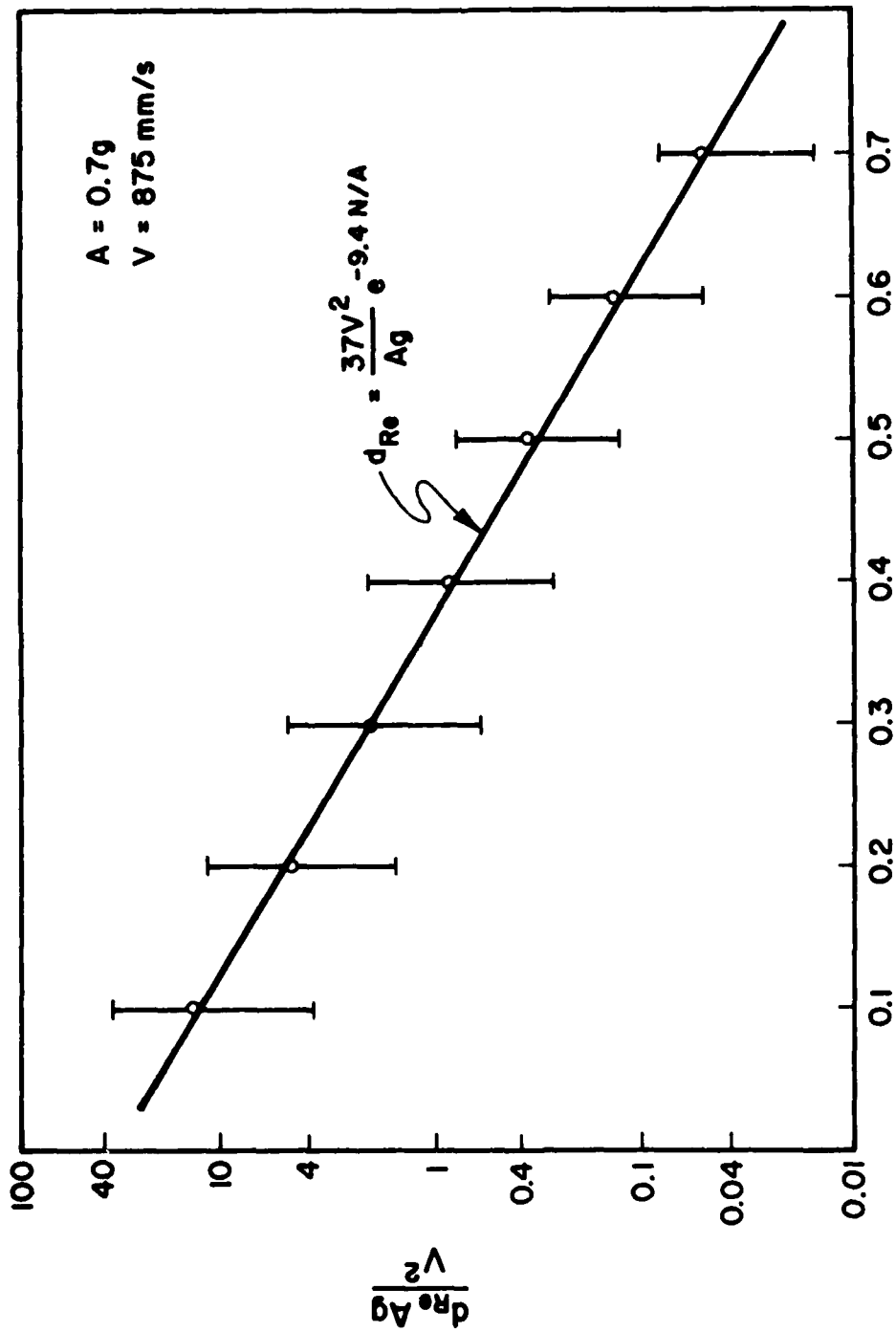

FIG. 6.3 DISPLACEMENT FROM NEWMARK'S MODEL WITH $N_V = 0$ AS A FUNCTION OF N/A.

scaled in the same ratio as the horizontal component. The influence of the vertical accelerations is indicated by the ratio $E_v = d_{Rv}/d_{Re}$ where d_{Rv} is the slip computed when vertical accelerations are considered. The ratio E_v was found to depend upon the strength of the input acceleration (the coefficient A) as well as upon N/A. For each pair of values for A and N/A, up to 56 values of E_v were computed (less those cases where $d_{Re} = \emptyset$ and cases where d_{Re} is so small that division by it would give a value of E_v which might be much in error). Average values are plotted in Fig. 6.4, and coefficients of variation are listed in the lower portion of Table 6.1.

Figure 6.4 indicates that, on the average, incorporating vertical ground accelerations causes greater residual displacements. This can be understood by considering a hypothetical case in which upward and downward accelerations both reach peak values of 1.0g. When the peak downward acceleration occurs, resistance to slip disappears entirely, whereas at the peak upward acceleration the resistance is merely double that for zero vertical acceleration. Clearly, the potential effect of downward acceleration on slip is greater than the influence of upward acceleration.

The coefficient of variation for the function E_v is small except when both A and N/A are large. As would be expected, with large N/A there are fewer intervals during which slip occurs, and hence the sense of the vertical acceleration in these moments is quite important. The influence of vertical accelerations would

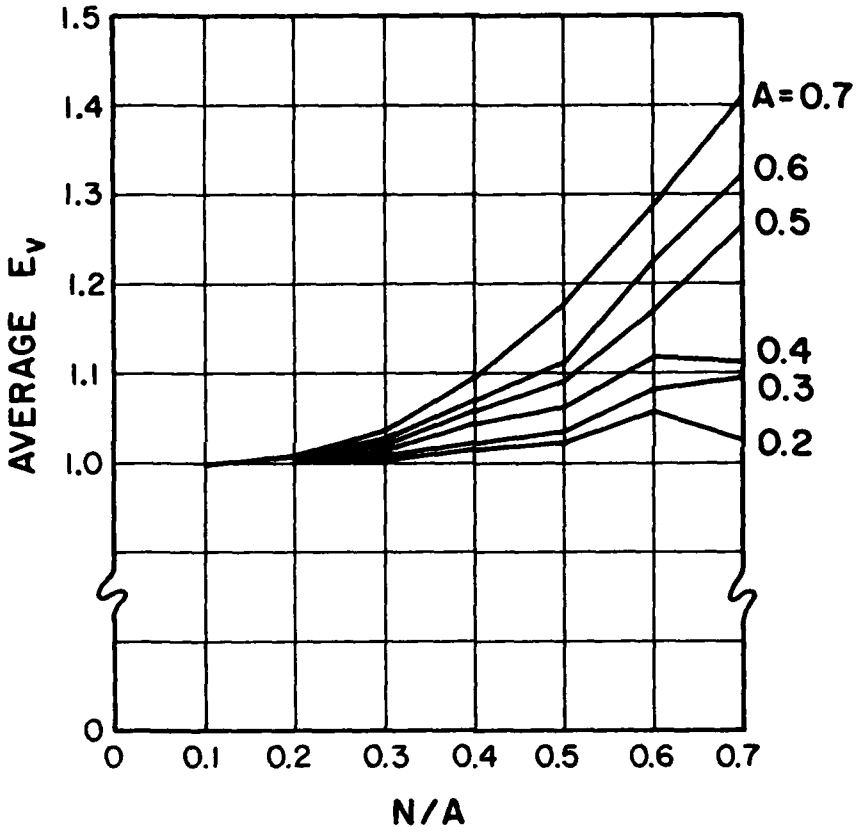

FIG. 6.4 EFFECT OF VERTICAL GROUND ACCELERATION ON RESIDUAL DISPLACEMENT OF BLOCK.

appear even greater if cases in which $d_{Re} = 0$ but $d_{Rv} \neq 0$ were included.

Wong suggested an equation for the average effect of vertical accelerations:

$$\bar{E}_v = 1.015 - 0.2N/A + 0.72(N/A)^2 \qquad (6.3)$$

which is valid for $0.2 \leq A \leq 0.7$ and $0.1 \leq N/A \leq 0.7$. "Average" in this sense implies averaging over a range of values of A as well as over a set of computed slips.

6.6 COMBINED UNCERTAINTY

One way to estimate the overall uncertainty arising from the combined effect of orientation of the wall, site-to-site and event-to-event differences, and vertical ground accelerations is to combine the coefficients of variation in Table 6.1. We would estimate the slip of a block as:

$$d_{Rv} = E_o E_s E_v \bar{d}_{Re} \qquad (6.4)$$

where $\bar{d}_{Re}$ is a deterministic function of N/A (as given in Eq. 6.2) and E_o, E_s, E_v are random variables which depend upon A and N/A. If we further assume that E_o, E_s and E_v are independent, then the coefficient of variation V_R of d_{Rv} is:

$$V_R^2 = (1 + V_O^2)(1 + V_S^2)(1 + V_V^2) - 1 \qquad (6.5)$$

where V_o, V_s and V_v are the coefficients of variation of E_o, E_s and E_v respectively. The resulting values of V_R are tabulated in Table 6.2. As would be expected from comparison of the individual V_o, V_s and V_v, vertical ground accelerations contribute relatively little to the overall uncertainty except at large values of N/A. Even here the predominant uncertainty comes from the unknown orientation of a wall relative to the principal axes of the ground motion.

Alternatively, values of V_R may be determined directly from the 56 computed values of residual slip for each A and N/A. These results are given in Table 6.3. Comparing Tables 6.2 and 6.3, it is seen that the directly-evaluated V_R (Table 6.3) are always less than those (Table 6.2) computed by assuming that the three effects discussed in Sections 6.3, 6.4, and 6.5 are independent. Clearly some degree of correlation actually exists among these effects. From the results at small N/A, it may be deduced that the orientation and site-to-site effects are correlated to a slight degree. At large N/A the V_R do not increase significantly as A becomes larger, implying that the effect of vertical ground acceleration is strongly correlated to one or both of the other two effects. This latter conclusion seems reasonable: vertical accelerations are important only when there are a very few spikes of horizontal acceleration that cause slip, and having only a few such spikes can also lead to a strong orientation effect.

For design considerations only the results in Table 6.3 are of interest. However, having looked at the various effects

Table 6.2

OVERALL COEFFICIENT OF VARIATION
ASSOCIATED WITH UNCERTAIN NATURE
OF GROUND MOTION, BY COMBINING
UNCERTAINTIES IN CONTRIBUTING EFFECTS

A	N/A						
	0.1	0.2	0.3	0.4	0.5	0.6	0.7
0.2	0.64	0.72	0.83	0.94	1.14	1.37	1.48
0.3	0.64	0.72	0.83	0.94	1.15	1.40	1.54
0.4	0.64	0.72	0.83	0.95	1.17	1.44	1.60
0.5	0.64	0.72	0.83	0.95	1.19	1.48	1.78
0.6	0.64	0.72	0.83	0.96	1.24	1.54	1.87
0.7	0.64	0.72	0.83	0.98	1.30	1.60	1.95

Table 6.3

OVERALL COEFFICIENT OF VARIATION
ASSOCIATED WITH UNCERTAIN NATURE
OF GROUND MOTIONS, FROM STATISTICS
OF COMPUTED RESIDUAL DISPLACEMENTS

A	N/A						
	0.1	0.2	0.3	0.4	0.5	0.6	0.7
0.2	0.63	0.68	0.78	0.88	1.02	1.17	1.39
0.3	0.63	0.68	0.78	0.88	1.02	1.17	1.40
0.4	0.63	0.68	0.78	0.88	1.02	1.17	1.41
0.5	0.63	0.68	0.78	0.88	1.01	1.16	1.42
0.6	0.63	0.68	0.78	0.88	1.01	1.16	1.43
0.7	0.63	0.68	0.78	0.88	1.01	1.16	1.43

separately has been of considerable value in understanding the importance of the several contributions to overall uncertainty.

6.7 PREDICTING RESIDUAL DISPLACEMENTS

If the effects of vertical ground acceleration are ignored, Eq. 6.2 provides a good prediction for the average residual displacement for a given A, V and N/A. There is a small "fitting error" and there is still some statistical uncertainty in the determination of the actual mean displacement owing to the limited size of the suite of earthquakes used in the calculation. However, these uncertainties are small compared to the scatter in residual displacement resulting from the random nature of ground motions. When vertical accelerations are introduced,Eq. 6.2 may be modified to:

$$\bar{d}_{Rv} = \bar{E}_v \bar{d}_{Re} \tag{6.6}$$

where $\bar{E}_v$ is given by Eq. 6.3. As discussed in Section 6.5, $\bar{E}$ is actually also a function of A, but the error introduced by using Eq. 6.3 is small compared to the scatter associated with orientation and event-to-event effects.

Table 6.3 provides estimates of the coefficient of variation of the residual displacements. If the distribution function for the displacements is known or assumed, Eq. 6.6 plus Table 6.3 provide a basis for estimating probability that various levels of ground motion might be exceeded. Since to some degree the uncertainty in d_{Rv} arises from a multiplication of the three

effects discussed in preceeding sections, it seems reasonable to assume a log-normal distribution function. Figure 6.5 compares cumulative distribution functions derived as suggested here with those developed from the actual computed residual displacements. In general the agreement is reasonable. In particular, it would appear that a satisfactory estimate can be obtained for the displacement which will not be exceeded with 95% probability.

Assume that the actual residual displacement can be written as:

$$d_{Rv} = \bar{d}_{Rv} Q \tag{6.7}$$

where Q is a log-normally distributed random variable with mean of unity and coefficient of variation $V_Q = V_R$. The mean and standard deviation for lnQ are:

$$\sigma_{lnQ} = \sqrt{\ln\ (1+ V_Q^2)} \tag{6.8}$$

$$m_{lnQ} = \ln(E[Q]) - \tfrac{1}{2} \mathrm{Var}[\ln Q]$$

$$= - \tfrac{1}{2} Q_{lnQ}^2 = - \tfrac{1}{2} \ln(1+V_Q^2) \tag{6.9}$$

The value of lnQ which will not be exceeded with 95% probabality is then:

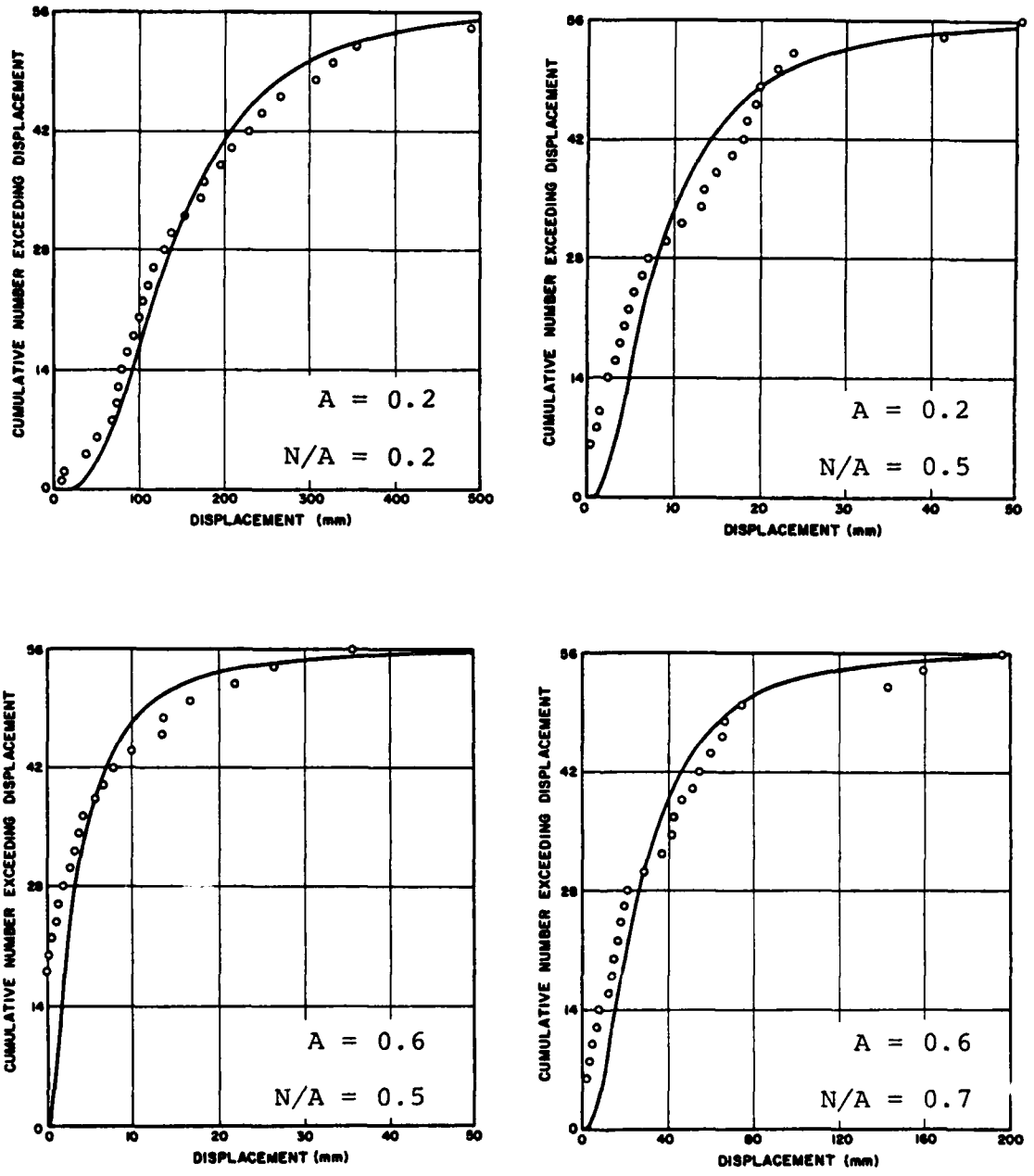

FIG. 6.5 COMPARISON OF RESULTS OF SLIDING BLOCK ANALYSES WITH DERIVED CUMULATIVE LOG NORMAL STATISTICAL DISTRIBUTIONS FOR DISPLACEMENT.

$$\ln Q_{95} = m_{\ln Q} + 1.645\, \sigma_{\ln Q} \tag{6.10}$$

or

$$\ln Q_{95} = -\frac{1}{2} \ln (1+V_Q^2) + 1.645 \sqrt{\ln (1+V_Q^2)} \tag{6.11}$$

or

$$Q_{95} = e^{-\frac{1}{2} \ln (1+V_Q^2) + 1.645 \sqrt{\ln(1+V_Q^2)}} \tag{6.12}$$

Values of Q_{95} are given in Table 6.4, for typical values of V_Q. The interpretation of these results is as follows. Suppose that the allowable residual displacement is d_L. Then, in order for there to be 95% probability that d_L will not be exceeded during an earthquake with given peak acceleration and peak velocity, then the expected (average) residual displacement for such an earthquake should be d_L/Q_{95}. This assumes that other parameters of a problem, such as the resistance of a block or wall to the initiation of sliding, are known with certainty. The effects of uncertainty in these parameters as discussed in the next chapter.

6.8 APPLICATION TO RETAINING WALLS

As discussed in Chapter 5, for a given A, V and N the residual displacement of a retaining wall, $\hat{d}_R$, is not equal to the residual displacement of a sliding block. Thus Equation 6.2 does not apply exactly for the mean residual slip of retaining walls. However, calculations by Wong (1982) have shown that the

coefficients of variation for $\hat{d}_{Re}$ are very nearly equal to those for d_{Re}, for each A and N. Hence Equation 6.11 and the results in Table 6.4 apply to retaining walls as well as sliding blocks.

6.9 IMPROVEMENTS TO PREDICTIONS

The procedure outlined here for predicting the average displacement of a sliding block is, of course, only as good as the suite of earthquakes used to develop the correlations and as the assumption that A and V are the best measures of intensity of shaking. It will certainly be desirable to refine and improve upon Equation 6.2 by using a larger suite of earthquake motions. Another improvement will be to use several such suites, each for a limited range of magnitudes (and perhaps epicentral distances) so as to reflect the influence of the duration of motion. It may also be that there are parameters other than A and V which are better indicators of the amount of residual displacement than can occur; for example, magnitude and epicentral distance. Explanatory studies into these questions are ongoing at MIT under the direction of Prof. Daniele Veneziano. Finally, as noted in Section 6.3, a more thorough treatment of the orientation effect would be desirable.

7 - UNCERTAINTY IN RESISTANCE PARAMETERS

1 INTRODUCTION

The analysis in Chapter 6 has assumed that the mean displacement $\bar{d}_{Re}$ is a known function of the properties of the wall and ckfill. Actually, $\bar{d}_{Re}$ is itself uncertain - partly because of certainty in these properties and partly because of uncertainty the model being used to compute displacement for given operties and given ground motion input. This chapter deals with e effect of uncertainties in the wall/backfill properties.

These properties include the weight of the wall; the unit ight of the wall; the friction angles at the base of the wall, thin the backfill and at the wall-backfill interface; and the ometry of the problem. While all of these properties are certain to some degree, the most important uncertainties are ose associated with the friction angles. The influence of certainties in the other properties generally is insignificant, d will be ignored in this analysis. That is to say, these other operties will be considered as deterministic.

Computation of the uncertainty in permanent displacement volves: (a) evaluation of uncertainty in the friction angles, d then (b) propagation of these uncertainties through the alysis connecting the friction angles to permanent displacement. e latter step is described in sections 7.3 and 7.4, beginning th the case of a sliding block on a horizontal plane.

7.2 UNCERTAINTY IN FRICTION ANGLES

The friction angles selected for analysis of a particular retaining wall seldom are based upon values measured using the actual soils at that wall, but rather are estimated based upon past experience with similar soils. Moreover, the actual friction angles may change as sliding progresses. The uncertainty in movement associated with this latter consideration should most properly be treated as part of the model error discussed in Chapter 8, but for purposes of this report it is considered as resulting from uncertainty in the evaluation of the friction angles.

When friction angles of a granular soil are measured, starting from a specified initial density, scatter is relatively small. It might reasonably be characterized by a standard deviation σ_ϕ of 1 or 2 degrees. However, because the backfill sometimes is poorly compacted and its actual density unknown, the possible variation about the actual mean value must be greater. Because backfill does tend to be loose, there is relatively little decrease in friction angle past the peak value as straining continues. Furthermore, ϕ for backfill is almost always selected conservatively, and it is rather unlikely that the minimum value can be more than several degrees less than the angle typically used for design. (It is the possibility that the actual ϕ may be less than the value assumed for design that is of primary concern to us). All in all, it seems reasonable to use σ_ϕ = 2 degrees or possibly 3 degrees.

These same arguments also apply to the friction angle ϕ_b at the base of the wall. Because foundation soils tend to be better compacted, ϕ_b usually is greater than ϕ. By the same token, decrease in ϕ_b with continued sliding is likely to be more significant. However, once again the values nominally used for calculations are likely less than the actual mean. Again it seems reasonable to use a standard deviation of 2 or 3 degrees.

Engineers tend to feel quite uncertain as to the choice of a suitable value of wall friction angle δ. It is not that the actual peak interface friction angle is in great doubt, but rather there is uncertainty as to how much frictional resistance is mobilized at a wall before static failure occurs. In the seismic problem where slip is actually expected, this type of uncertainty should not be so important. Nonetheless, it is considered that a larger standard deviation should be considered in the case of wall friction; say $\sigma_\delta = 5^\circ$.

For the calculations in the following sections, it is necessary to pay careful attention to the units for the standard deviations of friction angles, and this is best handled by re-expressing the foregoing results in radians. Appropriate values are summarized in table 7.1.

7.3 BLOCK ON HORIZONTAL PLANE

When uncertainty in resistance is considered, the term $\tilde{d}_{Rv}$ in Equation 6.7 becomes a function of the random variable N; that is, this term is itself a random variable. The variance of d_{Rv} may be found by:

Table 7.1

ESTIMATED STANDARD DEVIATIONS
FOR FRICTION ANGLES

Location	σ in radians
Backfill	0.035 to 0.052
Base	0.035 to 0.052
Wall	0.035 to 0.087

$$\text{Var}[d_{Rv}] = \left[\frac{\partial \bar{d}_{Rv}}{\partial N}\right]^2 \text{Var}[N] \tag{7.1}$$

Alternatively, but less precisely, we may rewrite Equation 6.6 as:

$$d_{Rv} = \bar{d}_{Rv} \; Q \; R_\phi \tag{7.2}$$

where now $\bar{d}_{Rv}$ is a deterministic function computed using average values for the friction angles involved in the problem at hand and R_ϕ is a random variable with mean unity reflecting uncertainty in the friction angles. The variance of R_ϕ is given by Equation 7.1. Computations show that $\partial \bar{d}_{Rv}/\partial N$ is closely approximated by $\bar{E} \cdot \partial \bar{d}_{Re}/\partial N$. Hence the variance of R_ϕ may be expressed as:

$$\text{Var}[R_\phi] = \bar{E}_v^{\,2} \cdot \left[\frac{\partial}{\partial N} \left(\frac{37V^2}{Ag} e^{-9.4N/A}\right)\right]^2 \text{Var}[N] \tag{7.3}$$

$$= \left[-\frac{9.4}{A} \bar{d}_{Rv}\right]^2 \text{Var}[N]$$

Taking the square root to obtain the standard deviation of R_ϕ and dividing by ϕ_{Rv}, the coefficient of variation of R_ϕ becomes:

$$V_{R_\phi} = \frac{9.4}{A} \sqrt{\text{Var}[N]} = \frac{9.4}{A} \sigma_N \tag{7.4}$$

Note that $V_{R\phi}$ is inversely related to the ground acceleration coefficient A. This means that, since it is ratio N/A that determines the amount of slip, a given uncertainty in N is much more important when A is small than when A is large.

For a sliding block of known weight on a horizontal plane, the transmittable acceleration N is determined entirely by the friction angle between the block and the supporting plane:

$$N = \tan\phi \tag{7.5}$$

The variance of N is then found by:

$$\text{Var}[N] = [\frac{\partial N}{\partial \phi}]^2 \text{ Var}[\phi] = \sec^4\phi \text{ Var}[\phi] \tag{7.6}$$

and the standard deviation σ_N is:

$$\sigma_N = \sigma_\phi/\cos^2\phi \tag{7.7}$$

Typical values for ϕ range from 30° to 35°. Using the values for σ_ϕ from Table 7.1, the range for σ_N is 0.05 to 0.08.

Combining Eqs. 7.4 and 7.7 leads to the results in Table 7.2. Note that some of the values of $V_{R\phi}$ - those for the smaller A - are quite large, much larger than the coefficients of variation discussed in Chapter 6. Thus it is evident that uncertainty in resistance parameters can be a very important consideration.

Table 7.2

COEFFICIENT OF VARIATION OF
RESISTANCE TERM

	V_{R_ϕ}	
A	$\sigma_N = 0.05$	$\sigma_N = 0.08$
0.2	2.35	3.76
0.3	1.57	2.51
0.4	1.18	1.88
0.5	0.94	1.50
0.6	0.78	1.25
0.7	0.67	1.07

7.4 RETAINING WALLS

For retaining walls one proceeds in a generally similar fashion. In this case, an exact solution would require derivatives for the product $\vec{d}_R \cdot R_{2/1}$. Values of the partial derivative have not been evaluated, although approximate results by Wong (1982) indicate that the value obtained for a sliding block are a good approximation for the retaining wall case. That is to say, Equation (7.3) may still be used. Hence interest then focuses upon evaluation of Var[N] for retaining walls.

The variance of N depends upon uncertainty in the three angles ϕ, ϕ_b and δ. If these angles are assumed independent of each other, then Var[N] may be evaluated by:

$$\text{Var}[N] = \left(\frac{\partial N}{\partial \phi}\right)^2 \text{Var}[\phi] + \left(\frac{\partial N}{\partial \phi_b}\right)^2 \text{Var}[\phi_b] + \left(\frac{\partial N}{\partial \delta}\right)^2 \text{Var}[\delta] \qquad (7.8)$$

The derivatives are obtained from Equation 4.4, which may be rewritten as:

$$N = \tan\phi_b - \frac{[\cos(\beta+\delta) - \sin(\beta+\delta)\tan\phi_b]P_{AE}}{W_w} \qquad (7.9)$$

Since P_{AE} is a function of N as well as of ϕ and δ, implicit differentiation must be used. Wong (1982) carried out the necessary steps, and the resulting equations are reproduced in Table 7.3.

Numerical evaluations of these equations have been performed for various combinations of values of the three angles and of N.

Table 7.3

EQUATIONS FOR PARTIAL DERIVATIONS OF N WITH RESPECT TO ϕ, ϕ_b AND δ.

$$\frac{\partial N}{\partial \phi_b} = \frac{\sec^2 \phi_b}{G} \left[\frac{\cot(\beta+\delta) - N}{(\cot(\beta+\delta) - \tan\phi_b)\ (\tan\phi_b - N)} \right]$$

$$\frac{\partial N}{\partial \phi} = \frac{1}{G} \left[2 \tan(\phi-\psi-\beta) + \frac{\cot(\phi+\delta)+\cot(\phi-\psi-i)}{1 + J} \right]$$

$$\frac{\partial N}{\partial \delta} = \frac{1}{G} \left[\frac{\cot(\phi+\delta) - J\tan(\psi+\beta+\delta)}{1 + J} + \frac{\tan(\beta+\delta)+\tan\phi_b}{1-\tan(\beta+\delta)\tan\phi_b} \right]$$

$$G = \frac{1}{1+N^2} \left[2\tan(\phi-\psi-\beta) + N + \frac{\cot(\phi-\psi-i)+H\tan(\psi+\beta+\delta)}{1 + J} \right]$$

$$+ \frac{1}{\tan\phi_b - N}$$

$$J = \sqrt{\frac{\cos(i-\beta)\cos(\psi+\beta+\delta)}{\sin(\phi+\delta)\sin(\phi-\psi-i)}}$$

(All have involved $\beta = i = 0$.) One special case of some interest is that when $\phi_b = \phi$ and $\delta = 0$. Then equation 7.8 may be rewritten as:

$$\text{Var}[N] = \left[\left(\frac{\partial N}{\partial \phi}\right)^2 + \left(\frac{\partial N}{\partial \phi_b}\right)^2\right] \text{Var}[\phi] \qquad (7.10)$$

The term in brackets is nearly constant for the several combinations investigated, at a value of about 0.85 radians^{-2}. Thus:

$$\sigma_N = \sqrt{0.85}\ \sigma_\phi = 0.92\sigma_\phi \qquad (7.11)$$

That is to say, the uncertainty in N is actually somewhat less than that in each of the two friction angles. This reduction occurs because, assuming independence, it is relatively unlikely that both friction angles will be simultaneously larger (or smaller) than mean values. If there is some actual dependence between the values taken on by these angles, then the ratio σ_N/σ_ϕ would be increased to some degree.

When wall friction is present, as indeed it must be, the situation is more complicated. Results from some typical calculations are presented in Table 7.4, for the case $\sigma_\phi = \sigma_{\phi b} = 2^\circ$, $\sigma_\delta = 5^\circ$ and $\beta = i = 0$. It may be seen that σ_N varies with the combination of values used for the three angles and N, and is greatest when N is smallest. Somewhat greater values of σ_N may be found when other combinations of parameters are used. Furthermore, depending among the three friction angles (especially

Table 7.4

STANDARD DEVIATION FOR RESISTANCE FACTOR N FOR GRAVITY WALLS WITH WALL FRICTION, ASSUMING $\sigma_{\phi} = \sigma_{\phi b} = 2°$ AND $\sigma_{\delta} = 5°$

			σ_N		
ϕ	ϕ_b	N	$\delta=0$	$\delta=20°$	$\delta=30°$
30°	30°	0.05	0.032	0.043	0.049
		0.1	0.031	0.041	0.047
		0.2	0.032	0.038	0.043
		0.3	0.033	0.036	0.039
30°	35°	0.05	0.034	0.051	0.061
		0.1	0.033	0.048	0.058
		0.2	0.033	0.044	0.052
		0.3	0.033	0.041	0.047
35°	35°	0.05	0.033	0.049	0.059
		0.1	0.033	0.047	0.057
		0.2	0.033	0.044	0.052
		0.3	0.033	0.042	0.048

between ϕ and δ) will cause the σ_N to increase. It was judged that an average of the numbers in the final column of Table 7.4 would be most representative of the uncertainty in N, and such average values are plotted in Fig. 7.1 as a function of N.

Values of σ_N may be entered into Equation 7.4, and Table 7.2 is still at least approximately valid. Once again the conclusion is that the overall effect of uncertainty in the friction angles is very significant.

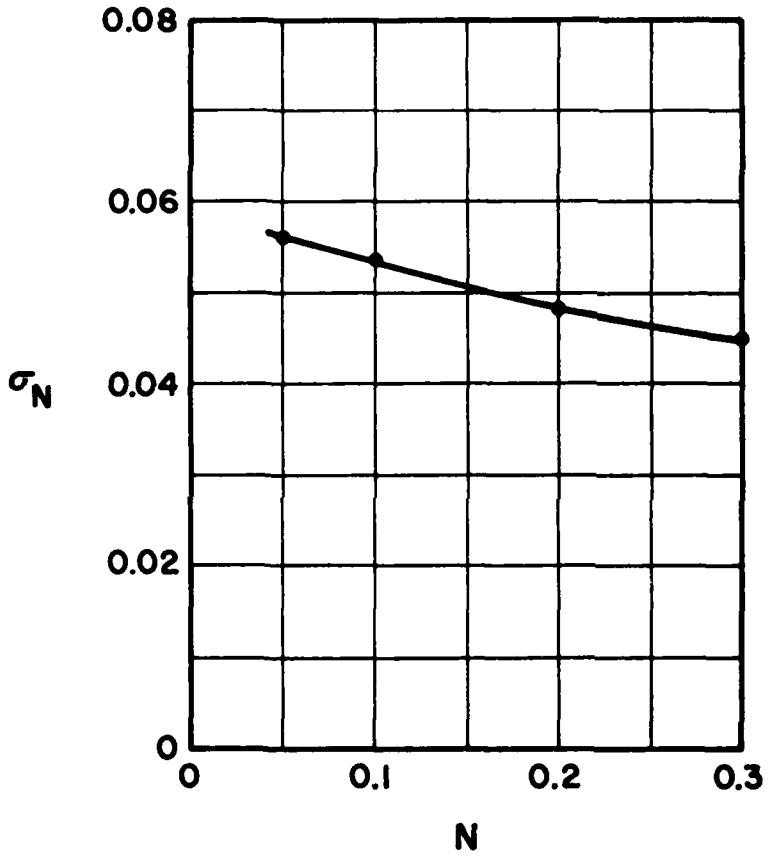

FIG. 7.1 TYPICAL VALUES FOR σ_N FOR RETAINING WALL WITH WALL FRICTION.

8 – MODEL ERRORS AND UNCERTAINTIES

This chapter discusses several ways in which the two block model of Chapter 5 is still imperfect, but where knowledge is inadequate to permit use of an improved model. These aspects include the proper choice of a failure plane, the effect of deformations within the backfill before sliding begins, and tilting of walls. In addition, there are errors because one may choose to use simpler approximate results in lieu of expending considerable effort in using the best methods of analysis that are available.

8.1 FAILURE PLANE INCLINATION

In Zarrabi's (1979) two-block model, it was assumed that the inclination of the failure plane in the backfill varies with the instantaneous ground acceleration. This is a natural assumption that arises from the formulation and application of the Mononobe-Okabe Equation. However, as described in Chapter 2, the model tests performed by Murphy (1960) and Lai (1979) indicate that it may be more reasonable to assume that the failure plane inclination remains constant during slip. Jacobsen's (1980) comparisons of Lai's (1979) model test results with calculations using the two-block model concur with this reasoning, in that the agreement is better between theory and experiment, when a fixed angle of inclination θ is assumed. Thus, it would be reasonable to use a fixed angle θ in the calculation of residual displacements.

depth more rapidly than linearly. At other times when the rotational acceleration of the wall reverses, the opposite is true and then the resultant horizontal force lies above the lower third point.

Once revealed by this simple conceptual model, these results are quite obvious. The analysis demonstrates clearly that conventional wisdom concerning the location of the resultant, which was derived for the case of a wall that does not tilt, may be quite misleading as regards the response of a wall which is free to tilt.

Nadim used this model to study the relative importance of sliding and tilting. Moment resistance at the base of the wall was assumed to be rigid-plastic in character, and it was further asumed that the axis of tilting was at a fixed location. A threshold transmittable acceleration, N_R, is reached when the base moment required for dynamic equilibrium just equals the maximum moment. (The dynamic stress from the backfill is assumed to increase linearly with depth in this calculation.) Any tendency for the thrust from the backfill to increase further is resisted by rotational inertia of the wall. The principal conclusions from Nadim's study were:

* If $N_R > N$, then only sliding will occur. That is, having resistance to sliding which is less than the resistance to tilting protects the wall against tilting.

* If $N_R < 0.85N$, then only tilting - and no sliding - occurs. In this case, the permanent displacement at the

'all may slide and/or rotate about its base. The horizontal
cceleration of each slice is just equal to the horizontal
cceleration of the wall at the point where the slice meets the
'all. Each slice also accelerates vertically, as necessary to
aintain contact between the slices. With these various
ssumptions, it is possible to develop an equation* giving the
istribution of stresses between the wall and backfill in terms of
he horizontal acceleration of the wall at its base (which may
iffer from the acceleration of the underlying ground) and the
otational acceleration of the wall. This equation is then used
ogether with equations for the dynamic equilibrium of the wall
as in Chapter 5) to compute the motions of the wall.

One result of this analysis - a rather surprising result at
irst sight - is that the resultant of the dynamic stresses
etween backfill and wall sometimes lies below the lower third
oint. This happens whenever the tilt of the wall away from the
ackfill is accelerating while the horizontal acceleration of the
round is towards the backfill (which is just the situation of
reatest concern to us). At such times (see figure 8.5b), the
bsolute acceleration at the top of the wall is less than the
bsolute acceleration at the base of the wall. With our
ssumptions, this means that the uppermost slice through the
ackfill has a smaller acceleration than the slices below it.
ence the horizontal stresses between soil and wall increases with

---

* It turns out that the thickness of the individual slices can in the limit be set to zero, so that a continuous equation is obtained.

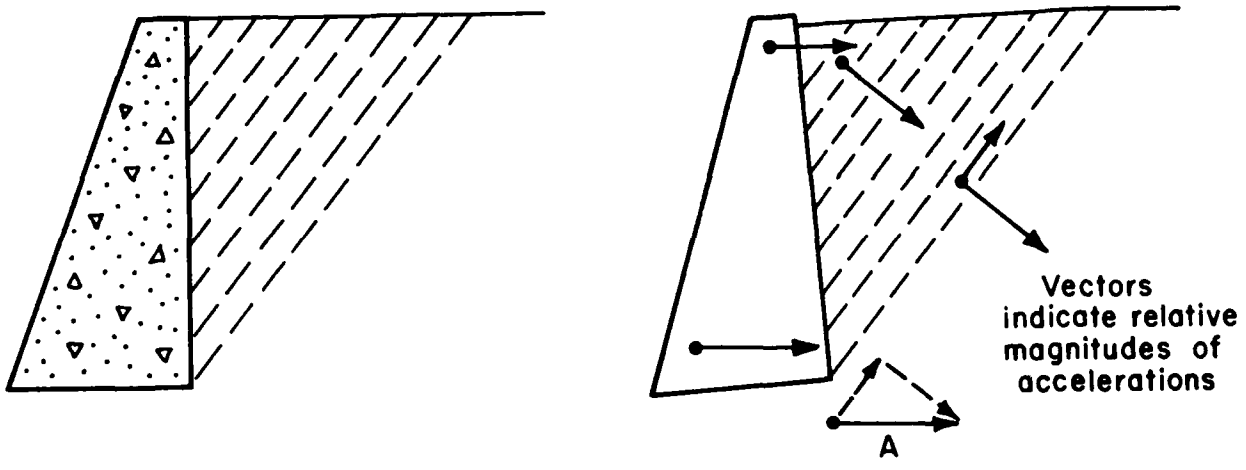

FIG. 8.5 MULTIPLE PARALLEL SLICE MODEL FOR TILTING OF WALL. WHEN ROTATIONAL ACCELERATION OF WALL IS OUTWARD, ABSOLUTE ACCELERATIONS ARE REDUCED NEAR TOP OF WALL AND BACKFILL.

depicted by the dashed "proposed design lines" shown in Fig. 8.4. The factor R_E obtained from these lines can be justifiably used as relatively conservative amplification factors to be applied to simpler sliding block analysis, in the same vein as previously suggested.

It should be noted that the fundamental frequency f_{BF} for backfills will typically range from 5 Hz to 25 Hz. Dominant frequencies of ground motions f_{E-Q} range generally from 2 Hz to 5 Hz. Thus, the most typical range of the frequency ratio f_{E-Q}/f_{BF} is 0.2 to 0.6.

8.3 TILTING

Observations in the field following earthquakes suggests that permanent displacement of gravity retaining walls usually involves tilting. This important aspect of behavior has received very little attention from a theoretical standpoint, and hence is still poorly understood. There have been model tests in which a wall is tilted while it and the backfill are subjected to earthquake like motions (Sherif, et al. 1981). These tests have confirmed the influence of tilting upon the development of active conditions behind a wall. However, they give no direct evidence as to the amount of tilting that might develop in a free-standing wall.

A preliminary study of this problem by Nadim (1980) used the conceptual model shown in Figure 8.5. The failing wedge of soil is subdivided into thin slices which may slide over each other once frictional resistance on the interslice failure surface is reached. Except for such sliding, the backfill is rigid, while the

idealization of the problem. In all of these cases, it was assumed that there is a rigid boundary beneath the backfill at the same level as the base of the wall. This means that seismic wave motions reflect back into the backfill from this boundary. However, in most real problems this boundary is not rigid, and a portion of the waves radiate away from the region of excitation at this boundary (radiation damping). Because of this effect, the actual amplification of ground motion through the backfill is probably not as large as one predicts from the finite element analysis with a rigid boundary at the level of the base of the wall, especially near resonance conditions.

Another trend shown in Fig. 8.4 is that the amplification of residual displacements is more significant for high values of N/A. If N/A = 1 and the rigid block model were correct, there would be no slip. However, because of amplification through the backfill the acceleration in the upper portions of the backfill would actually exceed N, and hence slip would occur. Thus for N/A equal to and slightly greater than unity, the ratio R_E is infinite. As previously noted, however, the usual range of practical values of N/A is from about Ø.3 to Ø.7.

The incorporation of preceeding observations into a practical design criteria can be done in several ways. Nadim (1982) and Nadim and Whitman (1983) have proposed modifying the values of A and V to reflect the amplification of ground motion, and using these amplified values of A and V as input into a block model analysis, such as the Richards-Elms Equation (Eqn. 4.1). An alternative method that is perhaps simpler and more direct is

$$R_E = \frac{d_R \text{ using elastic finite elements}}{d_R \text{ using rigid 2-block model}}$$

The variables f_{E-Q} and T_{E-Q} are respectively the dominant frequencies and period of the earthquake excitation, and f_{BF} and T_{BF} refer to the first fundamental frequency and period of the backfill.

From Fig. 8.4, it is clear that much larger displacements than predicted by the rigid-block model can occur if the elasticity of the backfill is considered, as in the finite element model. The ratio R_E can become very large (on the order of 10) as the ratio of the frequencies f_{E-Q}/f_{BF} approaches 1.0, which is analogous to a resonance condition for a SDOF vibrating system. Since the fundamental frequency of the backfill can be approximated as

$$f_{BF} = \frac{C_s}{4H} \tag{8.4}$$

where C_s is the shear wave velocity of the soil and H is the height of the wall. This implies a direct correlation between the frequency ratio and the height of the wall. Thus the amplification problem is more pronounced for higher walls.

It should be noted the finite element results obtained for excitation frequencies near the resonance condition are conservative because of the boundary conditions that are imposed in the

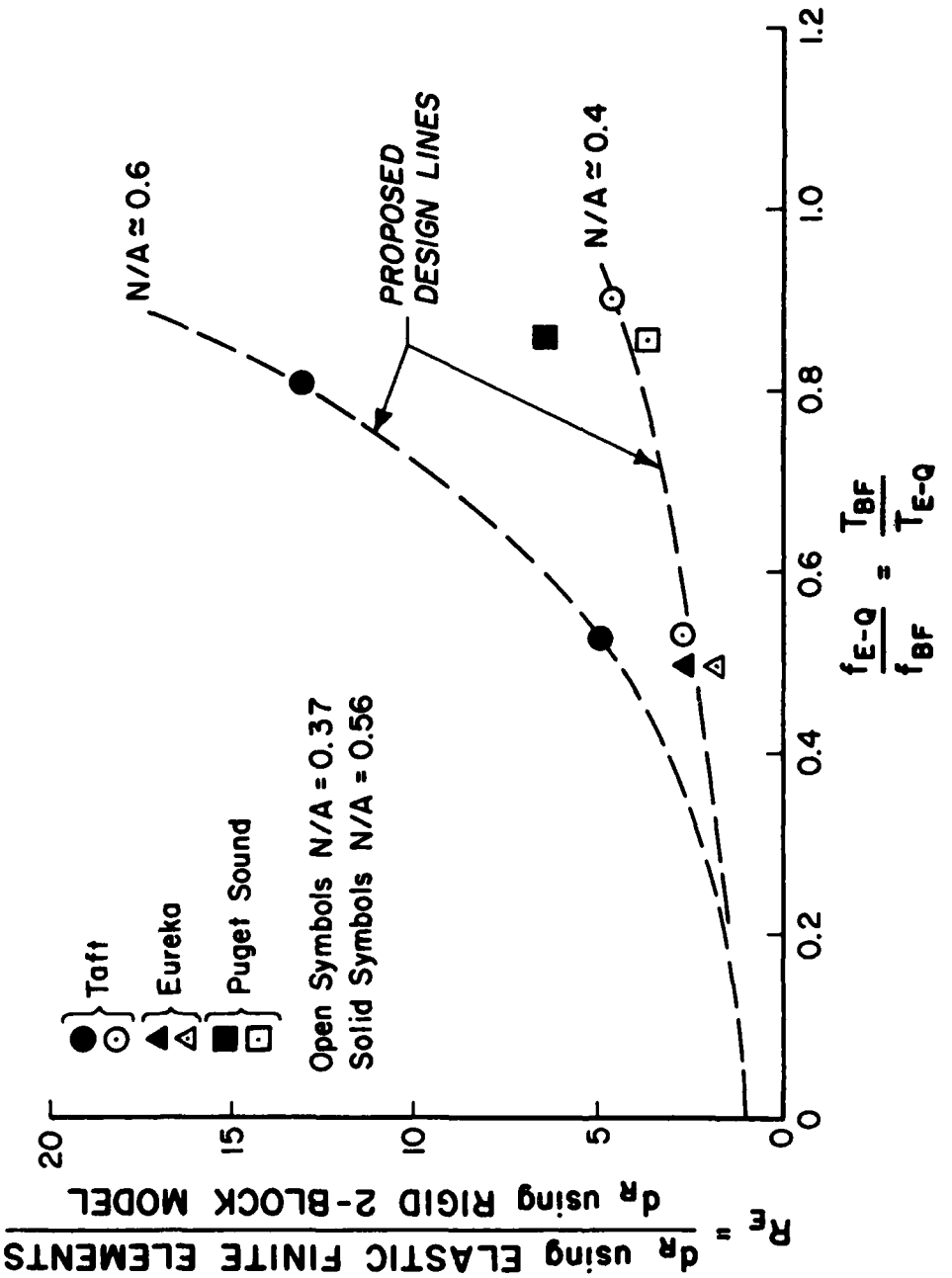

FIG. 8.4 COMPARISON OF RESULTS OF ELASTIC FINITE ELEMENT MODEL WITH RIGID TWO-BLOCK MODEL (ASSUMING CONSTANT θ).

increases the ground accceleration coefficient A. Assuming that the transmittable acceleration Ng is approximately the same regardless of the flexibility assumption, the effective N/A ratio would be lower for the flexible backfill than for the rigid backfill case. Consequently, considering the results from rigid block models, larger residual displacements would be expected. Also, there is additional amplification of the transmittable acceleration coefficient, such that larger earth pressures would be expected to develop, if envisioned in the context of seismic coefficients.

Obviously, the preceeding statements are only intuitive arguments for explaining how ground motion amplification affects residual displacements. It should be recognized that the concepts of rigid block models, including strict quantifications of N, A, the ratio N/A, and notions of normalizing displacement using V^2/Ag are no longer valid in view of the non-uniform distribution of these quantities in an elastic finite element model. However, the corresponding rigid block model quantities can be calculated and can serve as useful references for comparison of results.

Numerical results from the elastic finite element model results as compared with those from the rigid two-block model (assuming constant θ) are in Fig. 8.4. Computations are shown for three earthquake records and two different values of N/A. The format of comparison is analogous to the frequency response cure for a single degree-of-freedom (SDOF) vibrating mass. The ratio R_E, a residual displacement amplification factor, is defined as:

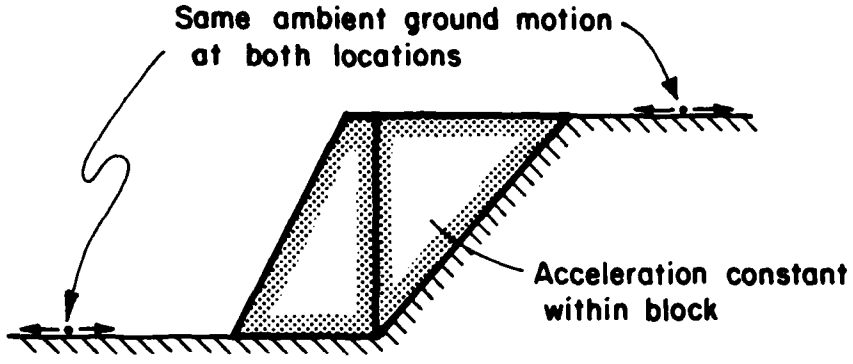

(a) Rigid Blocks and Backfill

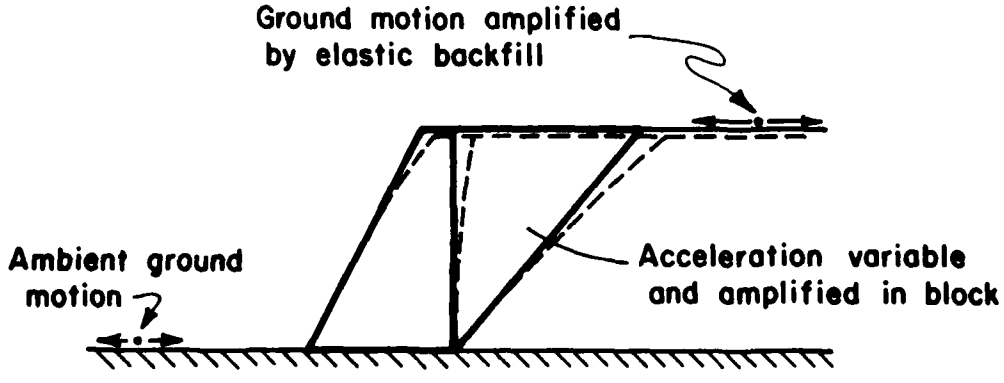

(b) Flexible (Elastic) Blocks and Backfill

FIG. 8.3 SCHEMATIC COMPARISON OF EFFECTS OF RIGIDITY AND FLEXIBILITY (ELASTIC) ASSUMPTIONS IN RETAINING WALL BEHAVIOR.

because of lack of data. However, in terms of practical significance, for the ranges of N and A commonly encountered, whether one uses a fixed or variable θ may not be important. This is especially true in light of the uncertanties in evaluating θ (as shown in Fig. 8.1) and the even larger uncertainties in the earthquake ground motion characteristics.

8.2 ELASTIC BACKFILL EFFECTS

The sliding block model developed by Zarrabi (1978) assume the blocks representing the retaining wall and the soil backfill wedge to be perfectly rigid. This is actually a fairly good assumption, particularly for walls with relatively low heights, where the effects of wall and backfill flexibility are essentially negligible. However, for high walls, the rigidity assumptions may lead to severe underestimation of the residual slip. The effects of assuming the wall and backfill to be elastic, and hence flexible, has been studied by Nadim (1982) using the finite element idealizations as described in Chapter 2. These result have also been reported in a paper by Nadim and Whitman (1983).

The basic effect on an elastic backfill is the resulting amplification of ground motion, similar to the phenomenon which is expected to occur in earth dams (see Seed and Martin, 1966 and Makdisi and Seed, 1979). The amplification phenomenon is schematically illustrated in Fig. 8.3 and compared to the rigid block case, without amplification.

Firstly, amplification of the ground motion occurs in the backfill outside of the soil failure wedge, and effectively

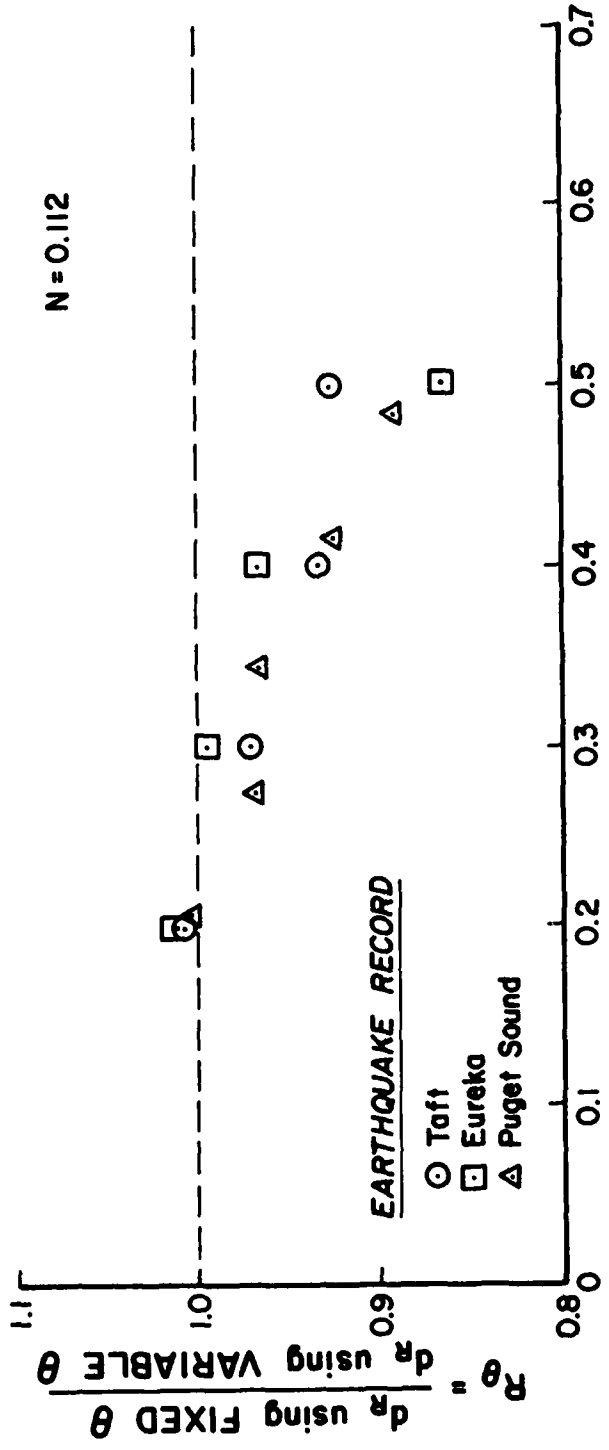

FIG. 8.2 COMPARISON OF CALCULATED DISPLACEMENTS USING FIXED VERSUS VARIABLE FAILURE PLANE INCLINATION ANGLE θ.

(increasing F_{ww}), a larger inertia force from the backfill is required to initiate slip. Thus a larger mass of backfill soil must be mobilized as reflected by a decrease in θ.

The experimental results for θ shown in Fig. 8.1 are consistently higher than the theoretical threshold θ_T, calculated based on measurements of ϕ, ϕ_b and δ evaluated by Lai (1979) and Jacobsen (1980). This may be attributed to frictional effects between the model and the glass sides of the model container, which would tend to effectively increase ϕ. There is also a range of possible interpretation of the failure angle θ due to the fact that the failure surface is actually a zone rather than a thin line of failure. Furthermore, there is a slight curvature to this failure zone, deviating from ideal linear conditions.

The numerical differences that arise in the calculated residual displacement between assuming a constant or variable plane of failure are illustrated in Fig. 8.2. The results shown are obtained from calculations performed separately by Nadim (1982) and Wong (1982) using three earthquake records and a constant value of N = 0.112. The Ratio R_θ is defined as:

$$R_\theta = \frac{\text{Residual displacement using fixed } \theta}{\text{Residual displacement using variable } \theta} \qquad (8.2)$$

The value of R_θ is generally less than or equal to one, with those values greater than one thought to be the result of numerical round-off errors. There is clearly a trend toward greater discrepancies for increasing accelerations, given a fixed value of N, but further generalizations of trends are difficult

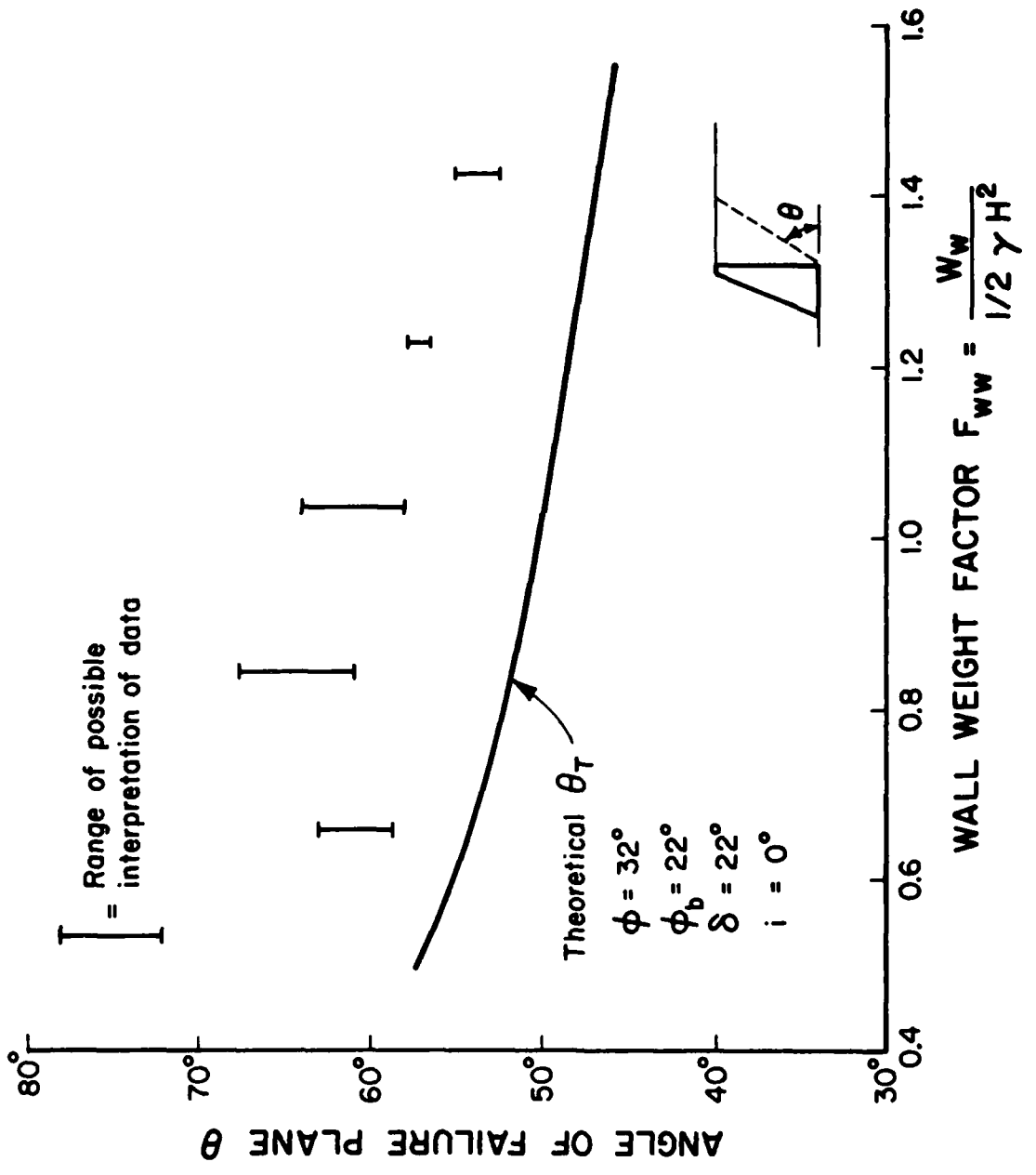

FIG. 8.1 COMPARISON OF THEORETICAL AND OBSERVED FAILURE PLANE INCLINATION ANGLE θ (DATA FROM LAI, 1979).

Physically, once a failure plane develops in the backfill, the plane may become slightly weaker than the surrounding soil and it would be the preferred plane of failure at subsequent stages of movement. Thus, the initial failure plane that develops should logically be used in the analysis. Thus the critical failure plane angle of inclination θ_T which would occur during earthquake motions is only dependent on the wall weight and the properties of the foundation and backfill soils. Nadim (1982) gave equations that determine the angle of inclination of this plane explicitly as:

$$\theta_T = 1/2(\alpha + \alpha_1) \tag{8.1}$$

where $\alpha = \tan^{-1}(B/A)$

$\alpha_1 = \cos^{-1}(-C.\cos\alpha/A)$

and

$$A = \cos(\phi+\delta+i)\sin(\phi_b-\phi) - \sin(\phi+\delta-i)\cos(\phi_b-\phi) - \cos(i)\cos(\delta+\phi_b)F_{ww}$$

$$B = 2\cos(i)\sin(\phi_b-\phi)\sin(\phi+\delta)$$

$$C = \sin(\phi_b+\delta+i) - \cos(i)\cos(\delta+\phi_b)/F_{ww}$$

$$F_{ww} = \frac{W_w}{1/2\gamma H^2} = \text{wall weight factor}$$

A comparison of the theoretical equation give by Nadim (1982) and the results from Lai's (1979) experiments is shown in Fig. 8.1. Both theory and experiment show a general downward trend for θ with increasing wall weight factor F_{ww}. This downward trend is explained physically by the fact that as the wall becomes heavier

top of the wall was found to be about 1 1/2 times the movement predicted using a sliding block with N set equal to N_R. Thus there's some reason to think that a sliding block model maybe useful in estimating permanent displacement even though tilting is the predominant mode of displacement.

These conclusions must, of course, be treated with great caution.

Unlike the case of sliding, significant tilting may occur before the maximum resistance against overturning moment is reached. There has been no adequate study of this aspect of the problem. Some results obtained using the finite element model of Figure 2.5 have confirmed that the resultant thrust from the backfill can lie below the lower third point at various times during a cycle of shaking. It does seem clear that any tendency for a wall to tilt will relieve the overturning moment acting upon the wall.

All in all, there is reason to believe that the sliding block model proposed by Richards and Elms is a reasonable model for predicting the permanent movement of actual gravity walls, provided they have been designed using a typically conservative safety factor against overturning by static loads.

8.4 APPROXIMATIONS TO 2-BLOCK ANALYSIS

If one knows the inclination of the failure plane through the backfill, or if one is willing to accept the assumption that this inclination varies continuously during shaking, the effect of kinematic constraints can be taken into account as discussed in

Chapter 5. However, the required analysis is at least moderately complex, and hence it generally is desirable to accept approximations in order to achieve simplicity.

Wong (1982) has suggested an equation for the factor $R_{2/1}$.

$$R_{2/1} = \begin{cases} 0.7 + 1.2N(1-N); & N < 0.5 \\ 1 & N > 0.5 \end{cases} \qquad (8.5)$$

This equation describes an average curve through the several curves in Figure 5.5. Each of those curves is itself drawn through a scattering of points calculated using different ground motions. However, the scatter in these points is quite small. The approximation in Eq. 8.5 lies in ignoring the effect of A.

Wong computed his results for the case $\beta = i = 0$ and for specific valus of ϕ and ϕ_β. Antia (1982) examined the effect of varying these parameters upon the ratio $R_{2/1}$ of permanent displacements computed by the two- and one-block models. His results are illustrated by the following tabulation (for A = 0.2, N = 0.4 and Taft earthquake record):

i	β	δ	Ratio of $R_{2/1}$
0	0	0	0.731
7.5°	0	0	0.767
0	15°	0	0.828
0	0	15°	0.764
7.5°	15°	15°	0.917

In all cases investigated, the effect is to decrease the difference between the residual displacements computed using the two models. Wong reached similar conclusions. Note that each case in the tabulation above corresponds to a different weight of wall, so as to hold N constant.

These results, plus those discussed in Section 8.1, emphasize the complexity of the so-called "2-block" effect. There is no doubt that the effect is real and that it acts to reduce the actual permanent sliding compared to that predicted using the Richard-Elms simple sliding block model. The problem is in predicting this reduction accurately by any simple calculation. Having the inclination of the failure plane fixed tends to make the reduction greater than suggested by Eq. 8.5. As the results in Figure 5.6 show, this reduction can be very large indeed. On the other hand, Antia's results show that this equation may not always be conservative.

Taking all these factors into consideration, it is reasonable to use a mean value of 0.65 for the factor $R_{2/1}$, and to represent the uncertainty in this factor by a standard deviation of 0.2.

9 - IMPROVED APPROACHES TO DESIGN

9.1 REVIEW OF OBJECTIVES

As discussed in Chapter 1, the general objective of this study has been to quantify the uncertainties invovled in using a displacement-limiting approach to the design of gravity retaining walls for seismic loadings. The specific goal has been to select, with greater confidence, a suitable safety factor for use with the Richards-Elms approach or, if possible, to develop an improved design methodology. In so doing, the desire to maintain the essential simplicity of the Richards-Elms approach has been an overriding consideration.

The various aspects of the problem have now been examined, to the extent that knowledge permits. The next step is to synthesize them into a unified approach to design.

9.2 EQUATION FOR PREDICTING MOTIONS

At the heart of any displacement-limiting approach to design is an equation for predicting displacements in terms of the specified ground motions and the physical parameters characterizing a gravity retaining wall and its backfill. To achieve the objectives of this study, such an equation must be probabilistic in nature. That is to say it is necesary to quantify the probability that various amounts of permanent displacement will be exceeded.

Equation 1.1 was suggested at the outset of this study for this purpose. In it, the permanent displacement of a retaining

wall is predicted by the product of five terms:

$\bar{d}_{R_v}$: The permanent displacement of a one-way sliding block with maximum transmittable acceleration Ng, averaged over all earthquake ground motions characterized by peak acceleration Ag and peak velocity V.

$R_{2/1}$: A deterministic factor accounting for the effect of a kinematic constraint ignored when using a sliding block to represent a retaining wall and its backfill.

Q : A random variable with mean of unity, describing the variation of permanent displacement aroused by different earthquake motions all having the same Ag and V.

R_ϕ : A random variable with mean of unity, describing the effect of random uncertainties in the resistance parameters for the wall and backfill.

M : A model error term, random in nature, which accounts for as yet poorly understood aspects of the problem.

The first four of these factors have been studied in considerable detail: $R_{2/1}$ in Chapter 5, d_R and Q in Chapter 6 and R_ϕ in Chapter 7. Methods for accounting for these several aspects of the problem have been developed in some detail. However, several of these methods are rather complicated.

The effect of vertical ground accelerations enters into the expression for d_R, and this causes the factors A and N to enter into computations in a complex fashion. Complicated calculations are necessary to arrive at exact values for the ratio $R_{2/1}$, and this ratio is influenced by A and N in a non-simple way. Similarly, it is not an easy matter to evaluate the effect of deformable backfill, even though guidelines for this purpose have been suggested in Chapter 7.

In order to retain simplicity, and keeping in mind the still imperfect state of our knowledge, Equation 1.1 has been simplified to:

$$d_{Rw} = \frac{37V^2}{Ag} e^{-9.4\bar{N}/A} \; Q \; R_{\phi} \; M \qquad (9.1)$$

The first term is Equation 6.2 for the mean displacement of a sliding block with no vertical ground accelerations. The errors caused by ignoring vertical accelerations, and those introduced by omitting the factor $R_{2/1}$, are lumped into the model error term M. $\bar{N}$ is the expected (in the average sense) threshold transmittable acceleration coefficient for the wall/backfill, evaluated using average values for the various friction angles. Q, $R_{2/1}$ and M are all random variables, Q and R having means of unity. Based in part upon available numerical results (see Chapter 6) and in part upon the form of Equation 9.1 (i.e. it is a product of random variables) it is assumed that d_R is lognormally distributed.

Using results from the theory of probability and assuming that Q, R_ϕ and M are also independent, it is now possible to write expressions for the mean and stantard deviation of d_{Rw}:

$$\text{Mean}[d_{Rw}] = \frac{37\bar{V}}{Ag} e^{-9.4\bar{N}/A} \bar{M} \qquad (9.2)$$

where $\bar{M}$ is the mean value of M; and *

$$\sigma^2_{\ln d_{Rw}} = \left(\frac{9.4}{A}\right)^2 \sigma_N^2 + \sigma^2_{\ln M} + \sigma^2_{\ln Q} \qquad (9.3)$$

Actually, Equation 9.3 gives the standard deviation for $\ln d_{Rw}$ rather than for d_{Rw} directly. $\sigma_{\ln M}$ and $\sigma_{\ln Q}$ are the standard deviations for lnM and lnQ, respectively.

Information concerning the parameters in Equations 9.2 and 9.3 has been summarized in Table 9.1. Coefficients of variation for Q are found in Table 6.3; since the mean of Q is unity, the standard deviation equals the coefficient of variation. $\sigma_{\ln Q}$ is computed by:

$$\sigma^2_{\ln Q} = \ln(1+V_Q^2) \qquad (9.4)$$

Estimates for σ_N were discussed in Chapter 7.

The model error term M is a composite of several factors, as indicated in Table 9.1. Figure 6.4 has been used to estimate

---

* In a more proper derivation, Equation 9.1 should have been written as:

$$\ln d_{Rw} = \ln\left(\frac{37V^2}{Ag}\right) - 9.4\,\frac{N}{A} + \log Q + \log M$$

where N is a random variable. The first term in Equation 9.3 is then obtained by employing:

$$\left[\frac{\partial(\ln d_{Rw})}{\partial N}\right]^2 \text{Var}[N] = \left(-\frac{9.4}{A}\right)^2 \sigma_N^2$$

Table 9.1

SUMMARY OF PARAMETERS IN EQUATION 9.1
FOR PREDICTION OF PERMANENT DISPLACEMENTS

Factor	Mean	Standard Deviation	Log normal Standard Deviation
Ground motion factor Q	1	0.6 -1.4	0.58-1.05
Resistance factor N	$\bar{N}$	0.04-0.065	-
MODEL ERROR			
Vertical acceleration	1.2	0.2	0.2
Ignoring $R_{2/1}$	0.65	0.2	0.3
Deform. backfill	3	2	0.6
Tilting	1.5	0.75	0.5
Combined model error	3.5	3.6	0.84

the mean and standard deviation of the error introduced by failing to take the effect of vertical accelerations into account directly. The discussion in Section 8.4 has provided the basis for estimating the effect of not accounting directly for the ratio $R_{2/1}$. Similarly, rather than introducing a correction for the effect of deformable backfill as a function of period ratio and N/A, a mean correction and a measure of scatter have been estimated from Figure 8.4. The possible effects of tilting have been discussed in Section 8.3. In arriving at these various values, attention has been focussed upon the range of A and N/A of greatest interest: A = 0.3 to 0.4 and N/A = 0.3 to 0.7.

Given the means and standard deviations for the several effects that enter into the model error term, the parameters for this term may be calculated. The mean of M is just the product of the means. The standard deviation is computed using:

$$\sigma^2_{\ln M} = \sum_i \ln(V_i^2 + 1) \qquad (9.5)$$

where V_i is the coefficient of variation for the ith factor in M. Applying these approaches to the values listed in Table 9.1 under the heading of model error leads to the results M = 3.5 and $\sigma_{\ln M} = 0.84$. V_M, and thence σ_M, can be found using Equation 9.4 (with Q replaced by M), leading to $V_M = 1.03$ and $\sigma_M = MV_M = 3.6$.

Table 9.2 presents results for the standard deviation of $\ln dR$, calculated using Equation 9.3 together with values of $\sigma_{\ln Q}$ based on Table 6.3, values for M and $\sigma_{\ln M}$ from Table 9.1

Table 9.2

σ_{lnd_R} FOR GRAVITY RETAINING WALLS

		N/A						
		0.1	0.2	0.3	0.4	0.5	0.6	0.7
V_Q		0.63	0.68	0.78	0.88	1.02	1.17	1.41
σ^2_{lnQ}		0.33	0.38	0.48	0.57	0.71	0.86	1.10
$\sigma^2_{lnQ} + \sigma^2_{lnM}$		1.04	1.09	1.19	1.28	1.42	1.57	1.81
A	0.2	2.9	2.9	2.8	2.8	2.8	2.8	2.8
	0.3	2.1	2.0	2.0	2.0	2.0	2.0	2.0
	0.4	1.7	1.6	1.6	1.6	1.7	1.7	1.7
	0.5	1.5	1.4	1.5	1.5	1.5	1.5	1.6
	0.6	1.3	1.3	1.3	1.3	1.4	1.4	1.5
	0.7	1.3	1.3	1.3	1.3	1.3	1.4	1.4

and values of σ_N interpolated from Fig. 7.1. For the smaller values of A, the first term in Equation 9.3 is quite dominant; that is to say, uncertainty in the resistance factor N is the controlling factor. At the larger A, all terms in Equation 9.3 are more-or-less of equal importance. The result is that $\sigma_{\ln dR}$ is substantially independent of N/A, but depends strongly on A.

9.3 APPROACH TO DESIGN USING SAFETY FACTOR AGAINST DISPLACEMENT

Taking logarithms on both sides of Equation 9.2 and rearranging the resulting equation gives:

$$\frac{\bar{N}}{\bar{A}} = \frac{1}{9.4} \ln \left[\frac{37\bar{M}V^2}{Ag\bar{d}_{Rw}} \right] \tag{9.6}$$

Equation 9.6 may be solved to find the value of N required if the mean residual displacement is to be equal to or less than a given d_R, when A and V are specified. According to the argument in section 9.2, M should be taken as 3.5.

If an engineer could accept having the average residual displacement of many walls be just equal to, or less than, a specified permissible displacement d_L, then d_R in Equation 9.6 may be replaced by d_L. The value of N found from this equation would, together with average values for soil weights and friction angles, be used to calculate the required weight of wall from (see Eq. 4.7).

$$W_w = \frac{[\cos(\beta+\delta) - \sin(\beta+\delta)\tan\phi_b]P_{AE}}{\tan \phi_b - N} \tag{9.7}$$

No safety factor would need to be applied to this weight of wall.

However, the discussion in this and previous chapters has emphasized that often the residual displacement will be much larger than the mean value. The engineer may wish to use a safety factor so as to reduce the likelihood that the actual displacement wil exceed d_L. One way to do this is to apply a safety factor F to d_L, such that:

$$F = \frac{d_L}{\bar{d}_{Rw}} \tag{9.8}$$

Then Equation 9.6 becomes

$$\frac{\bar{N}}{\bar{A}} = \frac{1}{9.4} \ln \left[\frac{37\bar{M}FV^2}{Agd_L} \right] \tag{9.9}$$

This equation would be used as before to calculate N and thence wall weight from Equation 9.7. No additional safety factor would be applied to W_w.

In the absence of extensive tests or field observations to use as a basis for selecting the safety factor F, theory of probability may be used to guide the choice of a suitable value. The engineer must first decide upon an acceptable risk for having d_L exceeded. Let us denote by P the desired probability of not exceeding d_L. Since we have already concluded that d_{Rw} is (approximately) lognormally distributed, probability theory gives the following expression for F (see Eq. 6.11):

$$F = \exp \left[-\frac{1}{2}\sigma^2 \ln d_{Rw} + D_P \sigma_{\ln d_{Rw}} \right] \tag{9.10}$$

where Dp is a factor dependent upon P, as listed in Table 9.3. The information in Tables 9.2 and 9.3 may then be combined to produce a table giving F as a function of P and A. (Note, in Table 9.2, that $\sigma_{\ln dR}$ is virtually independent of N/A: an

Table 9.3

FACTOR D_P FOR VARIOUS PROBABILITIES OF NON-EXCEEDANCE

Probability of Non-Exceedence P-%	Factor D_P in Eq. 9.12
50	0
75	0.675
85	1.037
90	1.286
95	1.645

average value has been used for each A.) The results are given in Table 9.4.

Several somewhat surprising aspects of this table may be noted. First, for P = 50% all of the safety factors are less than unity. This result actually reflects a well-known fact concerning lognormal distributions: the median (point for which half of values are smaller and half are larger) is always less than the mean. For the $\sigma_{lnd_{Rw}}$ of interest, this situation is almost always true for P = 75%.

Second, for P = 95% the safety factor first increases somewhat as $\sigma_{lnd_{Rw}}$ increases (A decreases) and then decreases again for large values of σ_{lndRw}. The trend for F to decrease with increasing $\sigma_{lnd_{Rw}}$ is evident for all other values of P. Thus, once $\sigma_{lnd_{Rw}}$ has increased past a certain point (which depends upon P), further increase causes the point for P percent non-exceedence to move back toward (and even past) the mean! The physical situation that accounts for this behavior may be explained as follows. It has been noted that uncertainty in N contributes very strongly to uncertainty in d_R, especially with smaller A. An N smaller than the mean will contribute an enormous number of cases with small displacements, while an N larger than the mean implies that a few cases with very large displacement are possible. The net effect is actually a decrease in the value exceeded (100-P) percent of the time.

: predicting the displacement of a sliding block has been veloped, and suitable safety factors have been suggested.

5. Based upon this analysis, it is possible to assess the liability of previously proposed methods for designing gravity taining walls.

* Use of a seismic coefficient corresponding to one-half of the peak acceleration for the design earthquake, together with safety factors on wall weight in the range of 1.0 to 1.2, gives satisfactory designs for a moderate seismic environment (probability of excessive displacement less than 10% for peak accelerations less than 0.2 g).

* In a severe seismic environment (peak acceleration of 0.5 g of more), there is generally an unacceptable risk (probability greater than 20%) that walls designed by the seismic coefficient approach will experience permanent deformations in excess of one or two inches.

* For walls designed by the Richards-Elms approach, with a safety factor of 1.1 to 1.2 on wall weight, there is at least 95% probability that the limiting displacement will not be exceeded.

.2 OPPORTUNITIES

Even though design of gravity retaining walls is not one the really major problems in earthquake engineering, the tire class of problems involving prediction of permanent splacements presents one of today's major challenges. Overall ere is considerable value to be derived from further work upon d understanding of one of the simpler cases within this class problems. The opportunities for further work upon the avity retaining wall problem fall in three categories.

1. There is need for further theoretical analysis, to udy the effect of deformability of the backfill upon both iding and tilting. A reasonably satisfactory finite element del is now available for study of sliding; it should be used

10 - CONCLUSIONS AND OPPORTUNITIES

0.1 CONCLUSIONS

The conclusions from this study may be summarized by the ollowing statements:

1. The design of gravity retaining walls against the ffects of earthquakes logically should be based upon a isplacement-limiting approach.

2. Use of a sliding block analysis is appropriate (but arginally so!) for a gravity wall.

3. The basic sliding block model must be modified to ccount for:

* The actual interaction between two sliding blocks, one representing the wall and the other the failing wedge of backfill. This effect is reasonably well understood.
* The effect of the deformability of the backfill prior to failure. This aspect of the problem is now partly understood.
* Tilting of the wall. This effect is as yet poorly understood.

4. The choice of a safety factor for use in the design of wall for the seismic loading case should be based upon the robability that a limiting permanent displacement will be xceeded. It is necessary to consider:

* Variability of ground motions
* Uncertainty in resistance parameters
* Approximations ("errors") in the model used as a basis for computation.

n analysis has been made of these considerations, using the urrently best available data and information. A new equation (9.1)

EXAMPLE 9.2

Given: A wall designed for A = 0.3 and safety factor of 1.1 on wall weight for seismic case, using $\phi = \phi_b = 30°$ and $\delta = 20°$. The height is H and the unit weight is γ.

Find: Probability that permanent displacement will exceed 1, 2 or 4 inches, during earthquake with A = 0.3 and V = 15 inches/sec.

Solution: The first step is to design the wall.

From Eq. 3.2b, with $N = \frac{1}{2} A = 0.15$; $K_{AE} = 0.407$

From Eq. 9.7: $W_w = 0.707 \frac{1}{2}\gamma H^2$

Applying the safety factor: $W_w = (1.1)(0.707)\frac{1}{2}\gamma H^2$

$= 0.778 \frac{1}{2}\gamma H^2$

Using Eq. 4.4 iteratively the actual N for this wall is 0.171.

For the actual earthquake, Eq. 9.2 gives $\bar{d}_{Rw} = 1.19$ inches.

The following table gives results for various d_L. From Table 9.2, the appropriate value of $\sigma_{lnd_{Rw}}$ for A = 0.3 is 2.0.

	d_L = 1 in	d_L = 2 in	d_L = 4 in	
$F = d_L/\bar{d}_{Rw}$	0.84	1.68	3.36	
D_P	1.09	1.26	1.61	Eq. 9.12
$P[\bar{d}_{Rw}<\bar{d}_L]$	0.82	0.90	0.95	Standard Probability Table
$P[\bar{d}_{Rw}>\bar{d}_L]$	0.18	0.10	0.05	

EXAMPLE 9.1

Given: The requirements in Example 4.3.

Find: Appropriate weight of wall using approach of Chapter 9.

Solution: W_w will be computed for two values of F.

	F = 2.5	F = 4	
$\bar{N}/A$	0.68	0.73	Eq. 9.13
$\bar{N}$	0.20	0.22	
ψ	11.3°	12.4°	Eq. 3.1
K_{AE}	0.473	0.491	Eq. 3.2b
P_{AE}	17.7 k/ft	18.4 k/ft	Eq. 3.2a
W_w	46.9 k/ft	51.5 k/ft	Eq. 9.7

These weights may be used directly to proportion the wall: no additional safety factor is required.

shearing through the backfill. In addition, pore water may exert a dynamic force on a wall more or less independently of the mineral skeleton. These are matters for future research.

displacement of such a wall actually results from the type of deformation pattern envisioned by a sliding block type of analysis. Even here, however, there are problems, such as the apparent importance of "elastic" deformations of the backfill, as discussed in Section 8.3. Indeed, when it becomes necesary to use a multiplicative correction factor of 3.5 (primarily to account for elastic backfill effects and tiltng), one must think that the usefulness of the sliding block method is being pushed to its limit.

Clearly more research is required concerning the importance of tilting and of the "elastic" deformability of backfill. It will be very important to conduct experiments in which these effects are properly simulated. Having reasonably correct stress-strain behavior in the soil used for these experiments will be critical. Thus model tests should be carried out on a centrifuge rather than in normal gravity.

Two other matters not dealt with in this report deserve mention. One is the effect of passive resistance at the toe of a wall. In principle this resistance might be incorporated into the analysis as an additional term in Eq. 4.2a. However, it is well known that some displacement must occur before full passive resistance is developed, and such a situation cannot be modelled well by a rigid-plastic model. Great care should be used in applying the methodology of this report if passive toe resistance is a significant part of the total resistance to sliding. The other effect is the influence of pore water within the backfill. Pore water of course can influence resistance to

There is one aspect of the probabilistic analysis which is incomplete. Eq. 6.2 for predicting permanent displacement of a sliding block was developed using data from earthquakes with magnitudes from 6 to 7. Presumably larger earthquakes, causing ground motions of greater duration, would result in greater displacements for the same A and V. It would be desirable to repeat the analysis leading to Eq. 6.2 using ground motions from larger earthquakes.

In the years since Newmark's paper suggesting the use of sliding block analysis, there have been numerous efforts to apply the method to predicting permanent displacements of earth structures as the result of earthquakes. Newmark originally suggested use of the method in connection with slopes, and the bulk of the applications have, in fact, been to slopes. As a conceptual aid to understanding the evolution of permanent deformations and in the development of general guidelines, the sliding block has indeed been very valuable. However, in the case of earth dams it appears that a significant amount of permanent displacement may result from distortions distributed throughout the dam, before a definite failure surface develops. Thus the quantitative use of the sliding block analysis as a tool for predicting the permanent deformation of earth dams may be limited.

Sliding block analysis has always seemed more suitable for the analysis of gravity retaining walls, since it usually takes very litle outward motion to develop a failure condition within the backfill. That is to say, the observable permanent

seismic environments, several different d_L ranging from 1 to 4 inches, and several values of safety factor applied to the calculated wall weight. The results of these calculations may be summarized as follows:

Safety factor applied calculated wall weight	Probability that d_L used for design will be exceeded if design earthquake occurs
1.0	~10%
1.1	~ 5%
1.2	< 5%

If 5% probability-of-exceedence is taken as a target, these results justify the use of a safety factor of 1.1 or 1.2 on wall weight in conjunction with the Richards-Elms procedure.

9.5 GENERAL DISCUSSION

The methodology developed in this report has focussed primarily upon predicting the probability that a retaining wall will experience various amounts of permanent displacement during an earthquake. Quantifying uncertainty requires good knowledge of the several aspects of a problem and adequate statistics for the pertinent parameters. Obviously there is yet not enough such information to do with great confidence. Nonetheless, the estimates developed in this report using the best available information appear to provide good guidance for purposes of design. The methodology itself should remain useful as additional data are developed, and may be applied to other types of problems for which a sliding block analysis is applicable.

Table 9.5

PROBABILITY THAT MOVEMENT OF WALLS WILL EXCEED VARIOUS LIMITING VALUES. WALLS ARE DESIGNED FOR STATIC SEISMIC COEFFICIENT OF 1/2 OF PEAK ACCELERATION WITH $\phi = \phi_b = 30°$ and $\delta = 20°$

SAFETY FACTOR ON WALL WGT. SEISMIC CASE	d_L inches	CHARACTERISTICS OF EARTHQUAKE		
		A = 0.2 V=10 in/s	A = 0.3 V=15 in/s	A = 0.5 V=25 in/s
1.0	1	10%	28%	56%
	2	7%	18%	38%
	4	4%	10%	22%
1.1	1	5%	18%	47%
	2	3%	10%	30%
	4	2%	5%	16%
1.2	1	2%	12%	40%
	2	2%	6%	23%
	4	1%	3%	12%

coefficient for this wall is N = 0.71. The actual earthquake is assumed to have the same peak acceleration as the "design earthquake (i.e. a = 0.3), together with a peak velocity V = 15 in/s. Note that the results are independent of the actual height of the wall and of the actual weight of the backfill.

Table 9.5 summarizes results for walls designed in this way using several different safety factors nad several different design (and actual) earthquakes. Similar results were obtained using other combinations for ϕ, ϕ_b and δ. (Changing these parameters changes the wall weight, but has little effect upon the N for a wall just meeting the design criteria.) For a moderate seismic environment (A = 0.2), a conventional design will have reasonably low probabilities of excessive displacements. However, in a severe seismic environment the probability of excessive movements is much larger, at least for safety factors of 1.0 to 1.2.

In computing these results, it has been assumed that average values of ϕ, ϕ_b and δ are used for design of a wall. If conservatively low values are used in design, the probability of excessive movements will be less than suggested by these calculations.

9.4.2 Design Following Richards-Elms

With the Richards-Elms method, the required weight of wall depends upon the allowable displacement d_L as well as upon the seismic environment. A number of calculations have been made, using various combinations of ϕ, ϕ_b and δ, various

2. The corresponding value of N is computed, using one of the techniques discussed in Section 4.3.

3. The value of $\bar{d}_R$ is computed, using Eq. 9.2 and the parameters appropriate for the earthquake of concern.

4. The factor F is calculated for the selected threshold permanent displacement.

5. The factor D_p is calculated by inverting Eq. 9.12. The appropriate value of $\sigma_{lnd_{Rw}}$ is selected from Table 9.2

6. The probability of exceedance corresponding to Dp is looked up in a standard normal cumulative probability table.

9.4.1 Conventional Design

While there are many different "conventional" ways to select a seismic coefficient for the design of gravity retaining walls (se Chapter 3),for purposes of illustration this coefficient will be taken as one-half of the peak acceleration in the earthquake used to define the seismic threat. Example 9.2 outlines a sample calculation of the probabilities that various levels of displacement will be exceeded, for a specific case. Note that the wall is "designed" for an earthquake with a peak acceleration of 0.3g, using a seismic coefficient N = (1/2)(0.3) = 0.15. Because of the safety factor applied to the calculated wall weight, the actual threshold acceleration

9.3.2 Examples

Using M = 3.5, Equation 9.11 now becomes:

$$\bar{N} = \begin{cases} \left[0.66 + \frac{1}{9.4} \ln \frac{V^2}{Agd_L}\right] A & F = 4 \quad (9.11a) \\ \left[0.61 + \frac{1}{9.4} \ln \frac{V^2}{Agd_L}\right] A & F = 2.5 \quad (9.11b) \end{cases}$$

The factor 37, M and F have all been combined in the first terms of these equations.

To illustrate the use of Equation 9.13, let us return to Example 4.3, which is reworked in Example 9.1 using the results developed in this chapter. Note that Eqs. 3.1 and 3.2 are used with $N_v = 0$; the possible effects of $N_v \neq 0$ have been accounted for by the analysis in this chapter. The wall weights computed using both values of the safety factor are larger than that determined in Example 4.3 before any safety factor was applied. However, in the current example no additional safety factor need be applied to the computed weight, and hence the design is more economical.

9.4 RELIABILITY IMPLICIT IN OTHER DESIGN APPROACHES

The results developed in Section 9.2 may be used to estimate the probability that walls designed by a conventional approach, or using the Richards-Elms method, will experience more than a given value of movement. The methodology is as follows:

1. The wall weight required by the approach, including any safety factor, is calculated.

9.3.1 Choice of Safety Factor

There is no standard to guide the choice of a suitable value for P. In the case of buildings, the probability of not failing during a major earthquake, as implied by good modern building codes, apparently is less than 1% (corresponding to P = 99%). A somewhat lower probability of nonfailure seems appropriate for gravity retaining walls: say P = 95% or even P = 90%. It should also be noted that P = 95% is about as far as the information concerning the distribution of d_R may comfortably be pushed. This is certainly the upper limit (perhaps even beyond the limit) of confidence in the statistical analysis of computed displacements in Chapter 6.

Referring to Table 9.4, with P = 95% the safety factor F should be about 3.6 to 3.9, except for the smallest ground accelerations where a smaller value is justified. However, design of gravity walls is little affected when expected ground accelerations are this small. In the interests of simplicity a single factor of 3.8 might be used at all levels of ground acceleration. Similarly, use of a safety factor of 2.4 seems reasonable if a somewhat less conservative design corresponding to P = 90% is desired.

Recognizing that one characterization of the distribution of d_R is uncertain at such higher levels of non-exceedence, one should not attempt to be too precise in the choice of safety factors. Hence values of F = 4 (conservative) or F = 2.5 (less conservative) are recommended.

Table 9.4

SAFETY FACTORS REQUIRED FOR VARIOUS PROBABILITIES OF NON-EXCEEDANCE, AS A FUNCTION OF PEAK GROUND ACCELERATION

		Probability of non-exceedance - %				
A	$\sigma_{lnd_{RW}}$	50	75	85	90	95
0.2	2.83	0.018	0.12	0.34	0.69	1.92
0.3	2.01	0.13	0.52	1.07	1.44	3.62
0.4	1.66	0.25	0.77	1.41	2.13	3.87
0.5	1.50	0.32	0.89	1.54	2.23	3.83
0.6	1.36	0.40	0.99	1.63	2.28	3.72
0.7	1.33	0.41	1.01	1.64	2.28	3.68

to study the influence of varying the several parameters. Further improvement of the model likely will be necesary for study of tilting; for this case it seems essential at least to have multiple parallel failure planes through the backfill. Modelling the resistance of the soil beneath the wall to tilting is a very poorly understood problem.

2. Valuable results can come from model tests of gravity walls carried out on a centrifuge. It is essential that the wall be free-standing; i.e. free to move relative to the soil as it will. A program of tests involving sliding has been underway at Cambridge University in England, but results are not yet available. Additional tests to explore the complex tilting problem should be even more valuable.

3. The analysis of uncertainty should be extended. A primary need is to bring the influence of the magnitude of the earthquake into the equation for predicting the displacement of a sliding block.

REFERENCES

Antia, H. 1982. "Predicting Relative Displacement for Limited-Slip Seismic Design of Gravity Retaining Walls with Non-Liquefying Backfills," S.M. Thesis, Research Report R82-34, Department of Civil Engineering, Massachusetts Institute of Technology.

ATC-3-06. Jun 1978. "Tentative Provisions for the Development of Seismic Regulations for Buidings," Applied Technology Council, Report No. ATC-3-06, Palo Alto, Calif.

Bolton, M. D., and Steedman, R. S. July 1982. "Centrifugal Testing of Microconcrete Walls Subjected to Base Shaking," Proceedings, Conference on Soil Dynamics and Earthquake Engineering, Southampton, Vol 1, pp 311-329.

Evans, G. L. 1971. "The Behavior of Bridges Under Earthquakes," Proceedings, New Zealand Roading Symposium, Victoria University of Wellington, Wellington, New Zealand, Vol 2, pp 664-684.

Franklin, A. G., and Chang, F. K. Nov 1977. "Earthquake Resistance of Earth and Rock-Fill Dams; Report 5, Permanent Displacement of Earth Embankments by Newmark Sliding Block Analysis," MP S-71-17, Soils and Pavements Laboratory, US Army Waterways Experiment Station, Vicksburg, Miss.

Jacobsen, P. N. 1980. "Behavior of Retaining Walls Under Seismic Loading," M.E. Report 79/9, Department of Civil Engineering, University of Canterbury, Christchurch, New Zealand.

JSCE. 1977. "Earthquake Resistant Design for Civil Engineering Structures, Earth Structures and Foundations in Japan," Japan Society of Civil Engineers.

Lai, C. S. 1979. "Behavior of Retaining Walls Under Seismic Loading," M.E. Report 79/9, Department of Civil Engineering, University of Canterbury, Christchurch, New Zealand.

Makdisi, F. I., and Seed, H. B. Dec 1979. "Simplified Procedure for Evaluating Embankment Response," Journal of the Geotechnical Engineering Division, ASCE, Vol 105, No. GT12, pp 1427-1434.

Mayes, R. L., and Sharpe, R. L. Oct 1981. "Seismic Design Guidelines for Highway Bridges," Report No. FHWA/RD-081-081, Federal Highway Administration, Washington, DC.

Mononobe, N., and Matsuo, H. 1929. "On the Deformation of Earth Pressure During Earthquakes," Proceedings, World Engineering Conference, Vol 9, p 177.

Murphy, V. A. 1960. "The Effect of Ground Characteristics on the Aseismic Design of Structures," Proceedings, Second World Conference on Earthquake Engineering, Japan, Vol 1, pp 231-247.

Nadim, F. 1980. "Tilting and Sliding of Gravity Retaining Walls," S.M. Thesis, Department of Civil Engineering, Massachusetts Institute of Technology, Cambridge, Mass.

_____. 1982. "A Numerical Model for Evaluation of Seismic Behavior of Gravity Retaining Walls," Sc.D. Thesis, Research Report R82-33, Department of Civil Engineering, Massachusetts Institute of Technology, Cambridge, Mass.

Nadim, F., and Whitman, R. V. July 1983. "Seismically Induced Movement of Retaining Walls," Journal of Geotechnical Engineering, ASCE, Vol 109, No. 7, pp 915-931.

NAVFAC. May 1982. "Foundations and Earth Structures, DM-7.1 and DM-7.2," Department of the Navy, Naval Facilities Engineering Command, Alexandria, Va.

Newmark, N. M. 1965. "Effects of Earthquakes on Dams and Embankments," Geotechnique, Vol 15, No. 2, pp 139-160.

Newmark, N. M., and Hall, W. J. 1982. "Earthquake Spectra and Design," Earthquake Engineering Research Institute, Berkeley, Calif.

Okabe, S. 1926. "General Theory of Earth Pressure," Journal, Japanese Society of Civil Engineers, Vol 12, No. 1.

Ortiz, L. A., Scott, R. F., and Lee, J. 1981. "Dynamic Centrifuge Testing of a Cantilever Retaining Wall," Soil Mechanics Laboratory, Division of Engineering and Applied Sciences, California Institute of Technology, Pasadena, Calif.

Richards, R. J., and Elms, D. Apr 1979. "Seismic Behavior of Gravity Retaining Walls," Journal of the Geotechnical Engineering Division, ASCE, Vol 105, No. GT4, pp 449-464.

Seed, H. B., and Martin, G. R. May 1966. "The Seismic Coefficient in Earth Dam Design," Journal of the Soil Mechanics and Foundations Division, ASCE, Vol 92, No. SM3, pp 25-59.

Seed, H. B., and Whitman, R. V. 1970. "Design of Earth Retaining Structures for Dynamic Loads," ASCE Specialty Conference, Lateral Stresses in the Ground and Design of Earth Retaining Structures, pp 103-147.

Sherif, M. A., Ishibashi, I., and Lee, C. D. Jan 1981. "Dynamic Earth Pressures Against Retaining Structures," Soil Engineering Research Report No. 21, University of Washington, Seattle, Wash.

USACE. Jan 1965. "Retaining Walls, EM 1110-1-1401 Change 3," Department of the Army, US Army Corps of Engineers, Washington, DC.

USACE. Apr 1970. "Stability of Earth and Rock-Fill Dams, EM 1110-1-1902," Department of the Army, US Army Corps of Engineers, Washington, DC.

_____. Feb 1982. "Stability of Earth and Rock-Fill Dams, EM 1110-1-1902 Change 1," Department of the Army, US Army Corps of Engineers, Washington, DC.

_____. May 1983. "Earthquake Design and Analysis for Corps of Engineers Projects," ER 1110-2-1806, Department of the Army, US Army Corps of Engineers, Washington, DC.

Wong, C. P. 1982. "Seismic Analysis and an Improved Design Procedure for Gravity Retaining Walls," S.M. Thesis, Research Report R82-32, Department of Civil Engineering, Massachusetts Institute of Technology.

Zarrabi-Kashani, K. 1979. "Sliding of Gravity Retaining Wall During Earthquakes Considering Vertical Acceleration and Changing Inclination of Failure Surface," S.M. Thesis, Department of Civil Engineering, Massachusetts Institute of Technology, Cambridge, Mass.

LIST OF SYMBOLS

A = Maximum horizontal ground acceleration coefficient of an earthquake record (max. acceleration is Ag).

A_H = Horizontal ground acceleration coefficient; varies with time.

A_V = Vertical ground acceleration coefficient.

a = Ground acceleration.

a_T = Transmittable (or threshold, or limiting) accelerations.

C_s = Shear wave velocity.

D_P = Standard normal deviate (i.e., number of standard deviations from the mean) corresponding to the probability P of non-exceedance of a given parameter (e.g. residual wall displacement).

d_L = Allowable residual displacement

d_R = Residual displacement calculated using the rigid single block model. Also, the residual displacement calculated using the Richards-Elms equation or one of Newmark's equations.

$\hat{d}_R$ = Predicted residual displacement for 2-block model.

d_{Re} = Residual displacement of a rigid single-block model; when no vertical component of an earthquake record is taken into account.

$\bar{d}_{Re}$ = Average of d_{Re} over a number of records.

$\bar{d}_{Ro}$ = Average residual displacement of a rigid single-block model; averaged over 4 orientation directions as shown in Fig. 6.1 for a single earthquake record.

d_{Rv} = Residual displacement of a sliding rigid single-block model, when vertical component of an earthquake record is taken into account.

$\bar{d}_{Rv}$ = Average of d_{Rv} over a number of records.

d_{Rw} = Residual displacement of a retaining wall.

$\bar{d}_{Rw}$ = Expected value of d_{Rw}.

$E[]$ = The expected value operator, with the quantity inside the brackets being the operand; equivalent to calculating the mean of the operand.

E_o = Correction factor to block model slip calculations, to account independently for wall orientations. A random variable.

E_s = Correction factor to block model slip calculations, to account independently for earthquake record variability. A random variable.

E_v = Correction factor to block model slip calculations, to account independently for vertical earthquake motions. A random variable.

$\bar{E}v$ = Average value of E_v at a given N/A.

F_{ww} = Wall weight factor, a non-dimensional indicator of wall weight.

f_{E-Q} = Central frequency of earthquake.

f_{BF} = Natural frequency of backfill.

g = Constant of gravitational acceleration.

i = Angle of inclination of the backfill with respect to horizontal.

K_A = Coefficient of active earth pressure (static).

K_{AE} = Coefficient of active earth pressure due to earthquake (includes static and dynamic effects).

K_o = Coefficient of earth pressure at-rest.

H = Height of the wall.

M = Correction factor, accounting for various modelling errors of the single block model. Also, mass of a sliding block.

$\bar{M}$ = Expected value of correction factor M.

M_s = Mass of the backfill soil.

M_w = Mass of the wall.

m = Mean of a quantity the particular quantity would be indicated by a subscript to m, e.g. m_Q, m_N, etc.

N = Maximum transmittable horizontal ground acceleration coefficient; also seismic coefficient depending on the context.

$\bar{N}$ = Expected value of N.

N_H = Transmittable horizontal ground acceleration coefficient, variable with time. Also, the seismic coefficient depending on the context.

N_o = Seismic coefficient number from Fig. 3.6.

N_R = Threshold transmittable acceleration coefficient for rotational mode of failure.

N_V = Transmittable vertical acceleration coefficient variable with time.

N_T = Threshold transmittable acceleration coefficient.

P = Probability; probability of non-exceedance.

P_{AE} = Total active thrust due to dynamic plus static earth pressure.

$(P_{AE})_H$ = Horizontal component of P_{AE}.

$(P_{AE})_V$ = Vertical component of P_{AE}.

Q = Correction factor, accounting for random nature of earthquake shaking.

R_E = Residual displacement amplification factor, accounting for effects of elastic backfill.

$R_{2/1}$ = Correction factor, ratio of 2-block to 1-block model displacement.

R_ϕ = Correction factor, accounting for uncertainties in parameters characterizing backfill, wall, and foundation soil.

$R\theta$ = Ratio of residual displacements of 2-block models using fixed θ vs. variable θ in analysis.

T_{BF} = Natural period of backfill.

T_{E-Q} = Central period of earthquake.

t = Time.

V = Maximum ground velocity of an earthquake record.

V_o = Coefficient of variation of E_o.

V_R = Combined coefficient of variation of E_o, E_s, and E_v assuming E_o, E_s, and E_v independent.

$V_{R\phi}$ = Coefficient of variation of $R\phi$.

V_s = Coefficient of variation of E_s.

V_v = Coefficient of variation of Ev.

Var[] = The variance operator, with the quantity inside the brackets being the operand; equivalent to σ^2.

W = Weight of a sliding block.

β = Angle of inclination of the back of a retaining wall with respect to vertical.

γ = Unit weight of soil.

γ_c = Unit weight of concrete.

δ = Friction angle between the back of the wall and the backfill soil.

ϕ = Friction angle of soil backfill.

ϕ_b = Friction angle between the base of the wall and the foundation soil.

μ = Coefficient of friction.

ρ_c = Unit mass of concrete.

ρ_s = Unit mass of the backfill soil.

σ = Standard deviation of a quantity; the particular quantity would be indicated by a subscript to σ, e.g. σ_Q, σ_N, etc.

θ = Angle of inclination of failure plane with respect to horizontal.

θ_T = Threshold angle of inclination of failure plane with respect to horizontal.

ψ = Equivalent angle of tilt to transform a dynamic analysis into a pseudo-static analysis.

APPENDIX A

CATALOGUE OF STRONG-MOTION EARTHQUAKES CHOSEN FOR STATISTICAL SLIDING BLOCK ANALYSES

APPENDIX A

CATALOGUE OF STRONG MOTION EARTHQUAKES CHOSEN FOR STATISTICAL SLIDING BLOCK ANALYSES

No.	Earthquakes	File No.	Date	M	I
1	El Centro Earthquake, Imperial Valley	A001	5/18/40	6.7	8
2	Kern County Earthquake, Taft Lincoln School	A004	7/21/52	7.7	7
3	Eureka Earthquake, Eureka Federal Building	A008	12/21/54	6.5	7
4	Eureka Earthquake, Ferndale City Hall	A009	12/21/54	6.5	7
5	Long Beach Earthquake, Vernon CMD Building	B021	3/10/33	6.3	6
6	Lower California Earthquake, Imperial Valley	B024	12/30/34	6.5	6
7	Western Washington Earthquake at Olympia, Washington, Highway Test Lab.	B029	4/13/49	7.1	8
8	Puget Sound, Washington Earthquake at Olympia, Washington, Highway Test Lab.	B032	4/29/65	6.5	7
9	San Fernando Earthquake at 8244, Orion Blvd., 1st floor	C048			
10	Old Ridge Route, Castaic	D056	2/ 9/71	6.6	7
11	Griffith Park Observatory	0198			
12	Imperial Valley Earthquake Station 7				
13	Station 10		10/15/79	6.4	-
14	Bonds Corner				

* M stands for Magnitude
I stands for Intensity
File No. refers to CIT files
Computed results are filed as numbered